Post-Fire Damage Inspection of Concrete Structures - Phase II

Principal Investigator (s)
Dr. Simos Gerasimidis
Dr. Scott Civjan

University of Massachusetts Amherst

Research and Technology Transfer Section
MassDOT Office of Transportation Planning

U.S. Department of Transportation
Federal Highway Administration

Technical Report Document Page

1. Report No. 23-039	2. Government Accession No.	3. Recipient's Catalog No.
4. Title and Subtitle Post-Fire Damage Inspection of Concrete Structures - Phase II		5. Report Date February 28, 2023
		6. Performing Organization Code
7. Author(s) James Viglas, Thomas Vitalis, Scott Civjan, Simos Gerasimidis		8. Performing Organization Report No. 23-039
9. Performing Organization Name and Address University of Massachusetts Amherst UMass Transportation Center 130 Natural Resources Way Amherst, MA 01003		10. Work Unit No. (TRAIS)
		11. Contract or Grant No.
12. Sponsoring Agency Name and Address Massachusetts Department of Transportation Office of Transportation Planning Ten Park Plaza, Suite 6500, Boston, MA 02116		13. Type of Report and Period Covered Final Report - February 2023 (June 2021 – February 2023)
		14. Sponsoring Agency Code n/a
15. Supplementary Notes Project Champion - John Czach, Tunnel Maintenance Engineer, MassDOT		

16. Abstract

In general, tunnels are designed with an abundance of safety regarding structural integrity, however, there can be uncertainty related to structural performance after a fire event. The residual condition of a tunnel after a fire is dependent on fire intensity and duration. The goal of this study is to correlate visual and material characteristics of structural and nonstructural components of tunnels with fire temperature and exposure time. This can be further related to the residual capacity of structural members in a tunnel, providing insight into safety and overall functionality. Experimental results show that the visual response of materials with heat exposure is variable and dependent on a number of factors. A wide range of materials were studied to establish a well-versed collection of data that may be used in a post-fire inspection. In addition, mechanical testing of three configurations of structural slabs exposed to different heating regimens was conducted. The influence of heat on a structural member may be complex, and was found to be minimal for the heating regimens and loading procedures applied. This work can serve as an aid for post-fire investigation by providing methods to estimate fire intensity and duration through visual observation and mechanical testing.

17. Key Word fire event, tunnels, safety, structural performance, post-fire inspection		18. Distribution Statement	
19. Security Classif. (of this report) unclassified	20. Security Classif. (of this page) unclassified	21. No. of Pages 142	22. Price n/a

Form DOT F 1700.7 (8-72) Reproduction of completed page authorized

i

Post-Fire Damage Inspection of Concrete Structures

Final Report

Prepared By:

James Viglas
Graduate Researcher
jviglas@umass.edu

Thomas Vitalis
Graduate Researcher
tvitalis@umass.edu

Scott Civjan, Ph. D.
Co-Principal Investigator
scivjan@umass.edu

Simos Gerasimidis, Ph. D.
Principal Investigator
sgerasimidis@umass.edu

University of Massachusetts Amherst

Acknowledgements

Disclaimer

Executive Summary

This study of post-fire damage inspection of concrete structures was undertaken as part of the Massachusetts Department of Transportation (MassDOT) Research Program. This program is funded with Federal Highway Administration (FHWA) State Planning and Research (SPR) funds. Through this program, applied research is conducted on topics of importance to the Commonwealth of Massachusetts transportation agencies.

Tunnels are a vital part of Massachusetts's transportation infrastructure, more so than ever since the completion of the Central Artery/Tunnel project. It is well known that fire can result in the loss of strength of tunnel structures and tunnel elements, hence the need for inspection protocols to help evaluate the structural condition of tunnels after fire events. Though the decision of whether to close a tunnel may be obvious in the case of a severe fire with extensive damage or a minor fire with no obvious damage, it may not be obvious in the case of a fire of intermediate intensity. The purpose of this research is to understand how fire affects the residual strength capacity of tunnel structures and tunnel elements and to develop a post-fire inspection protocol that can be quickly and easily implemented.

This report documents the findings of the research work done in Phase II of this project. The primary goals of Phase II of the project include a thorough investigation of the visual changes and the mechanical behavior of components found in tunnel structures after heat. exposure. A wide range of materials and tunnel components were heated under different regimens to understand how different temperatures and durations of heat exposure would influence their appearance. Also, structural reinforced concrete slab members were tested mechanically to understand the influence of heat on the residual capacity of these members.

An extensive collection of data was compiled which shows the influence of heat on various materials and tunnel components. The materials primarily consist of concrete, steel, and aluminum, and the tunnel components include structural concrete slabs as well as other tunnel utilities (phenolic conduit, aluminum wireways, light fixtures). Results show that different temperatures and durations of heat exposure can influence materials and components differently depending on a range of factors. In general, unique visual changes of materials and components can be associated with specific temperatures, and the duration of heat exposure can cause variances in visual appearances depending on material properties. Specific temperatures correlated with visual changes including melting, charring, discoloration, and other physical changes are reported. Unique visual changes associated with specific temperatures are important as these can be used as aids by a tunnel inspector to estimate temperatures reached in a tunnel fire, which can be further used to assess overall structural damage. This testing also provides insight into the functionality of tunnel utilities at different temperatures.

Structural reinforced concrete slab members were tested mechanically to investigate the residual capacity of members when exposed to various heating regimens. Slab specimens were heated to temperatures ranging from 300°C (572°F) to 500°C (932°F) for three hours to investigate the effects of intermediate tunnel fires. Test results suggest that the residual

capacity of structural reinforced concrete slab specimens was not significantly influenced by the applied heating regimens. Also, the associated deflections with maximum capacity were measured, and test data show that deflections of slabs exposeed to heat were approximately equal to or greater than that of control slabs.

The collection of visual data in conjunction with the results of mechanical testing may be used by MassDOT and other agencies to enhance post-fire inspection of tunnel structures. The data reported in this document can help better the judgement of fire intensity and duration during inspection and provide insight into the mechanical behavior of structural members.

Section 1 is a brief introduction to the problem and a description of the scope of the research. Section 2 describes the effects of fire on structural materials. Section 3 overviews existing post-fire inspection methods for concrete structures. Section 4 explains methods of testing for nonstructural components. Section 5 details the results of testing of nonstructural components. Section 6 presents results of testing of structural components. Section 7 overviews conclusions of the report. Section 8 suggests recommendations for future testing.

Table of Contents

List of Tables

List of Figures

List of Acronyms

Acronym	Expansion
ACI	American Concrete Institute
ASCE	The American Society of Civil Engineers
ASTM	American Society for Testing and Materials
CEN	European Committee for Standardization
FHWA	Federal Highway Administration
fib	International Federation for Structural Concrete
HC	Hydrocarbon
HCM	Hydrocarbon Modified
ISE	Institute of Structural Engineers
ISO	International Organization for Standardization
MassDOT	Massachusetts Department of Transportation
RWS	Rijkswaterstaat
SPR	State Planning and Research
TC	Thermocouple

This page left blank intentionally.

1.0 Introduction

This study of post-fire damage investigation of concrete structures was undertaken as part of the Massachusetts Department of Transportation (MassDOT) Research Program. This program is funded with Federal Highway Administration (FHWA) State Planning and Research (SPR) funds. Through this program, applied research is conducted on topics of importance to the Commonwealth of Massachusetts transportation agencies.

This report is a continuation of Phase I of this project and describes the findings of Phase II in detail. The Phase I report is referenced for further information *(1)*.

The assessment of a structure after an extreme damaging event is of primary interest for structural engineers and stake holders who are involved in decision-making regarding the resumption of the operation of the structure (building, bridge, tunnel etc.). Recently, there has been significant interest in the concept of infrastructure resiliency; some of the factors that affect that measure are the immediate response of the structure (the extent of damage), the available redundancy in the structure to withstand a partial or complete collapse, the available resources to repair the structure, and the process to recovery. Although there has been great theoretical progress in this field, targeted solutions are needed, and these solutions are always dependent on the type of extreme event (blast, fire, collision, etc.) and the type of structure. Due to the difficulty of quantifying resilience for every different event/structure, there are even threat-independent methods that have been developed for this purpose *(2, 3, 4, 5, 6, 7, 8)*.

MassDOT identifies fire events as a major concern regarding the safety and functionality of tunnel structures. This research project was initiated in response to the described concerns, which aims to establish a post-fire inspection protocol that may be used by inspectors to assess the condition of a tunnel after a fire event. Many challenges are associated with post-fire investigation. An inspector must be able to identify damage to structural components and any potential hazards post-fire. This can be especially difficult when addressing an intermediate tunnel fire, which is the focus of this report. Also, there may be urgency to safely reopen a tunnel shortly after a fire event to minimize interruptions of commerce, negative economic impacts, and social ramifications. Closure of a tunnel can cause traffic issues through disruption of commuting and emergency services. Depending on levels of damage, the cost of repair or replacement of tunnel components and structural members can be expensive. It is also important that the response to a tunnel fire be appropriate and handled with proper judgement, as this can have social impacts on the groups involved.

The interest in tunnel fires and their influence on structures is widespread across industry and academia. Fire is known to contribute to losses in strength and stiffness, excessive deflections/distortions, and a reduction in long-term durability of structural elements. The primary purpose of this report is to investigate the effects of fire exposure on the residual strength of structural members and to establish methods of visual inspection that can be used for rapid assessment of fire intensity and duration.

Three topics are prominent in the field of research regarding fire and structures:
- Residual condition of structures post-fire
- Fire resistance design
- Material response to fire

Post-fire residual condition of a structure can include losses in strength and stiffness, negative influence (increase) of deflections/distortions, and a reduction in the long-term durability of structural elements. Fire resistance design can be defined as the "ability of an element (not a material) of building construction to fulfill its designed function for a period of time in the event of a fire" *(9)*. Materials respond differently to heat exposure based on a wide range of factors, and their response can have implications on structural behavior. The primary focus of this report is the residual condition of structures post-fire, as this relates directly to post-fire evaluation. Current literature in the field of structural fire research is primarily focused on fire resistance design. Many questions persist in literature regarding the residual evaluation of structures, and this research project aims to better explore this topic, specifically relating to tunnel structures.

The content of this report is as follows:
- Section 2 describes the effects of fire on structural materials
- Section 3 overviews existing post-fire inspection methods for concrete structures
- Section 4 explains methods of testing for nonstructural components
- Section 5 details the results of testing of nonstructural components
- Section 6 presents results of testing of structural components
- Section 7 overviews conclusions of the report
- Section 8 suggests recommendations for future testing

1.1 Introduction to Residual Condition of Structures after a Fire

The primary focus of this report is the evaluation of the residual condition of concrete structures when exposed to intermediate tunnel fires. Evaluation of structures after a minimal or large tunnel fire can be relatively straightforward due to obvious implications of little damage or severe damage, respectively. Uncertainty arises when a tunnel fire is intermediate, and damage to the structure is not obvious and must be evaluated in greater detail. Literature has demonstrated that the residual strength, stiffness, serviceability, and durability of a structure can be significantly influenced by a fire event *(9, 10)*. These effects are a result of the degradation of the mechanical properties of structural materials, specifically concrete and steel, resulting from heat exposure. Heat exposure is also associated with spalling of concrete, which alters an element's cross section and can directly expose reinforcing steel to heat in a fire event. Due to the difficulties associated with mechanically testing full scale structural elements exposed to fire scenarios, the literature is dominated by studies of material properties after heat exposure. This project investigates the residual mechanical response of full-scale structural elements (prestressed concrete ceiling panels) exposed to specific heating regimens to enhance post-fire inspection protocols. Also, tunnel components

were tested to better understand associated material behaviors when exposed to heat, so that temperature and duration of heat exposure can be correlated with collected data and used to further evaluate potential damage of a structure.

Factors influencing the residual condition of structural elements in a fire event include:
1. Maximum temperature of fire
2. Proximity of fire to a structural element
3. Duration of heat exposure

The maximum temperature experienced during a fire can be crucial in evaluating the residual condition of structural elements. Of primary concern is the maximum temperature that the structural element experiences, as this directly relates to the element's mechanical response to heat exposure *(10)*. The maximum temperature that an element experiences can be influenced by the fire's fuel source and proximity to the element. The duration of heat exposure can influence the thermal penetration in an element. The extent of thermal penetration in an element can be indicative of the volume and location of material damaged as well as which materials are damaged (concrete and/or reinforcing steel).

1.2 Introduction to Fire Resistance Design

Fire resistance design is the performance of an element to withstand a fire with respect to its structural integrity during a fire event, and directly relates to the immediate safety of occupants and the functionality of a tunnel structure during a fire event *(1, 11)*. Codes and standards have been established for designers to aid in fire resistance design. Three approaches are generally used for fire resistance design:
- Fire testing
- Prescriptive methods
- Performance-based methods

Fire testing is the process of exposing a structural element or sub-assembly of a structure to fire conditions, generally while the element is subjected to service load conditions and expected support conditions. Fire design curves have been established that represent the air temperature in a fire over a defined amount of time. Fire design curves can represent a range of fire scenarios, considering variables such as the source of fire and boundary conditions.

The ISO 834 standard fire curve is a cellulosic curve based on the burning rate of general building materials. The ASTM E119 fire curve and its criteria are similar to the ISO 834 standard fire curve. The hydrocarbon (HC) fire curve is representative of the burning of hazardous materials like fuels and chemicals, and the hydrocarbon modified (HCM) fire curve represents a similar but more severe variation of the HC curve. The Rijkswaterstaat (RWS) fire curve represents an extreme, worst case, tunnel fire. The two RABT/ZTV fire curves represent highway and railway tunnel fires respectively *(12, 13, 14)*.

Prescriptive methods of fire resistance design define requirements of minimum concrete cover to steel reinforcement for specific design fires. These methods also establish maximum temperatures that certain elements may reach in a design fire *(1)*.

Performance-based methods utilize engineering calculations and/or finite element analysis to demonstrate a structure's response to fire design criteria, including a structure's ability to withstand fire loads without collapse *(9, 15)*.

1.3 Documents on the Residual Condition of Structures After a Fire

Table 1.1 shows a collection of standards, codes, and technical reports relating to the subjects of the residual condition of structures post-fire and fire resistance design. The *Structural Fire Protection* standard provides techniques to improve fire safety in buildings by providing standards to determine fire resistance of structural members *(16)*. The Eurocode documents (*EN 1992 1-2, EN 1993 1-2, and EN 1994 1-2*) describe requirements, rules, and principles for structural design of buildings exposed to fire in order to limit associated risks *(17, 18, 19)*. The *Assessment, Design, and Repair of Fire-Damaged Structures* report focuses on damage assessment, structural design, and repair methods, discussing standards, testing, and case studies *(20)*. *Fire Design of Concrete Structures—Structural Behavior and Assessment* is intended to enhance the understanding of fire resistance design as well as analysis and repair of fire-damaged structures *(21)*. The technical report *Appraisal of Existing Structures* was designed to guide structural engineers in checking and reporting the adequacy of an existing structure *(22)*. *Code Requirements for Determining Fire Resistance of Concrete and Masonry Construction Assemblies* has design and analytical procedures to aid in evaluating fire resistance properties of concrete and masonry members and building assemblies *(23)*.

Table 1.1: Standards, codes, and technical reports on the subject of fire and structures *(5)*

Organization	Country/ Region	Document Title	Document Type	Date of Publication
American Society of Civil Engineering (ASCE)	USA	Structural Fire Protection	Standard	1992
Eurocode (CEN)	EU	EN 1992 1-2, EN 1993 1-2, EN 1994 1-2	Building Code	2004 & 2005
Concrete Society	Britain	Assessment, Design, and Repair of Fire-Damaged Structures	Technical Report	2008
International Federation for Structural Concrete (fib)	EU	Fire Design of Concrete Structures – Structural Behavior and Assessment	Technical Report	2008
Institution of Structural Engineers (ISE)	Britain	Appraisal of Existing Structures	Technical Report	2010
American Concrete Institute (ACI)	USA	Code Requirements for Determining Fire Resistance of Concrete and Masonry Construction Assemblies	Building Code	2019

This page left blank intentionally.

2.0 Effects of Fire on Structural Materials

Concrete and steel, the two primary structural components in tunnels, experience degradation in material properties while and after being exposed to elevated temperatures, leading to a potential reduction in strength *(24, 25)*. It is essential to understand the relationship of these materials to heat exposure to evaluate the condition of a structure after a fire event. Numerous studies investigating the material properties related to elevated temperatures of concrete and steel have been published. Due to the impracticality of testing full structural elements, a large number of studies use specimens such as concrete cylinders and steel coupons when conducting laboratory tests. Notably, this allows for well-controlled tests, where variables of interest can be adjusted accordingly.

The material properties of concrete and steel at elevated temperatures and at residual condition must be distinguished. When a material is at an elevated temperature, this means that it is in the "hot" state, which is representative of a material's state during a fire event. A material in its residual condition refers to a material that has returned to ambient temperatures after being heated to elevated temperatures (post-fire). The residual condition is most applicable for a post-fire scenario.

When testing materials to investigate material properties related to heat exposure, they are typically tested in the following ways:
- **Unstressed test:** Unloaded specimens are heated to a specified temperature until steady-state conditions are reached, then the specimen is loaded until failure while at an elevated temperature. *This is applicable to understanding the performance of specimens under low stresses and ultimate loading during a fire event.*
- **Stressed test:** Specimens loaded under service conditions are heated to a specified temperature until steady-state conditions are reached, then the specimen is loaded until failure while at an elevated temperature. *This is applicable to understanding the performance of specimens under service level stresses and ultimate loading during a fire event.*
- **Unstressed residual test:** Unloaded specimens are heated to a specified temperature until steady-state conditions are reached, then the specimen is cooled to ambient temperatures and is loaded until failure. *This is applicable to understanding the performance of specimens under low stresses during a fire event and ultimate loading after a fire event.*
- **Stressed residual test:** Specimens loaded under service conditions are heated to a specified temperature until steady-state conditions are reached, then the specimen is cooled to ambient temperatures and is loaded until failure. *This is applicable to understanding the performance of specimens under service level stresses during a fire event and ultimate loading after a fire event.*

A brief overview of literature reviewed in Phase I as well as new literature studied in Phase II is provided in the following sections of this chapter. For further details of the Phase I literature, reference the Phase I report of this project.

2.1 Concrete

With concrete being the most used material in modern tunnel engineering and structural engineering in general, the literature on concrete behavior at elevated temperatures and in its residual condition is extensive. With respect to fire, concrete has two primary advantages: it is incombustible and it has good thermal insulating properties (low thermal diffusivity) *(13)*. Concrete can also experience negative impacts from fire, such as spalling and losses in strength and stiffness *(9)*. This section focuses on literature relating to physical and chemical changes experienced in concrete with heat exposure.

2.1.1. Physical and Chemical Changes During Heating and Cooling of Concrete

Concrete that experiences elevated temperatures can undergo irreversible physical and chemical processes which can lead to damage and decay of mechanical properties *(9, 21)*. The main contributing factors to concrete damage are:
- Physical and chemical changes in the cement paste
- Physical and chemical changes in the aggregate
- Differential thermal strains between the aggregate and the cement paste
- Pore pressure build up from water.

The physical and chemical changes in cement paste and aggregate are summarized in Table 2.1. Differential thermal strains between aggregate and cement paste are a result of cement paste expanding in volume until temperatures ranging from 150°C (302°F) to 200°C (392°F) and contracting at higher temperatures while the aggregate continuously expands with temperature increase. This behavior can be attributed to chemo-physical responses occurring in the concrete constituents *(21)*.

Table 2.1: Physical and chemical changes in concrete with heat exposure adapted from *(26)*

Approximate Temperature °C (°F)	Physical & Chemical Changes in Cement Paste and Aggregate	Strength Changes
70 – 80 (158 – 176)	Dissociation of ettringite	Minimal to none
105 (221)	Water begins losing physical bond in aggregate and cement paste	Minimal to none
120 – 163 (248 – 325)	Gypsum begins decomposing	Minimal to none
250 – 350 (482 – 662)	Oxidation of iron compounds causes pink/red color in concrete and physical bond of water continues to diminish degrading cement paste further	Minimal
450 – 500 (842 – 932)	Dehydroxylation of portlandite	Intermediate
600 – 800 (1112 – 1472)	Carbon dioxide releases from carbonates, causing cracking and contraction of concrete	Intermediate to severe
800 – 1200 (1472 – 2192)	Thermal stresses cause disintegration of calcareous constituents causing white/gray color change and further cracking	Severe

2.1.2. Strength of Concrete at Elevated Temperatures and at Residual Conditions

Concrete can experience loss in strength from a fire event due to physical and chemical changes in concrete with heat exposure. How concrete strength will be influenced depends on factors including *(24, 27, 28)*:
- Maximum temperature of concrete
- Loading conditions/constraints
- Concrete mixture design
- Type of aggregate in concrete (siliceous, calcareous, etc.)

Notably, the strength of concrete at elevated temperatures and in its residual condition after cooling to ambient temperatures may be different than its initial strength after exceeding a threshold temperature.

2.1.2.1. Codes and Standards of Concrete Exposed to Heat

Design codes and standards produced by several organizations, including CEN (Eurocode) and the American Concrete Institute (ACI), feature equations and curves which describe the strength and stiffness of concrete both at elevated temperatures and in residual conditions.

As shown in Figure 2.1, the residual strength reduction of concrete is slightly greater than than when concrete is at elevated temperatures. The additional strength reduction in the residual state can be attributed to differences in thermal strains between aggregate and

cement paste *(21)*. Figure 2.2 illustrates that in general, concrete with siliceous aggregate has more severe strength reductions than concrete with calcareous aggregate.
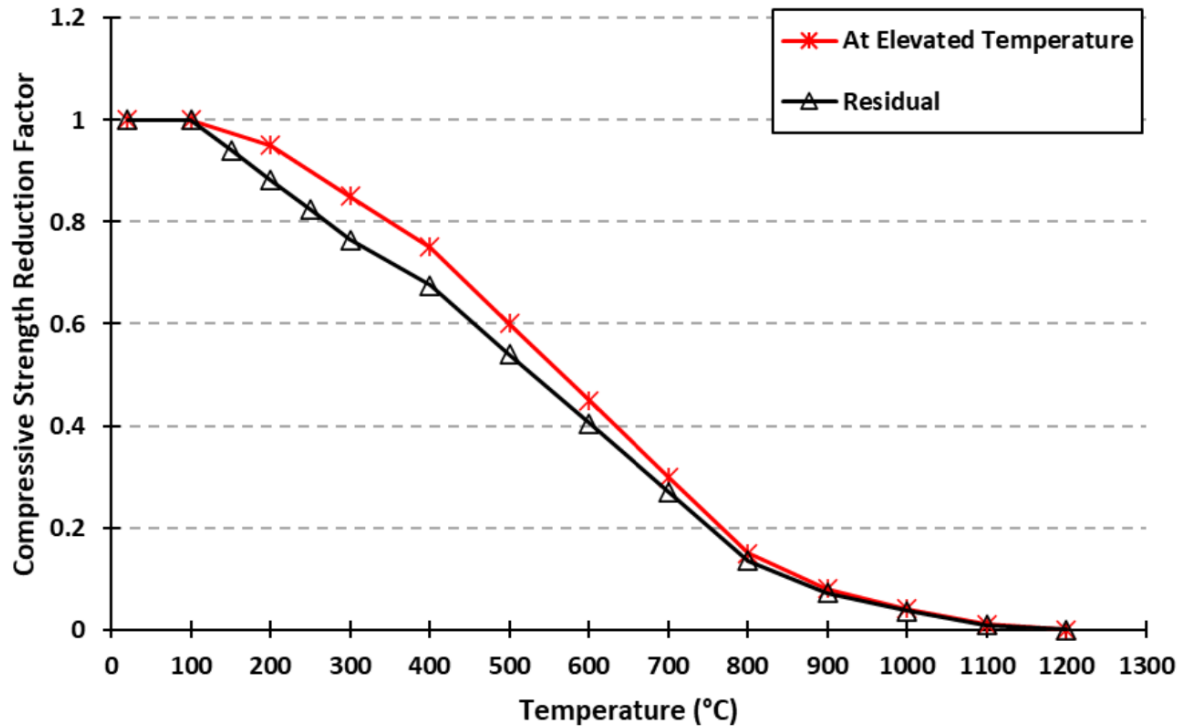
Figure 2.1: Comparison of reduction factors for compressive strength of concrete at elevated temperatures and in residual conditions per EN 1994 1-2 (1)
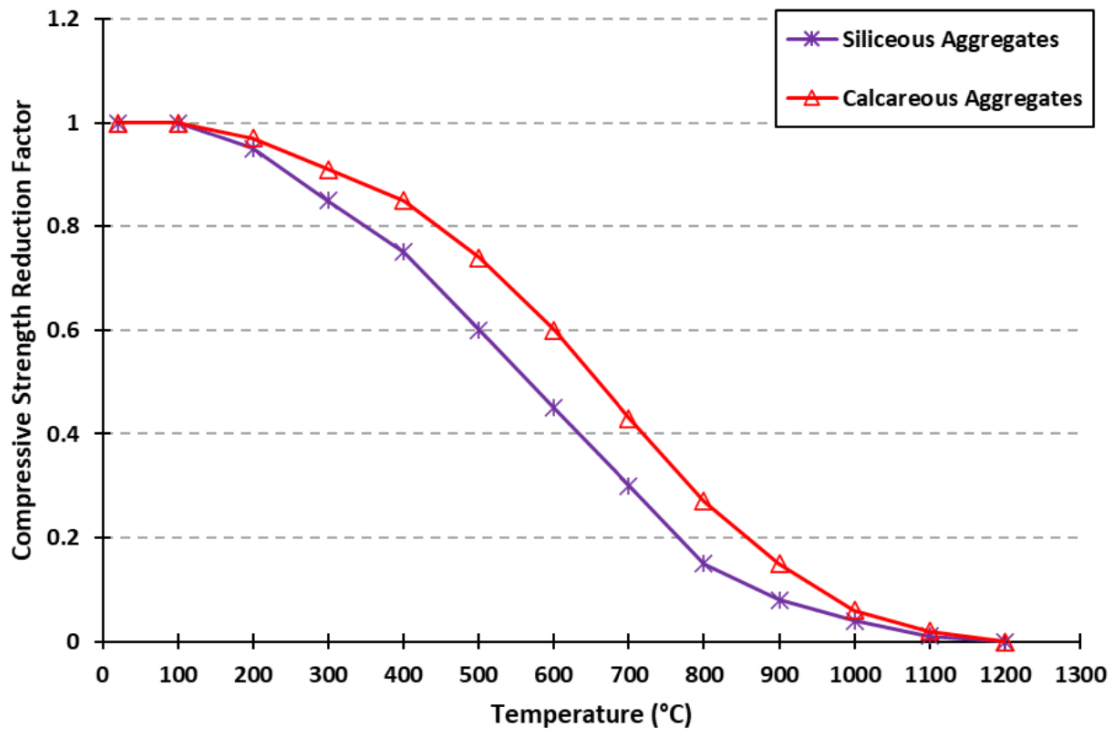
Figure 2.2: Compressive strength reduction factors for concrete at elevated temperatures per *EN 1992 1-2 (1)*

2.1.2.2 Experimental Studies of Concrete Exposed to Heat

A collection of experimental studies provides conclusions of concrete strength at elevated temperatures and at residual conditions. The Phase I report of this project further details experimental findings and differences between findings and codes.

2.1.3. Stiffness of Concrete at Elevated Temperatures and at Residual Conditions

The stiffness of concrete at elevated temperatures and at residual condition can be degraded. A study compiled results from several other studies and showed the relationship between the modulus of elasticity and maximum temperature *(27)*. The compiled data showed that in general, the stiffness of concrete will decrease with higher temperature exposure. Further detail may be referenced in the Phase I report of this project.

2.1.4. Thermal Spalling of Concrete

Thermal spalling of concrete is a phenomenon that can occur when concrete is brought to elevated temperatures and has been researched extensively *(29, 30, 31, 32, 33, 34, 35, 36, 37)*. Spalling of concrete has four general categories *(9)*:
- Explosive spalling
- Surface spalling
- Aggregate spalling
- Corner sloughing off

11

Explosive spalling is potentially the most significant type of spalling that is associated with heat exposure in regard to structural capacity of a member. Explosive spalling can lead to losses in strength and stiffness of a structural element as it can lead to alterations of a member's cross-section. The literature suggests that thermal stresses, pore pressure theory, or a combination of these are the likely causes of explosive spalling in heated concrete *(9)*. In general, many influences can contribute to spalling, making exact causes difficult to define for specific cases. Examples of factors contributing to spalling may include heating rate, thermal expansion rates of concrete member constituents, moisture content, maximum temperature, and other physical characteristics of the concrete *(9)*.

2.1.5. Thermal Gradient of Concrete Exposed to Heat

The thermal gradient experienced in a concrete element through its depth can be variable. Due to concrete's strong insulating properties, the outer surface of a concrete element may be at temperatures much higher than the internal temperatures depending on depth and time of exposure. Understanding the distribution of heat in a member can enhance post-fire analysis as the extent of damaged material may be more accurately assessed. This can help an inspector understand if reinforcement behind concrete cover may be damaged as well, as detailed in Section 2.2. The Phase I report of this project explains the distribution of temperatures in concrete slabs during ASTM E119 fire tests *(38)*. The data show that with an increase in depth, thermal penetration decreases. The data also show that with time, thermal penetration increases at a given depth.

2.2 Steel

Steel, companioning concrete as a common and essential structural material, is influenced by heat exposure. Many studies have been conducted to investigate the mechanical properties of steel at elevated temperatures and in residual conditions *(39, 40, 41, 42, 43, 44, 45, 46)*. Steel used in structures can be divided into four categories:

- Hot rolled structural steel
- Reinforcing steel
- Heat treated/cold worked or work hardened steel
- Prestressed steel

Because the topic of this report is primarily concrete structures, reinforcing and prestressed steel are of most relevance and are detailed in this report. For further detailing of other steel types, reference the Phase I report.

2.2.1. Strength and Stiffness of Steel at Elevated Temperatures and at Residual Conditions

The mechanical properties of reinforcing and prestressed steel, including both their strength and stiffness, are degraded when brought to elevated temperatures and at their residual conditions *(47)*. When steel is at elevated temperatures, it experiences a significant loss in strength. Figures 2.3 and 2.4 show both strength and stiffness for hot rolled and cold-worked

reinforcing steel, as well as for different types of prestressed steel. Notably, hot rolled and cold-worked reinforcing steel regain much of their strength once returned to ambient temperatures, however, this is not the case for prestressed steel. Prestressed steel experiences significant reductions in strength in its residual condition, as detailed in Table 2.2.
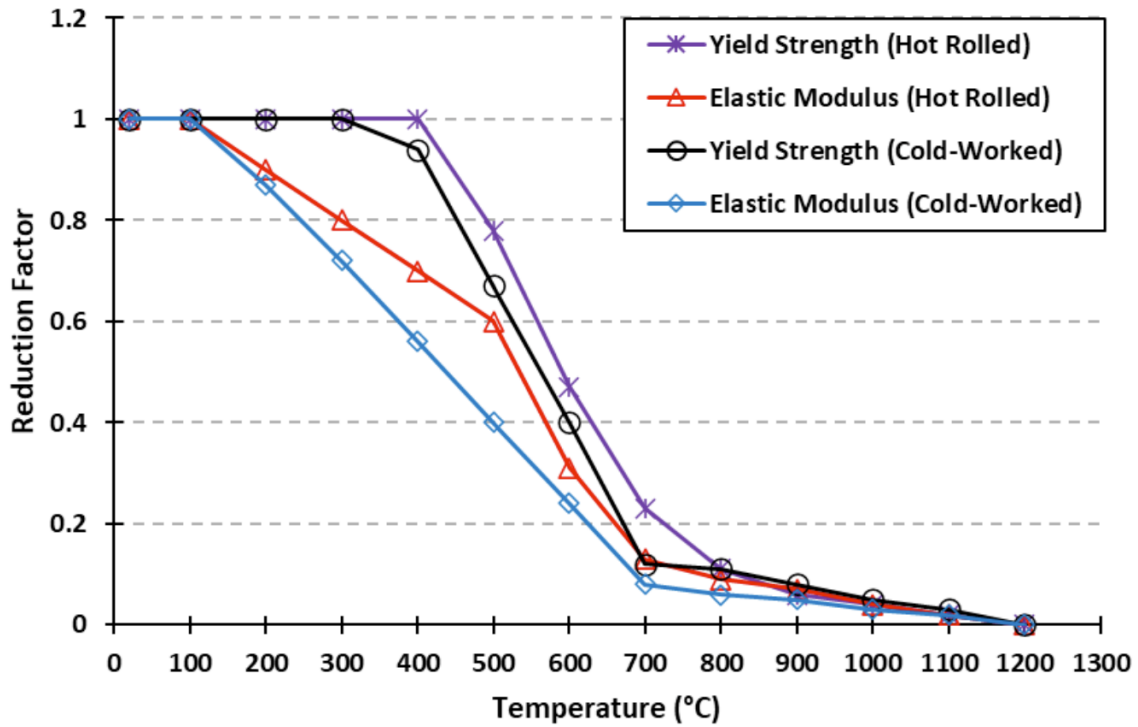
Figure 2.3: Comparison of yield strength and elastic modulus reduction factors for hot rolled and cold-worked reinforcing steel per EN 1992 1-2 *(1)*
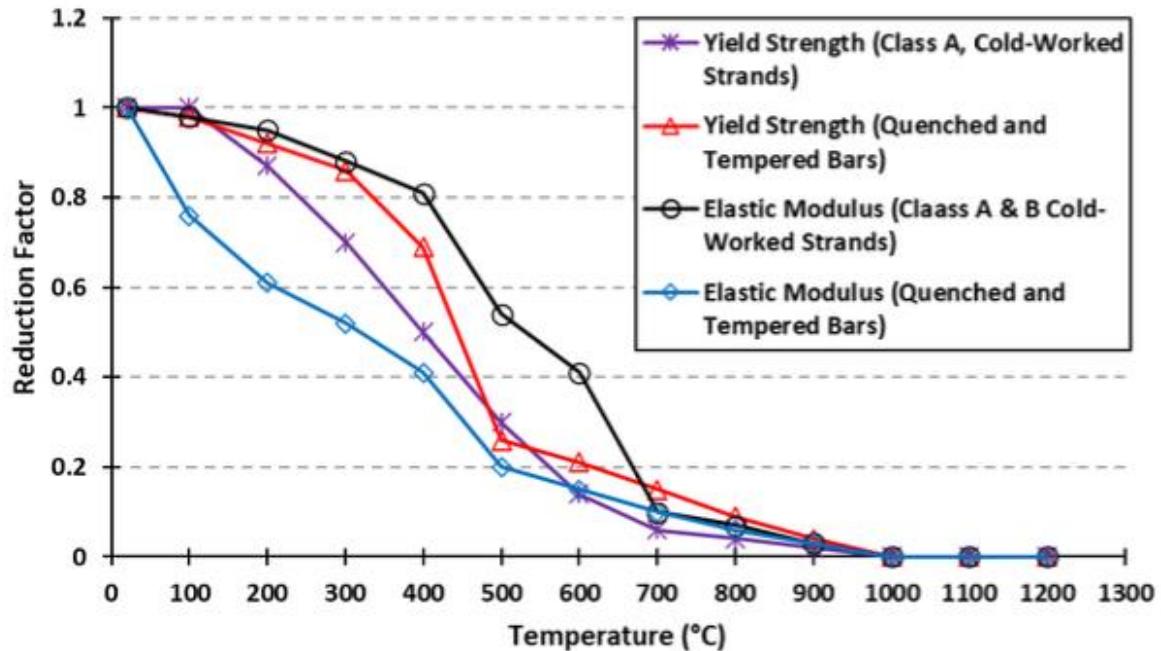
Figure 2.4: Comparison of yield strength and elastic modulus reduction factors or different types of prestressed steel per EN 1992 1-2 *(1)*

Table 2.2: Approximate reduction in ultimate capacity of prestressed steel with temperature exposure per *(39)*

Temperature °C (°F)	Approximate Reduction in Ultimate Capacity
300 (572)	5%
500 (932)	25%
700 (1292)	40%
900 (1652)	70%

2.3 Residual Bond Between Concrete and Steel

The residual bond between concrete and steel after heat exposure is of structural relevance. Steel that loses its bond with concrete can influence a structure negatively as composite behavior will degrade with this effect. The residual strength of the concrete and steel bond when returned to ambient conditions after being heated declines with the increase in maximum experienced temperature *(9, 48)*. Two bond failure modes, pullout failure and splitting failure, can occur as a result of bond strength decay *(49, 50)*. Generally, greater embedment length results in smaller decreases in residual bond strength, and increases in concrete cover can protect bond strength through concrete's natural insulative properties *(50, 51)*.

14

2.4 Effects of Fire on Structural Members

The Phase I report of this project details multiple studies conducted on structural members exposed to heat and their mechanical and physical responses *(52, 53, 54, 55, 56)*. Structural members referenced include reinforced concrete beams, high-strength reinforced concrete beams, super-high-strength reinforced concrete beams, and prestressed concrete box beams. A summary of results is as follows:

- Greater durations of heat exposure and higher exposure temperatures are generally associated with more significant losses in residual strength
- Spalling seemed to result in greater residual strength losses when compared with no spalling, depending on specimen geometry
- Specimens with high-strength concrete are more likely to experience spalling
- Residual strength losses varied greatly among studies. Specimens varied widely in dimensions and types, materials, and their experienced heating regimens

A new study focusing on structural members in fire has been published since Phase I that is of interest. This study focuses on large-scale reinforced concrete tunnel slabs and their response to heat exposure.

2.4.1. Hua et al. 2021 – Experimental study of fire damage to reinforced concrete tunnel slabs *(57)*

Hua et al. explored the effects of fire on concrete tunnel lining ceiling slabs. Parameters of interest included

- Concrete composition, specifically the presence/absence of polypropylene fibers
- The level of structural restraint from post-tensioned strands
- Fire intensity and duration

These parameters were adjusted to investigate crack patterns, spalling, discoloration, nondestructive testing, and deflection trends while specimens were at elevated temperatures and after returning to ambient conditions. Slabs were made with siliceous aggregate satisfying requirements of Type CA 1 and Type CA 2 as per NYSDOT. Four slab specimens measuring 1830mm x 2440mm x 300mm were constructed for experimental testing, three with polypropylene fibers (S1 – S3) and one without (S4). Twenty-seven concrete cylinders were cast with the slab specimens to investigate certain material characteristics of the concrete (both with and without polypropylene fibers).

Concrete cylinders were used to demonstrate the appearance and material properties of the concrete and can be referenced in the original paper. General results showed discoloration trends with increased temperature exposure as well as increased cracking. The residual strength of cylinders exposed to different levels of heat was also measured and can be referenced in Table 2.3. The experimental results of tests on the cylinders agree with those reported in other literature.

Table 2.3: Approximate residual strength reduction of concrete cylinders exposed to heat per *(57)*

Temperature °C (°F)	Approximate Residual Strength Reduction
200 (392)	15%
400 (752)	50%
600 (1112)	70%
800 (1472)	90%
900 (1652)	95%

All slab specimens were statically loaded on their top surface. A load was applied to each specimen at a rate of 3kN/sec until reaching 310kN. This is the equivalent weight of three meters of overburden soil with an additional surcharge load of 14kPa. Once the desired static load was achieved, it was held constant as heat loading began on the bottom surface of specimens covering an area of 1530mm by 1530mm. Three fire curve scenarios were applied to slab specimens. Temperatures described represent the gas temperature in the furnace that was used to heat the specimens. S1, S2, and S4 were tested under a fire curve scenario where a heating rate of 40°C/min (72°F/min) was applied until achieving 850°C (1562°F) which was then maintained for sixty minutes after which the furnace was shut off. Specimen S3 was first tested with a fire curve scenario where a heating rate of 40°C/min was applied to the specimen until reaching 700°C (1292°F) after which the furnace was immediately shut off. Specimen S3 was retested forty-eight hours later with a fire curve similar to the first, achieving 850°C (1562°F) and maintaining this temperature for sixty minutes, but using a slower ramp rate to achieve this target temperature. All fire scenarios were meant to be representative of different types of train fires in tunnels. Static loading was held on the specimens for four to six hours after heat testing was concluded (during the cooling phase of specimens).

Thermocouples measured temperatures at various depths and locations of the slabs to better understand the distribution of heat during testing. The temperature at which concrete residual capacity begins to show a decline in strength is 300°C (572°F). With regard to maximum depth from the heated face, specimen S1 achieved 300°C (572°F) at 25mm, S2 at 25mm, S3 at <5mm (test 3A), S3 at 25mm (test 3B), and S4 at 50mm. The authors explain that experimental temperatures among the tests were somewhat variable, as insulation was damaged after Test 3A. Also, spalling occurred in Test 4, influencing heat propagation as a section of the specimen's heated face spalled off and damaged the insulation. Interestingly, the specimen S4 in Test 4 was the only specimen without polypropylene fibers and it experienced spalling. Thermocouples were also used to measure rebar temperatures at the bottom (heated face) of the specimens and at the top (unheated face) of the specimens. Rebar temperatures never exceeded 300°C (572°F) on the bottom in all testing, and top rebar temperatures were consistently lower, only exceeding 100°C (212°F) in Test 4, most likely due to spalling.

All slabs began with a similar initial deflection trend which increased rapidly with heat exposure. A slow recovery of deflection was observed once heating was concluded and the cooling process began. The authors suggest that the applied static loads did not cause any

nonlinear behavior, so all residual displacements are due to heating once static loads were removed. All deflection trends among specimens are similar, and the differences in residual deflections depend on a number of factors in each test, which can better be referenced in the original study.

An investigation of the effectiveness of a Schmidt rebound hammer was conducted. The authors explain that rebound hammer tests generally showed more severe strength loss than the calculated strength loss. The calculated strength loss was based on an average strength loss of slabs after each fire test using the maximum temperature data at certain depths of concrete.

This page left blank intentionally

3.0 Existing Post-Fire Inspection Methods for Concrete Structures

The report for Phase I of this project explains existing post-fire inspection methods for concrete structures in detail. This chapter will serve as a brief summary of information covered in the Phase I report. For further detail, refer to the Phase I report.

Inspection of tunnels after a fire comes with many challenges. Damage can be severe, requiring extensive repairs depending on the fire intensity and duration. Also, many different materials and structural elements are present within tunnels, adding complexity to an inspector's understanding of the tunnel structural system. With pressure to reopen tunnels in efforts to reduce the interruptions of transportation networks, the need for rapid and safe inspection methods is necessary. Three categories of techniques are generally used for post-fire investigation:
- Visual inspection methods
- Nondestructive testing methods
- Laboratory testing methods

Visual inspection methods and nondestructive testing methods can be the most appropriate methods for rapid assessment.

3.1 Visual Inspection Methods

Visual inspection methods can be used to indirectly evaluate the structural condition of tunnel components. Visual inspection can give insight into fire intensity and duration, which can further be related to residual condition of materials and members.

3.1.1. Examination of Debris Materials

Debris material can be useful for evaluating post-fire conditions as it will be present in a post-fire scenario. Debris material can vary widely and has potential to be plentiful in a tunnel structure. This can include material that is part of the tunnel itself as both structural and/or nonstructural components and that present in vehicles or other objects in the tunnel. Table 3.1 illustrates a wide range of materials and their physical and visual conditions associated with a wide range of temperatures.

Table 3.1: Visual and physical conditions of materials associated with temperature adapted from *(22)*

Approximate Temperature °C (°F)	Substance/Material	Condition
100 (212)	Paint	Begins to deteriorate
120 (248)	Polystyrene	Collapse
120 – 140 (248 – 284	Polystyrene	Softens
150 – 180 (302 – 356)	Polystyrene	Melts
120 (248)	Polyethylene	Shrivels
120 – 140 (248 – 284)	Polyethylene	Softens and melts
130 – 200 (266 – 392)	Polymethyl methacrylate	Softens
250 (482)	Polymethyl methacrylate	Bubbles
100 (212))	PVC	Degrades
150 (302)	PVC	Fumes
200 (392)	PVC	Browns
400 – 500 (752 – 932)	PVC	Chars
200 – 300 (392 – 572)	Cellulose	Darkens
240 (464)	Wood	Ignites
250 – 400 (482 – 752)	Lead	Melts
400 – 420 (752 – 788)	Zinc	Melts
400 (752)	Aluminum (and alloys)	Softens
660 (1220)	Aluminum (and alloys)	Melts
500 – 600 (932 – 1112)	Glass	Softens
800 (1472)	Glass	Melts
900 – 950 (1652 – 1742)	Silver	Melts
900 – 1050 (1652 – 1922)	Brass	Melts
900 – 1000 (1652 – 1832)	Bronze	Melts
1000 – 1100 (1832 – 2012)	Copper	Melts
1100 – 1250 (2012 – 2282)	Cast iron	Melts
1371 – 1540 (2500 – 2800)	Steel	Melts

3.1.2. Concrete Color Change Due to Heat

As concrete structures are the primary topic of this report, understanding the color change in concrete that can result from heat exposure is critical. One study was able to produce high quality images of concrete, mortar, and cement paste at different temperatures ranging from 20°C (68°F) to 1000°C (1832°F) and can be referenced in the Phase I report of this project *(58)*. That study used normal-strength and high-strength concrete with CEM II/A-V 42,5 R cement and natural riverbed aggregates. It found that concrete, mortar, and cement paste all behaved similarly in regard to appearance with heat exposure. At temperatures of 300°C (572°F) – 600°C (1112°F), specimens turned pink/red in color, and color change was more prominent at the latter end of the temperature range. At 700°C (1292°F) and 800°C (1472°F), specimens began to turn gray in color. At 900°C (1652°F) and 1000°C (1832°F), specimens lightened in color significantly. The pink/red discoloration in concrete can be attributed to the

oxidation of iron compounds (ferric salts) in aggregates, and the gray/white discoloration in concrete is often associated with calcination of calcareous constituents *(26)*.

Aggregate type has been found to influence color change in concrete. One study compared concrete with aggregate composed of

- Siliceous gravel
- Crushed limestone
- Crushed granite
- Lytag

This study found that siliceous gravel showed the most significant color changes with heat exposure and that the color change with other types of aggregate was less observable *(59)*.

3.1.3. General Visual Damage Classification

In an effort to understand the residual condition of structural members, classification systems to evaluate the extent of concrete damage have been established *(26, 60)*. Examples of these systems can be referenced in Phase I of this report. The purpose of this report is to establish a similar system, adapted for MassDOT-owned tunnels specifically, that may be useful to others.

3.2 Non/Partially Destructive Testing Methods

Some non/partially destructive testing methods can be used to more directly evaluate the condition of a structure after a fire event. A wide variety of these methods exist, with their usage and practicality being variable. Figure 3.1 shows testing techniques and their applications. The report for Phase I should be referenced for further detail.

Test Type	Method	Material	
		Concrete	**Steel**
Nondes-tructive	Visual inspection	✓	✓
	Hammer soundings	✓	✓
	Rebound hammer	✓	
	Ultrasonic testing	✓	✓
	Magnetic particle imaging		✓
	Breakout/drilling	✓	
Partially destructive	Load test	✓	✓
	Petrographic examination	✓	
	Metallography		✓
	Hardness test		✓
	Compressive strength	✓	
	Tensile strength		✓

Figure 3.1: Non/partially destructive inspection methods *(60)*

This page left blank intentionally.

4.0 Methods of Testing for Nonstructural Components

In this research, both structural and nonstructural components of tunnels were studied. This section details methods of testing nonstructural components, including the equipment used, different types of heat loading regimens, and various types of test setups.

4.1 Equipment

Heat testing utilized three Watlow Ceramic 2030 Style Heaters (Figure 4.1). The heating elements of the heaters are capable of reaching temperatures of 1100°C (2021°F). A Watlow F4T temperature controller and data logging system (Figure 4.2) was used to supply power to the heaters and to record heat data. Heat data was recorded using type K thermocouples (TC) (Figure 4.3).
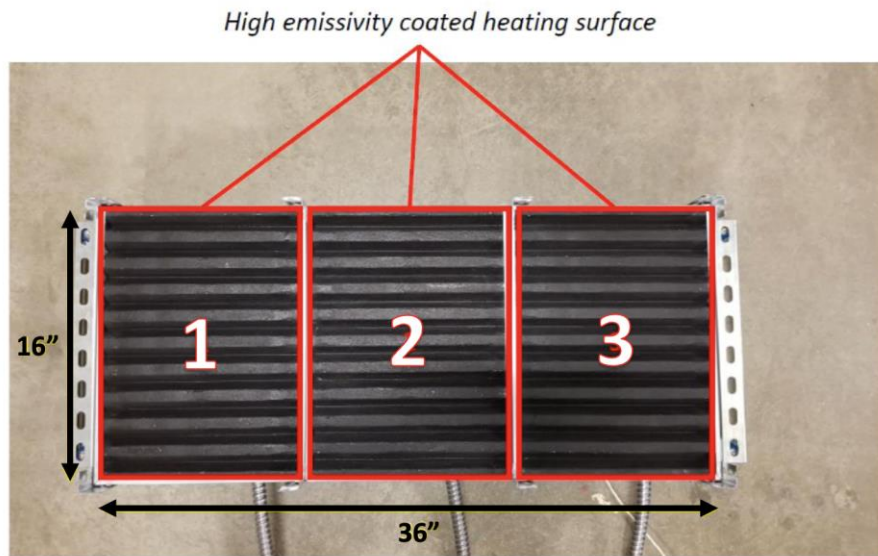
Figure 4.1: Watlow ceramic 2030 style heaters *(1)*

Figure 4.2: F4T temperature controller and data logging system

Temperature Probe   Connection Port
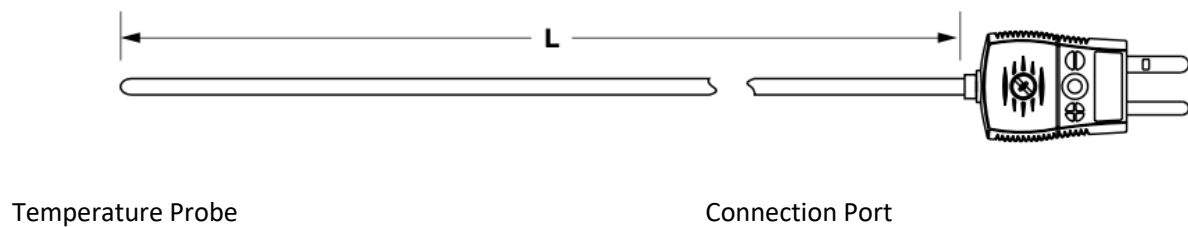
Figure 4.3: Type K thermocouple schematic *(61)*

4.2 Heat Loading Regimens

When heating specimens, two main types of heat loading regimens were followed:
- Direct loading
- Stepped loading

Direct loading (Figure 4.4) is the process of applying heat to a specimen to achieve a single target temperature. The rate of heat loading when ramping to a specified target temperature and the duration that the target temperature is maintained can vary depending on the goal of the testing.
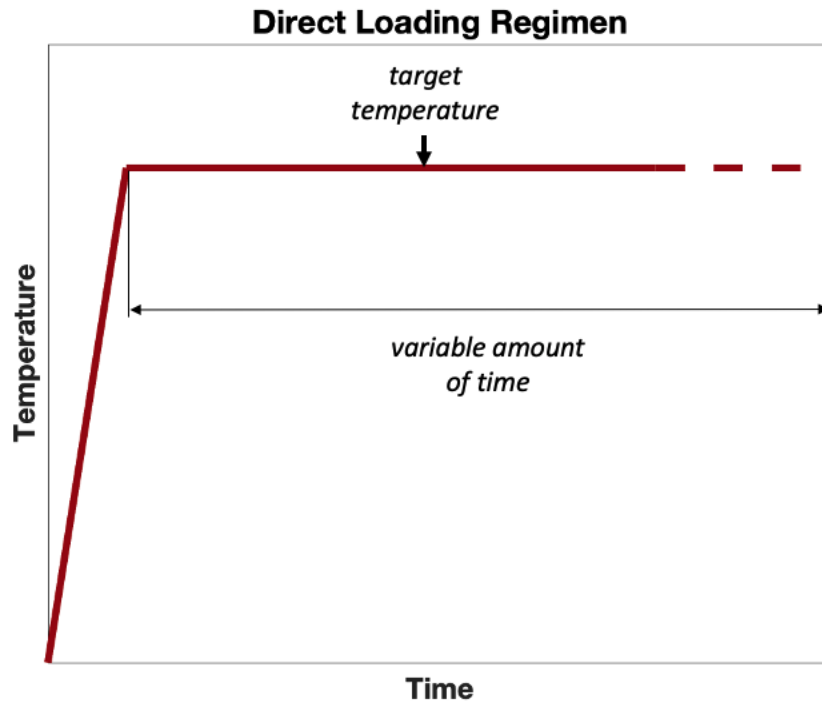
Figure 4.4: Direct heat loading regimen

Stepped loading (Figure 4.5) is the process of applying heat to a specimen to achieve multiple target temperatures in a single test. The rate of heat loading when ramping to a specified target temperature, the duration that the target temperature is maintained, and the number of steps can vary depending on the goal of the testing.
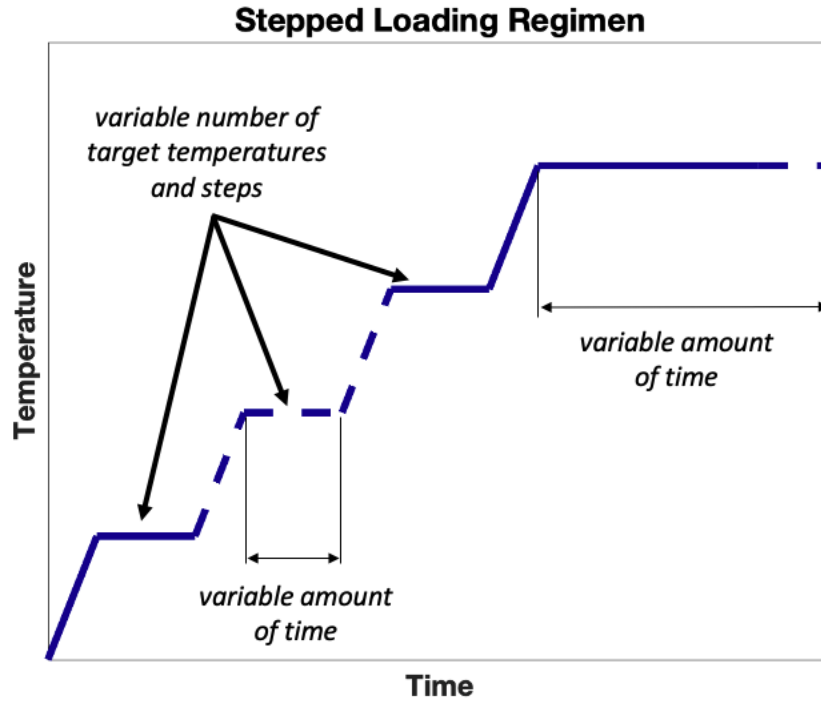
Figure 4.5: Stepped heat loading regimen

By applying both direct and stepped heat loading to specimens, a comparison between the two methods can be established to understand how different heating regimens can influence specimens. In addition, stepped loading can allow for significantly more information to be obtained from a single test, but prior loading steps may influence later loading step results.

4.3 Test Setup

The test setups for investigating nonstructural components of structures varied depending on the specimens being investigated. In order to use the Watlow heaters effectively, a unique furnace-like chamber was constructed for each test with the use of firebricks and fiber insulation roll material. Together, these materials provided the insulative properties necessary for the desired testing. The location of thermocouples also varied depending on the test being conducted.

5.0 Testing of Nonstructural Components

Heat testing of a wide range of specimens took place to investigate both visual changes and mechanical properties associated with heat exposure. Specimens can be categorized into two groups:

1. Nonstructural components of tunnels
2. Structural components of tunnels

This section focuses on the testing of the nonstructural components of tunnels. The purpose of testing nonstructural components of tunnels was to create an extensive collection of data on visual information that may be used by an inspector to identify aspects of fire intensity and duration in a post-fire event.

5.1 Nonstructural Utilities

Nonstructural utilities that are common elements of MassDOT-owned tunnels were tested. These elements include

- Phenolic Conduits
- Aluminum Wireways
- A light Fixture

5.1.1. Phenolic Conduit

The primary use of phenolic conduits is to provide a closed pathway for wires. Phenolic conduit is a common nonstructural tunnel component in some MassDOT-owned tunnels. In order to investigate the response of phenolic conduit exposed to elevated temperatures, multiple testing regimens were applied to specimens. Phenolic conduit specimens used in testing measured 2 inches in diameter and ¼ inch in wall thickness.

5.1.1.1 Phenolic Conduit Test 1

First, a general visual inspection of the conduit during and after a fire scenario was of interest and investigated. Figure 5.1 shows visual changes in a piece of phenolic conduit exposed to different levels of heat. The temperatures denoted express the air temperature at the height and location of the phenolic conduit specimen. The outer surface of the phenolic conduit is of most interest when considering visual responses to heat, as the outer surface would be directly exposed to a fire in a tunnel and is most easily observable by an inspector. A stepped heat loading procedure was applied to the specimen.

When analyzing visual data of the phenolic conduit specimen, it was observed that temperatures of 300°C (572°F) and 400°C (752°F) did not significantly influence the outer surface of the phenolic conduit. At the temperature 500°C (932°F), the outer surface began to show color changes as the black resin started burning off, creating a speckled pattern and

introducing a gray color shift. Temperatures of 600°C (1112°F) and 700°C (1292°F) showed a full transition of the outer surface of the phenolic conduit to a gray/silver color. The gray/silver color was maintained once the conduit returned to ambient temperature conditions.
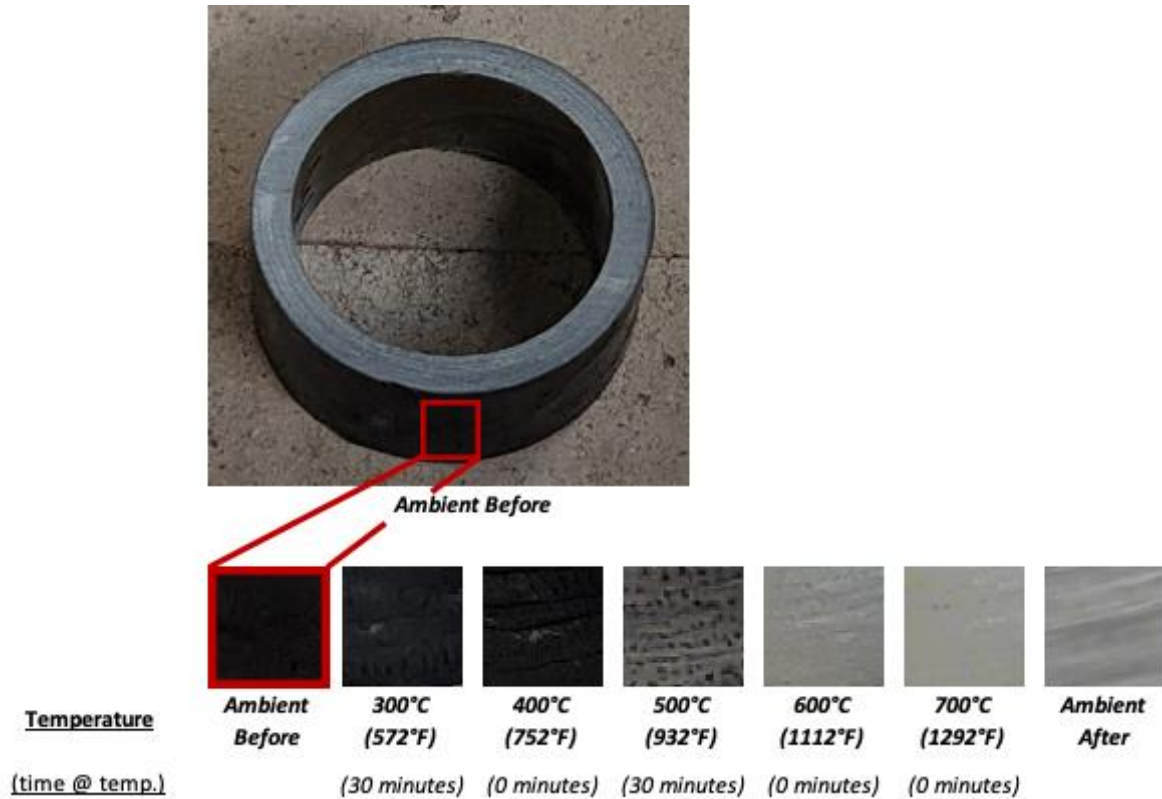
Figure 5.1: Phenolic conduit visual response to stepped heat loading

5.1.1.2 Phenolic Conduit Test 2

Also of interest was the distribution of heat inside and around phenolic conduit in a scenario more accurately representing its use in a tunnel structure. A piece of phenolic conduit was placed to span supports and set up in a furnace-like chamber with insulative material and firebrick (Figures 5.2 and 5.3). The ends of the conduit were located outside of the chamber so that the ends of the conduit would not be exposed to direct heat. The ends of the conduit were also filled with insulation to stop airflow inside the conduit that would influence the conditions of internal temperature measurement. The described setup is intended to imitate a fire scenario where a section of conduit is directly exposed to a fire while supported outside the heated region without significant interior air flow that could cool the inside of the conduit.
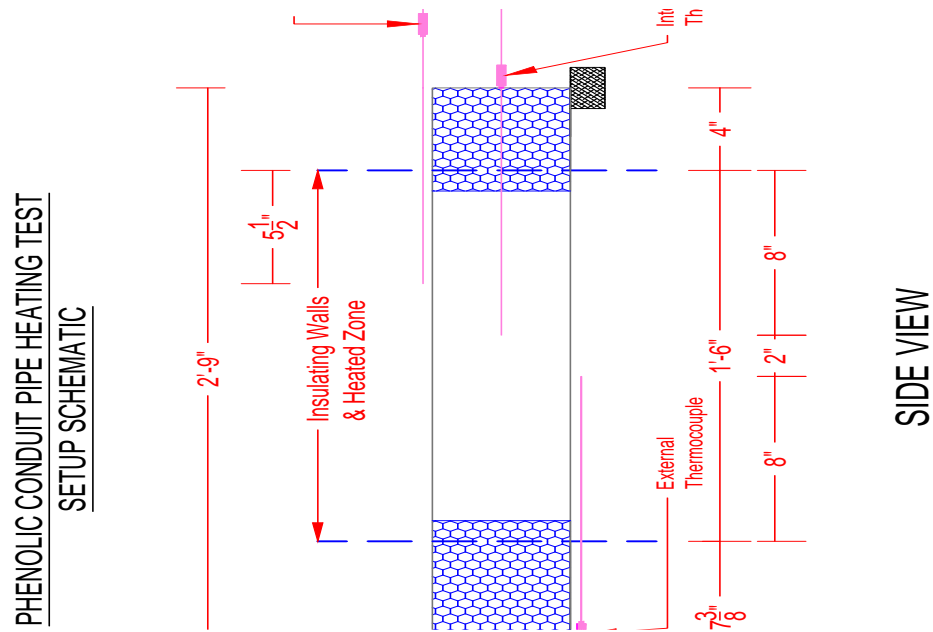
Figure 5.2: Phenolic conduit test schematic (not including firebrick/insulative fiber roll)

Figure 5.3: Phenolic conduit test setup (a) heating chamber open (b) heating chamber closed

During heat testing of the phenolic conduit, the air temperature at the top surface of the phenolic conduit was brought to a target temperature of 600°C (1112°F) and maintained for two hours. A thermocouple was also positioned to record the air temperature at the bottom surface of the phenolic conduit. The bottom thermocouple showed that for the given test setup, the bottom surface of the conduit was exposed to temperatures that were always lower than those of the top surface (Figure 5.4). A thermocouple placed inside the conduit showed that a steady state condition of approximately 100°C (212°F) after about one hour was reached and maintained for the duration of the test. Temperature-time data can be referenced in Figure 5.4. Figure 5.5 shows the visual results from the test, which agree with the visual results presented in Figure 5.1.
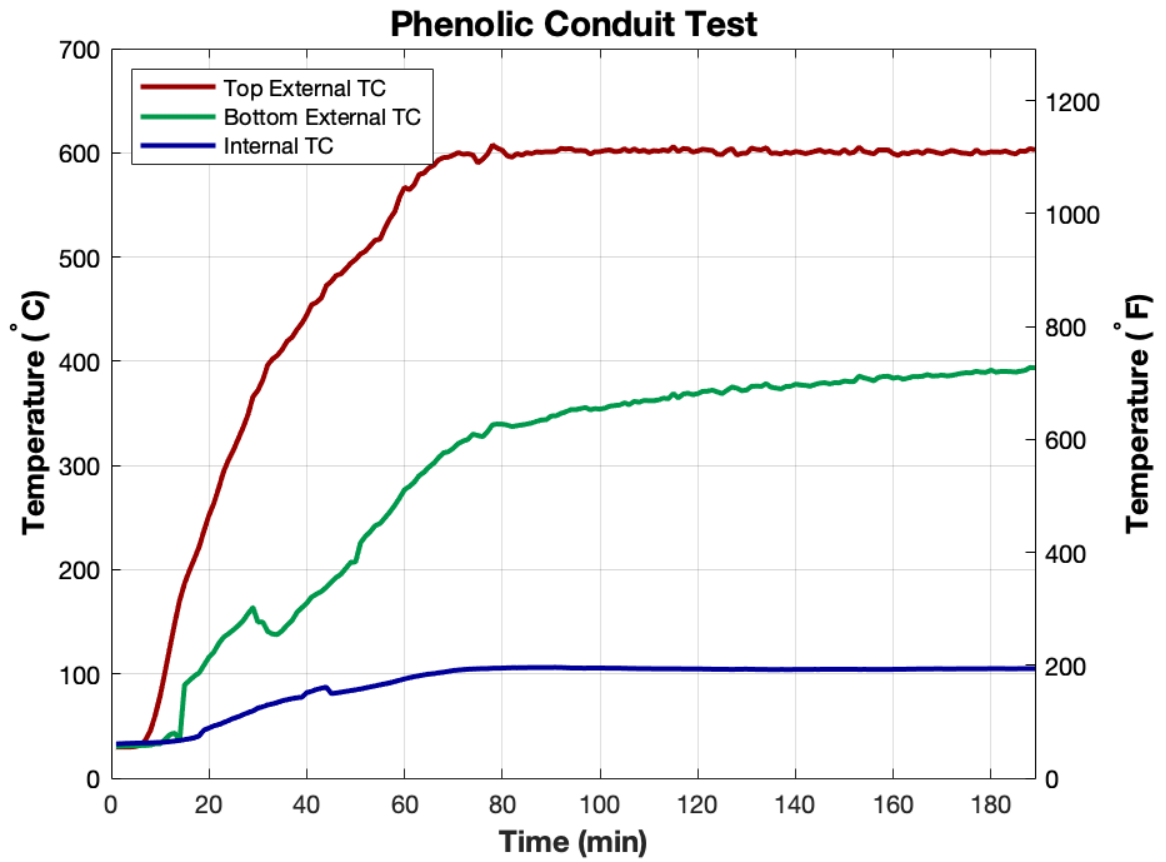
Figure 5.4: Phenolic conduit test temperature-time curve
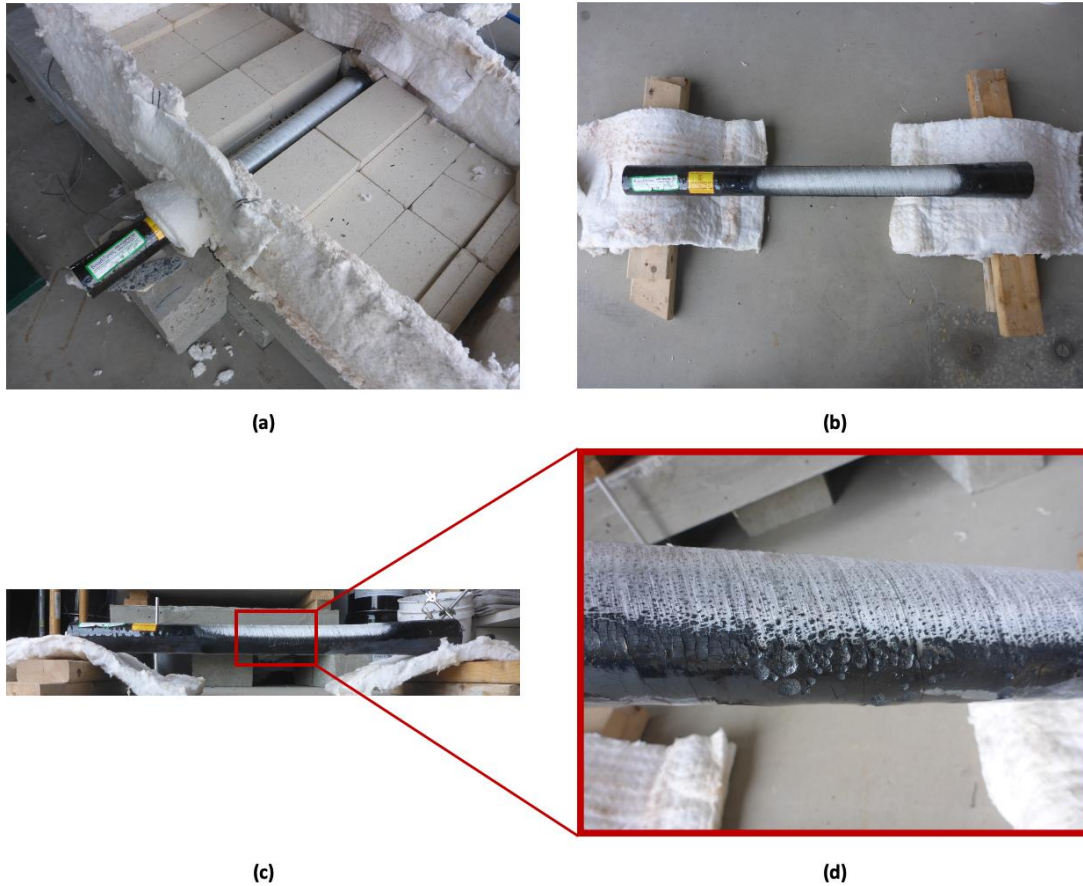
Figure 5.5: Phenolic conduit appearance after heat loading (a) in open heating chamber (b) top view (c) side view (d) close up side view, top exposed to 600°C (1112°F) and bottom exposed to 400°C (752°F)

5.1.2. Aluminum Wireway

Aluminum wireways serve as a support for wires travelling through a tunnel structure. Aluminum wireways are a common nonstructural component in some MassDOT-owned tunnels. In order to investigate the response of aluminum wireways exposed to heat, multiple tests with different loading regimens were applied to aluminum wireway specimens.

5.1.2.1 Aluminum Wireway Test 1

A piece of an aluminum wireway was directly heat loaded to investigate the specimen's response at elevated temperatures (Figure 5.6). The specimen was exposed to 700°C (1292°F) conditions for two hours and showed significant signs of discoloration and deformation.

Temperature (time @ temp.)	Visual Condition	Observations
Ambient Before		
700°C (1292°F) *(120 minutes)*		*-Discoloration of specimens (yellow in color)* *-Melting of aluminum*

Figure 5.6: Aluminum wireway physical response to direct heat loading

5.1.2.2 Aluminum Wireway Test 2

A second piece of an aluminum wireway was used to investigate the physical response of the aluminum subject to a stepped heat loading regimen (Figure 5.7). This specimen was

exposed to temperatures ranging from 300°C (572°F) to 900°C (1652°F) in intervals of 100°C (180°F). At 300°C (572°F), the exterior paint began to darken. At 400°C (752°F), the paint continued to discolor and began to bubble. At 500°C (932°F), the specimen's paint returned to a lighter shade. At 600°C (1112°F), yellow discoloration of the paint began. At 700°C (1292°F), the paint was yellow and the specimen was melting, undergoing significant deformations. At 800°C (1472°F) deformations continued. At 900°C (1652°F) no difference was observed from the previous heat step. Visual results can be referenced in Figure 5.7. Notably, the wireway specimen at 800°C (1472°F) and 900°C (1652°F) in the stepped loading test is comparable to the wireway specimen at 700°C (1292°F) in the direct loading test. This is most likely a result of the deformation being a function of time after reaching its melting point of 660°C (1220°F).

Temperature (time @ temp.)	Visual Condition	Observations
Ambient Before	~10" ~1"	
300°C (572°F) *(30 minutes)*		*-Initial color change*
400°C (752°F) *(0 minutes)*		*-Color change continues*
500°C (932°F) *(30 minutes)*		*-Color change continues*
600°C (1112°F) *(0 minutes)*		*-Color change continues*
700°C (1292°F) *(30 minutes)*		*-Color change continues* *-Melting of aluminum*
800°C (1472°F) *(0 minutes)*		*-Melting of aluminum continues (red lighting due to heaters)*
900°C (1832°F) *(0 minutes)*		

Figure 5.7: Aluminum wireway physical response to stepped heat loading (lighting is not consistent between pictures)

5.1.2.3 Aluminum Wireway Test 3

Small pieces of an aluminum wireway were used to investigate visual changes of the wireway at elevated temperatures and in its residual condition (Figure 5.8). Five pieces of aluminum wireway were step heated, exposed in steps to temperatures of 300°C (572°F), 400°C (752°F), 500°C (932°F), 600°C (1112°F), and 700°C (1292°F), with pieces being removed at each heat step. Specimens were visually inspected immediately after being removed and thirty minutes after being removed (once cooled to ambient temperatures). With exposure to temperatures of 400°C (752°F) and above, specimens showed discoloration trends immediately after being removed,. A temperature of 400°C (752°F) caused an initial darkening of the paint, 500°C caused graying of the paint, 600°C (1112°F) caused a lighter shading of the paint, and 700°C (1292°F) caused a yellow discoloration of the paint. Thirty minutes after being removed, all specimens except for the specimen removed at 700°C (1292°F) looked the same as they had upon removal. The specimen removed at 700°C (1292°F) changed from yellow to white when cooled to ambient temperature.
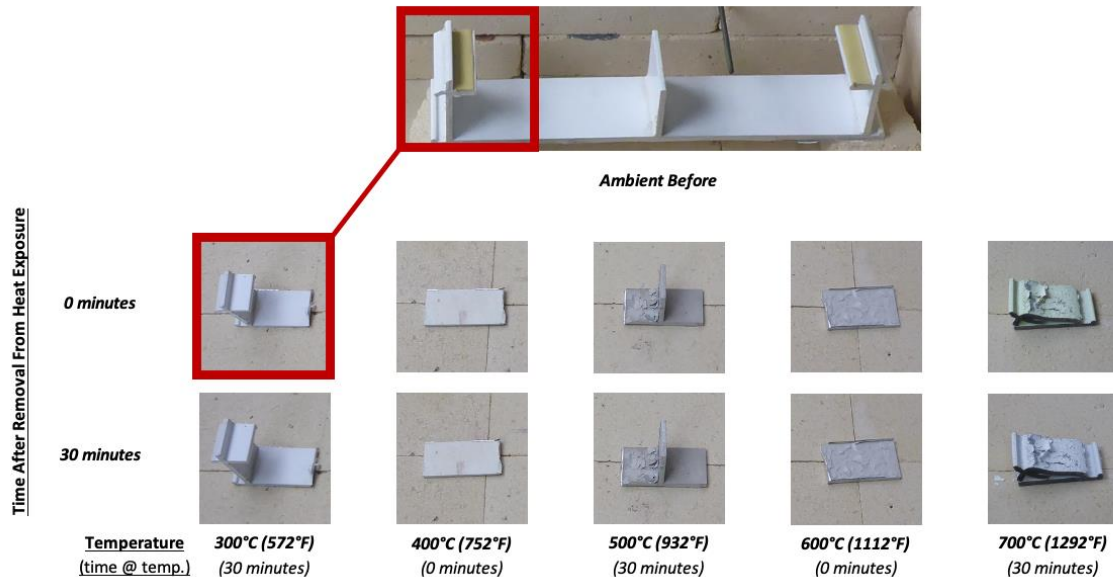
Figure 5.8: Aluminum wireway visual and physical response to stepped heat loading

5.1.3. Light Fixture

Light fixtures are a common utility found in MassDOT-owned tunnels. Since light fixtures are a common utility found in tunnel structures, they can potentially be a common visual indicator of temperatures reached in a fire if present. Table 5.1 provides a generic list of materials that may be found in a commercial LED light fixture and their associated melting points.

Table 5.1: Generic materials found in commercial LED light fixtures and associated melting points

Material	Potential Use	Approximate Melting Temperature °C (°F)
Glass (polycarbonate)	Light refractor	288 – 316 (550 – 600)
Glass (borosilicate)	Light refractor	1648 (3000)
Steel	Screws, latches, and mounting brackets	1371 – 1540 (2500 – 2800)
Brass	Wire insertion point plug	930 (1710)
Aluminum (A360 alloy)	Body/casing	660 (1221)
Hard plastic	Reflectors and miscellaneous electronics	120 – 170 (248 – 338)
Soft plastic	Wire tubing	120 – 170 (248 – 338)
Thermoset powder coating	Paint for body/casing	95 – 188 (203 – 370)

A light fixture specimen was tested under a stepped heat loading regimen. The light fixture was step loaded from 300°C (572°F) to 700°C (1292°F) in intervals of 100°C (180°F). The glass lens of the specimen was monitored for visual and physical chnages (Figure 5.9). At 500°C (932°F), initial discoloration of the lens began. At 600°C (1112°F) the lens was discolored significantly, covered in smoke residue. At 700°C (1292°F) smoke residue continued to build up. Once cooled to ambient temperature, the lens showed no visual changes from the last elevated temperature. The painted aluminum body of the light fixture was also monitored (Figure 5.10). It was observed that at 400°C (742°F), the paint of the body began to discolor. The paint began charring at 500°C (932°F) and after being held at 500°C (932°F) for thirty minutes it began to flake. At 600°C (1112°F), discoloration of the paint continued. At 700°C (1292°F), some of the aluminum began to deform as it exceeded its melting point of 660°C (1220°F). While returning to ambient temperature during the first hour, the paint of the body shifted slightly in color.
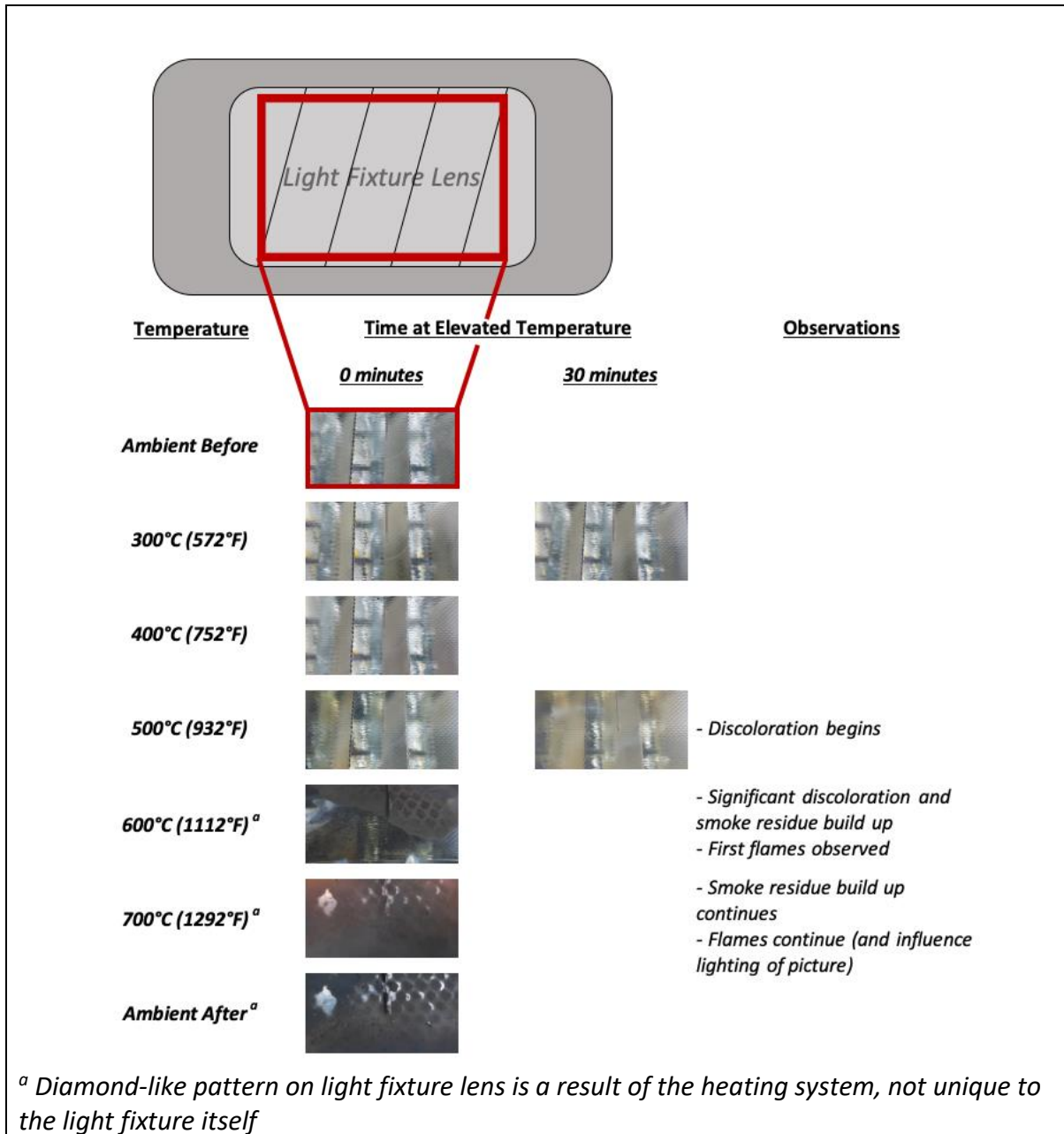
Figure 5.9: Light fixture lens visual response to stepped heat loading
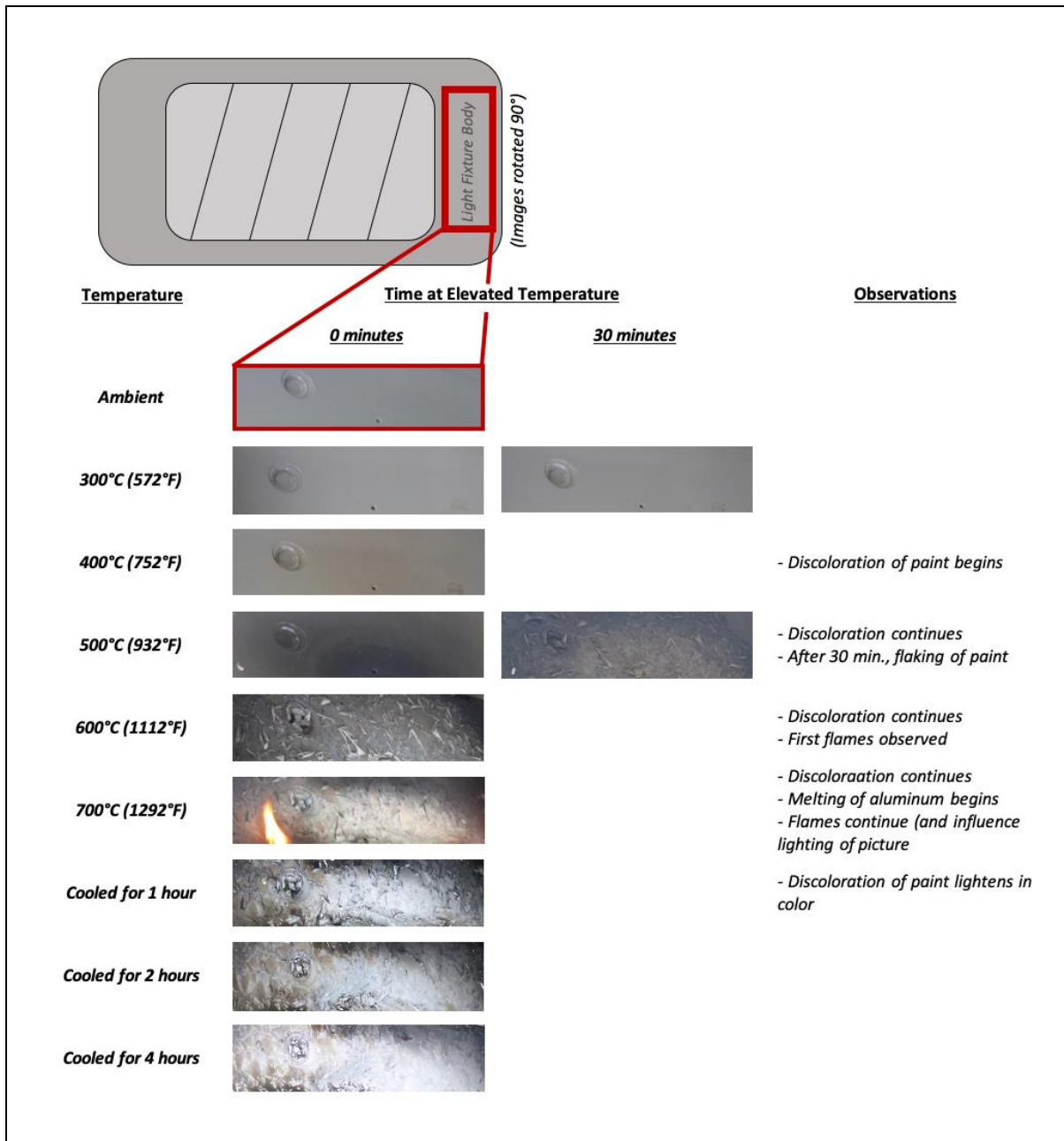
Figure 5.10: Light fixture body visual response to stepped heat loading

5.2 Nonstructural Miscellaneous

Many miscellaneous materials were tested to investigate their visual response to heat exposure. These materials consisted of
- Steel
- Aluminum
- Concrete

The types of steel, aluminum, and concrete varied in properties such as cross-sectional geometry, finish/outside coating, and specimen composition.

5.2.1. Nonstructural Galvanized Steel

Galvanized cold formed steel specimens were subjected to direct and stepped loading procedures. Galvanized specimens measured approximately 6 in. in length, 4 in. in width, 1.5 in. in height, and varied in thickness, measuring 33 mils, 54 mils, and 97 mils (where 1 mil is 1/1000 of an inch). Galvanized cold formed steel showed differences in visual response depending on the specimens' thicknesses and heat loading regimens. In general, it was observed that the galvanized coating on thinner specimens burned off at lower temperatures than that on thicker specimens. This resulted in thinner specimens experiencing discoloration and charring at lower temperatures. It also appears that temperature duration can have an influence on appearance, when comparing heat loading procedures. Detailed visual observations can be referenced in Figures 5.11, 5.12, and 5.13.

Figure 5.11 shows the results of a stepped loading test up to 700°C (1292°F) that was conducted on three galvanized specimens of different thicknesses. It was observed that the thinnest specimen (33 mil) began dulling at 300°C (572°F). The 54-mil and 97-mil specimens began dulling at a higher temperature of 500°C (932°F). Discoloration began in the 33-mil specimen at 400°C (752°F) and in the other two specimens at 700°C (1292°F). Notably, the discoloration in all specimens changed between zero minutes at 700°C (1292°F) and thirty minutes at 700°C (1292°F).

Figure 5.12 presents the results of another test that was conducted with 54-mil and 97-mil specimens which involved a stepped loading procedure to 900°C (1652°F). The specimens showed visual trends identical to the previously presented results up to 700°C (1292°F). At 800°C (1472°F), the specimens began to glow red as a result of the extreme heat. At 900°C (1652°F), the specimens showed significant charring.

Figure 5.13 summarizes the results from specimens that were directly heated to 700°C (1292°F) and held there for 120 minutes to see if direct heating and the duration of the temperature hold caused differences in the visual results. Notably, the time duration did not seem to have a significant influence on the appearance of specimens at this temperature. Also observed in this test was that the appearance of the specimens changed once they returned to ambient temperature conditions.

Temperature (time @ temp.)	Visual Condition			Observations
	33 mil[a]	54 mil[a]	97 mil[a]	
Ambient Before	~4" ~6"			
300°C (572°F) (30 minutes)				-Initial dulling of 33-mil specimen
400°C (752°F) (0 minutes)				-Initial discoloration of 33-mil specimen
500°C (932°F) (30 minutes)				-Dulling of all specimens
600°C (1112°F) (0 minutes)				-Discoloration of 33-mil specimen continues (yellow in color)
700°C (1292°F) (0 minutes)				-Discoloration of all specimens (yellow in color)
700°C (1292°F) (30 minutes)				-Discoloration of all specimens continues, with darker colors showing charring of specimens

[a]mil refers to the thickness of the specimen, in 1/1000 of an inch

Figure 5.11: Galvanized steel of different thicknesses response to stepped heat loading

Temperature (time @ temp.)	Visual Condition		Observations
	54 mil[a]	97 mil[a]	
Ambient Before			
300°C (572°F) (30 minutes)			
400°C (752°F) (0 minutes)			
500°C (932°F) (30 minutes)			-Dulling of specimens
600°C (1112°F) (0 minutes)			
700°C (1292°F) (30 minutes)			-Discoloration of specimens (yellow in color)
800°C (1472°F) (0 minutes)			-Discoloration of specimens continues (darker in color)
900°C (1832°F) (0 minutes)			-Charring of specimens

[a]mil refers to thickness of specimen, in 1/1000 of an inch

Figure 5.12: Galvanized steel of different thicknesses response to stepped heat loading

Temperature (time @ temp.)	Visual Condition		Observations
	54 milᵃ	**97 milᵃ**	
Ambient Before			
700°C (1292°F) (120 minutes)			*-Discoloration of specimens (yellow in color)*
Ambient After			*-Discoloration changes when specimens return to ambient temperatures*

ᵃmil refers to thickness of specimen, in 1/1000 of an inch

Figure 5.13: Galvanized steel of different thicknesses response to direct heat loading

5.2.2. Nonstructural Steel

Six miscellaneous steel specimens were step loaded to 700°C (1292°F) (Figure 5.14) and showed differences in appearance with temperature increase. Duplicate specimens were directly loaded to 700°C (1292°F) (Figure 5.15) and showed no differences in comparison to the specimens subjected to the stepped loading procedure, with exception of specimen S6 which showed different discoloration trends. Detailed visual observations can be found in Figures 5.14 and 5.15. Dimensions and physical properties of the miscellaneous steel specimens can be found in Table 5.2.

Table 5.2: Miscellaneous steel specimens and associated physical properties

Cross-Sectional Shape/Geometry (Specimen Nomenclature)	Length (in)	Width (in)	Thickness (in)	Finish/Outside Coating
Hollow Square (S1)	4	0.75	0.075	N/A
Solid Rectangle (S2)	4	1.15	0.40	N/A
Hollow Circle (S3)	4	1.50	0.25	Stainless
Hollow Circle (S4)	4	1.40	0.25	Rusted
Hollow Triangle (S5)	4	0.50[a] 0.60[b]	0.08	N/A
Angle (S6)	4	1.00[a] 1.60[b]	0.07	Black paint

[a] Some specimens have two width dimensions – this is the shorter of the two
[b] Some specimens have two width dimensions – this is the longer of the two

Temperature (time @ temp.)	Visual Condition	Observations
Ambient Before		-Specimens referred to from left to right as S1, S2, S3, S4, S5, and S6
300°C (572°F) (30 minutes)		-S2: Charring -S3: Slight browning -S4: Slight charring -S6: Darkening of paint
400°C (752°F) (0 minutes)		-S3: Significant browning -S5: Dulling -S6: Minor bubbling of paint
500°C (932°F) (30 minutes)		-S6: Significant flaking and discoloration of paint
600°C (1112°F) (0 minutes)		-S1: Flaking of exterior -S2: Significant charring -S3: Slight charring -S5: Color darkens
700°C (1292°F) (30 minutes)	**No Additional Changes**	

Note: If a specimen is not shown at specific time step, no change occurred

Figure 5.14: Miscellaneous steel response to stepped heat loading

Temperature (time @ temp.)	Visual Condition	Observations
Ambient Before		*-Specimens referred to from left to right as S1, S2, S3, S4, S5, and S6*
700°C (1292°F) (120 minutes)		*-S1: Flaking of exterior* *-S2: Significant charring* *-S3: Slight charring and browning* *-S4: Slight charring* *-S5: Color darkens and dulling* *-S6: Significant flaking and discoloration of paint*

Figure 5.15: Miscellaneous steel response to direct heat loading

5.2.3. Nonstructural Aluminum

Four miscellaneous nonstructural aluminum specimens were tested with a stepped heat loading regimen: 300°C (572°F) for thirty minutes, 400°C (752°F) for zero minutes, 500°C (932°F) for thirty minutes, 600°C (1112°F) for zero minutes, 700°C (1292°F) for thirty minutes, 800°C (1472°F) for zero minutes, and 900°C (1652°F) for thirty minutes. All specimens began deforming at 700°C (1292°F) and were severely deformed at 800°C (1472°F) and 900°C (1652°F) (Figure 5.16). Duplicates of the four aluminum specimens were subjected to direct loading to a temperature of 700°C (1292°F) for 120 minutes (Figure 5.17). When comparing specimens that were step loaded to those direct loaded at 700°C (1292°F), specimens that were direct loaded appear to have slightly more significant deformation. This may be due to deformation being a function of time after aluminum reaches its melting point of 660°C 1220°F).

45
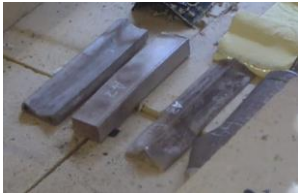
Temperature (time @ temp.)	Visual Condition	Observations
Ambient Before		
300°C (572°F)		
	No Changes	
600°C (1112°F)		
700°C (1292°F) (30 minutes)		-Discoloration of all specimens -Softening of aluminum/ deformation of all specimens
800°C (1472°F) (0 minutes)		-Significant deformation of all specimens (red light due to heaters)
900°C (1652°F) (30 minutes)		-All specimens charred -All specimens significantly deformed

Figure 5.16: Miscellaneous aluminum response to stepped heat loading

Temperature (time @ temp.)	Visual Condition	Observations
Ambient Before		
700°C (1292°F) (120 minutes)		-Slight discoloration of all specimens -Significant deformation of all specimens

Figure 5.17: Aluminum of different geometry response to direct heat loading

5.2.4. Nonstructural Concrete

The concrete specimens detailed in this section were used to investigate the effects of heat exposure on nonstructural concrete. Small blocks, measuring 12 in. x 6 in. x 4 in., representing concrete sidewalks were used to investigate the influence of heat on different mixture designs of concrete with different curing methods and degrees of surface scaling (Figure 5.18). Surface scaling of the specimens was a result of freeze-thaw cycles in the presence of deicing chemicals. These specimens were provided through a former research project at the University of Massachusetts Amherst, *Construction and Materials Best Practice for Concrete Sidewalks (62)*.

Concrete Sidewalk Block Specimen - No Scaling   Concrete Sidewalk Block Specimen - Scaling

Figure 5.18: Example concrete sidewalk specimens (left) specimen with no scaling (right) specimen with scaling

The loading regimens of specimens varied and can be referenced in Table 5.3. Each specimen's nomenclature describes its curing method and mixture design (Figure 5.19). There were six different mixture designs of concrete sidewalk specimens (Figure 5.20). Specimens were treated with three curing methods:

- "0" – no curing
- "MC" – moisture curing
- "CC" – chemical curing

Two of each specimen were tested, one scaled specimen and one non-scaled specimen.

Figure 5.19: Nomenclature describing specimen design

2019 CEMENT CONCRETE MIX DESIGN SHEET

RMS 043

Rev. 02/12/2019

PLANT INFORMATION

PLANT NAME	J G MACLELLAN CONCRETE	
CITY/TOWN, XX	GRAFTON, MA	
STREET NO. & ADDRESS	180 Phoenix Ave.	
MAILING ADDRESS	CITY/TOWN, XX	Lowell, MA 01852
EMAIL ADDRESS	alextn@jgmaclellan.com	

CONTRACT: SIDEWALK
MIX SHEET IDENTIFICATION / SHEET IDENTIFICATION NO.: 19-11-06-09-20-48

AGGREGATE SOURCES

ID	SOURCE	LOCATION	S.G.
FINE1	OSSIPEE AGGREGATES	OSSIPEE, NH	2.62
FINE2			
3/8"1	AGGREGATE INDUSTRIES	LITTLETON, MA	2.66
3/8"2			
3/4"1	AGGREGATE INDUSTRIES	LITTLETON, MA	2.67
3/4"2			
1.5"1			
1.5"2			

CEMENTITIOUS & SUPPLEMENTARY CEMENTITIOUS MATERIALS (SCM) SOURCES

ID	SOURCE	LOCATION	TYPE	S.G.
C1	LAFARGE	ST CONSTANT, QC	I / II	3.15
C2				
C3				
C4				
FA1	CHARAH (MIAMI FORT)	NORTH BEND, OH	F	2.64
FA2				
SLAG	LAFARGE NEWCEM	BALTIMORE, MD	120	2.85
SF				

ADMIXTURE SOURCES (* = NTPEP / TRIAL REQ'D)

ID	COMPANY & PRODUCT	TYPE	QCML
AD1	SIKA - SIKA AEA-14	AEA	Y
AD2	SIKA - SIKAMENT AFM	A	Y
AD3			
AD4			
AD5			
AD6			
AD7			
AD8			

SIEVE ANALYSIS AND LA ABRASION

SIZE	2"	1 1/2"	1"	3/4"	1/2"	3/8"	#4	#8	#16	#30	#50	#100	#200	F.M.	L.A.
FINE					100	100	95-100		45-80	10-30	2-10	0-3		2.5-3.0	INFO
FINE1					100	99	93	70	43	16	5	1.3		2.69	<30
FINE2															
3/8"					100	85-100	10-30	0-5							<30
3/8LW					100	80-100	5-40	0-20	0-10						INFO
3/8"1					100	90	25	8	3						3.65
3/8"2															
3/4"			90-100	20-55	0-10	0-5									<30
3/4LW			90-100	10-50	0-15	0-5									<30
3/4"1			94	42	9	3									19.0
3/4"2															

CLASSIFICATION OF CONCRETE

ID NO.	PSI	TYPE	SIZE
1	4000	SIDEWALK	3/4"1
2	4000	SIDEWALK	3/4"1
3	4000	SIDEWALK	3/4"1
4	4000	SIDEWALK	3/4"1
5A	4000	SIDEWALK	3/4"1
5B	4000	SIDEWALK	3/4"1
5C	4000	SIDEWALK	3/4"1
6	4000	SIDEWALK	3/4"1

AGGREGATE (LBS.) / CEMENT (LBS.) / SCM (LBS.) / WATER (GAL.) AND ADMIXTURES (OZ.) / CALCULATION

ID NO.	1.5"1	1.5"2	3/4"1	3/4"2	3/8"1	3/8"2	FINE1	FINE2	C1	C2	C3	C4	FA1	SLAG	SF	WTR.	AD1	AD2	AD3...AD8	W/C	AIR	PASTE
1			1416.9		357		1091.9		556							33.6	3.0	46.0		0.43	6.3%	29.5%
2			1409.8		345		1086.4		328				196			31.1	3.8	31.2		0.49	10.2%	26.1%
3			1420.1		355		1099.6		492							33.6	2.0	46.2		0.43	6.0%	29.5%
4			1393.9		345		1094.2		328					330		33.1	3.2	39.6		0.42	6.9%	29.6%
5A			1098.5		698		1169.3		418					180		30.3	4.8	60.0		0.42	6.4%	27.2%
5B			1098.5		698		1169.3		418					180		31.6	4.8	60.0		0.44	5.7%	27.8%
5C			1098.5		698		1169.3		418					180		32.0	4.8	60.0		0.45	5.5%	28.0%
6			1085		682		1164		300					300		31.7	3.0	42.7		0.44	6.5%	27.8%

We agree to furnish mixes to MassDOT projects that are produced from only the referenced materials listed on the RMS 043 Cement Concrete Mix Design Sheet. We also understand that designs are to be submitted annually, prior to production for state work, and any subsequent change in materials or design will require resubmission for approval.

Figure 5.20: Concrete sidewalk block specimen mixture designs *(62)*

49

Table 5.3: Heating regimens of concrete sidewalk block specimens

Specimens	Type of Heat Loading	Temperature °C (°F), (time at temperature, minutes)
101 102	Stepped	300°C (572°F), (30) 400°C (752°F), (30) 500°C (932°F), (30) 600°C (1112°F), (120)
201[a] 202[a]	Direct	600°C (1112°F), (120)
201[b] 202[b]	Stepped	500°C (932°F), (0) 600°C (1112°F), (0) 700°C (1292°F), (0) 800°C (1472°F), (120)
601 602	Stepped	500°C (932°F), (0) 600°C (1112°F), (0) 700°C (1292°F), (0) 800°C (1472°F), (120)
6MC1 6MC2	Stepped	500°C (932°F), (0) 600°C (1112°F), (0) 700°C (1292°F), (0) 800°C (1472°F), (120)
6CC1 6CC2	Stepped	500°C (932°F), (0) 600°C (1112°F), (0) 700°C (1292°F), (0) 800°C (1472°F), (120)
1MC1 1MC2	Stepped	500°C (932°F), (0) 600°C (1112°F), (0) 700°C (1292°F), (0) 800°C (1472°F), (120)
1CC1 1CC2	Stepped	500°C (932°F), (0) 600°C (1112°F), (0) 700°C (1292°F), (0) 800°C (1472°F), (120)
401 402	Stepped	800°C (1472°F), (0) 900°C (1652°F), (120)

Visual results of the concrete sidewalk specimens are variable. Consistent visual trends associated with specific temperatures are not clearly observed in the results of these tests. Most specimens seemed to show some extent of reddening between the temperatures of 500°C (932°F) and 800°C (1472°F) and appeared to lighten slightly in color at 800°C (1472°F). The described visual changes are not easily observable and can be better noticed when referencing a control visual of the specimens at an ambient temperature for comparison.

There are no distinct differences between mixture designs and curing methods in relation to the visual changes resulting from heat exposure. When comparing scaled and non-scaled specimens, it seems that the visual changes are more apparent in general for scaled specimens. This may be attributed to the fact that more aggregate is exposed on the scaled side than the non-scaled side and oxidation in aggregate as well as the disintegration of calcium carbonate in calcareous aggregate both contribute to visual changes. No spalling was observed in any of the concrete sidewalk specimens.

This page left blank intentionally.

6.0 Testing of Structural Components

In order to assess the condition of a tunnel after a fire event, it is necessary that inspectors can determine the condition of structural components. To better understand the response of structural components of a tunnel in a fire, reinforced, precast, prestressed, concrete ceiling panels were designed and tested. These specimens were designed to be similar to ceiling panels found in MassDOT-owned tunnels so that specimens used in laboratory testing would be representative of tunnel components in the field.

6.1 Concrete Slab Specimen Design

Concrete slab specimens were cast in three batches. All three batches of specimens include six 140 in. x 30 in. x 4 in. reinforced, precast, prestressed specimens with variances in concrete strength, number of prestressed strands, exterior coating of mild reinforcement wire mesh, inclusion/location of metal pipe inserts, and type of lifting anchors. Mild reinforcement of all specimens is WWF 4x4 – W2.9xW2.9 and all prestressed reinforcement is seven-wire strand. Once concrete slab specimens arrived at the University's testing facility, specimens were cured in an ambient indoor laboratory environment until they were tested. Twenty-four concrete cylinder specimens were cast with each batch of concrete slab specimens and stored in the laboratory under similar conditions as the slabs.

Table 6.1: Concrete slab specimens' summary

Batch	Specimens	Number of Prestressed Strands	Specimens with Epoxy Coated Mild Reinforcement Mesh	Specimens with Metal Pipe Inserts	Type of Lifting Anchor
1	CS-1A CS-1B CS-1C CS-1D CS-1E CS-1F	2	-	CS-1A CS-1B CS-1C	F63B-B
2	CS-2A CS-2B CS-2C CS-2D CS-2E CS-2F	3	CS-2B CS-2D	CS-2A CS-2B CS-2C CS-2D CS-2E CS-2F	P-52
3	CS-3A CS-3B CS-3C CS-3D CS-3E CS-3F	3	CS-3E CS-3F	-	F63B-B

6.1.1. Concrete Cylinders

Concrete cylinder specimens measuring 4 in. x 8 in. were also cast with each batch of concrete slab specimens to investigate the compressive strength of each batch at twenty-eight days and six months. Concrete cylinders were also exposed to elevated temperatures to study their mechanical and visual response to heat exposure.

### 6.1.1.1. Concrete Cylinder Compressive Strength

At twenty-eight days and six months, two concrete cylinders from each batch were tested to evaluate the average compressive strength of concrete slab specimens. The compressive strength of each batch was found to be variable, as detailed in Table 6.2. The compressive strength of each batch increased between the twenty-eight-day and six-month time-period.

**Table 6.2: Concrete cylinder compressive strength results**

Batch	28-Day Compressive Strength (psi)	6-Month Compressive Strength (psi)
1	9,468	10,883
2	6,273	7,758
3	7,083	9,645

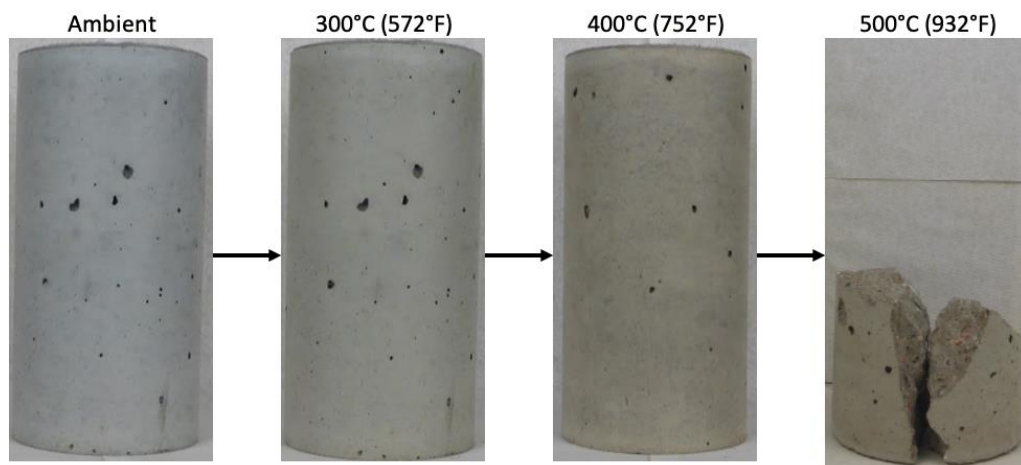### 6.1.1.2. Concrete Cylinder Visual Response to Heat Exposure

Additional concrete cylinders were cast to investigate their behavior with heat exposure. These cylinders were heated in a kiln where they were exposed to target temperatures of 300°C (572°F), 400°C (752°F), or 500°C (932°F) for three hours. The visual results are presented in Figure 6.1. A slight shift in color was observed in cylinders heated to 300°C (572°F) as a red tint was established in the concrete. At 400°C (752°F), the red tint became more apparent, and at 500°C (932°F) it was slightly more significant. Surface cracking was observed in all the concrete cylinder specimens exposed to elevated temperatures and was more apparent in the cylinders exposed to higher temperatures. Notably, a cylinder from batch 3 spalled explosively while at 500°C (932°F). The cylinders were heated in a kiln, and the temperatures described represent the gas temperature in the kiln.
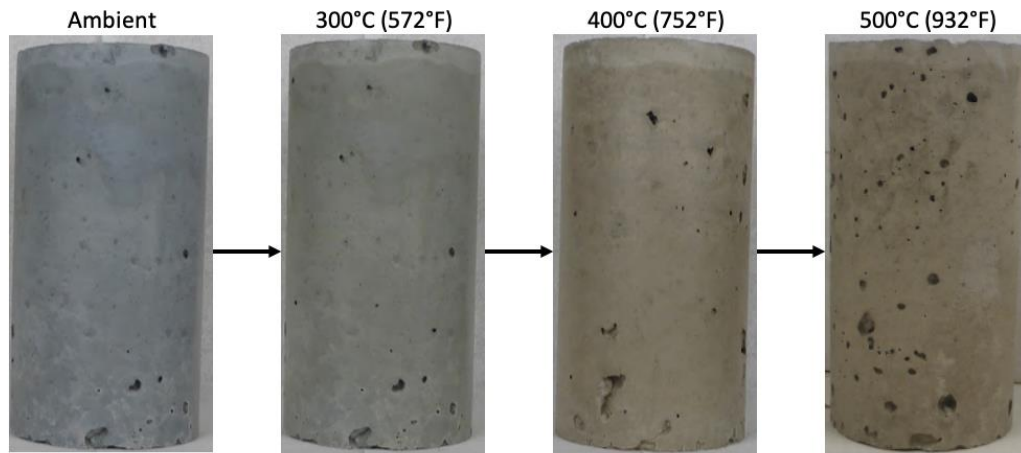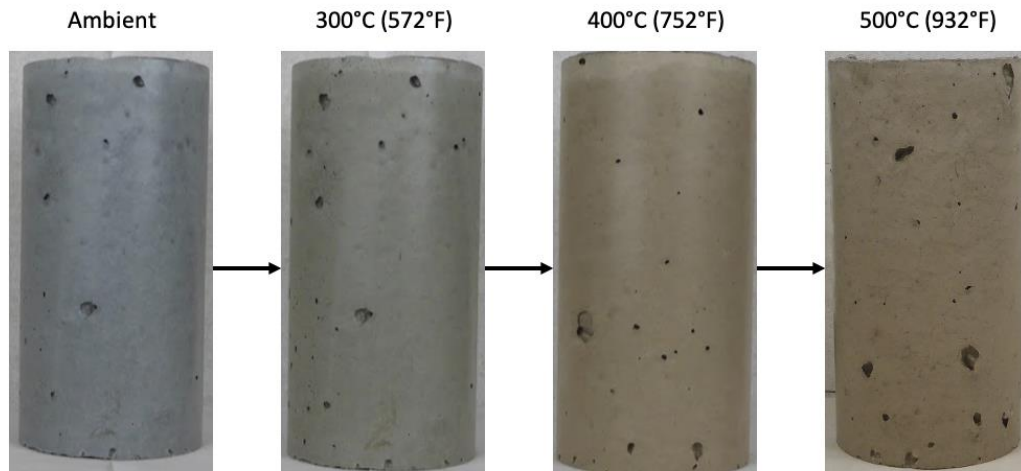
Figure 6.1: Concrete cylinder visual and physical responses to elevated temperatures (a) batch 1 (b) batch 2 (c) batch 3

6.1.2. Concrete Slab Specimen Shop Drawings

Original shop drawings of typical ceiling panel slabs from MassDOT-owned tunnels were used as a basis for the design of the concrete slab specimens. The actual ceiling panel slab shop drawings can be seen in Figure 6.2. The concrete slab specimens had some alterations when compared to the original ceiling panel slabs to enhance the scope of this research.
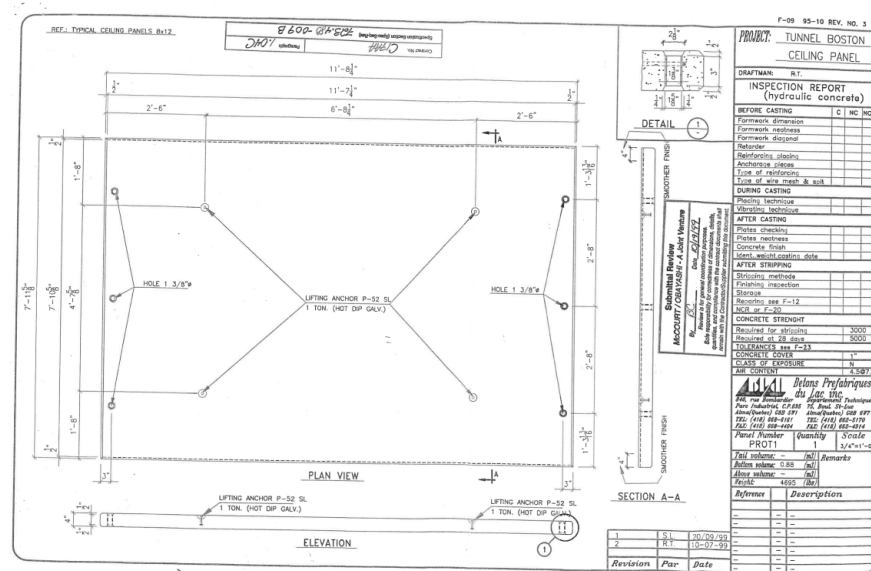
(a)
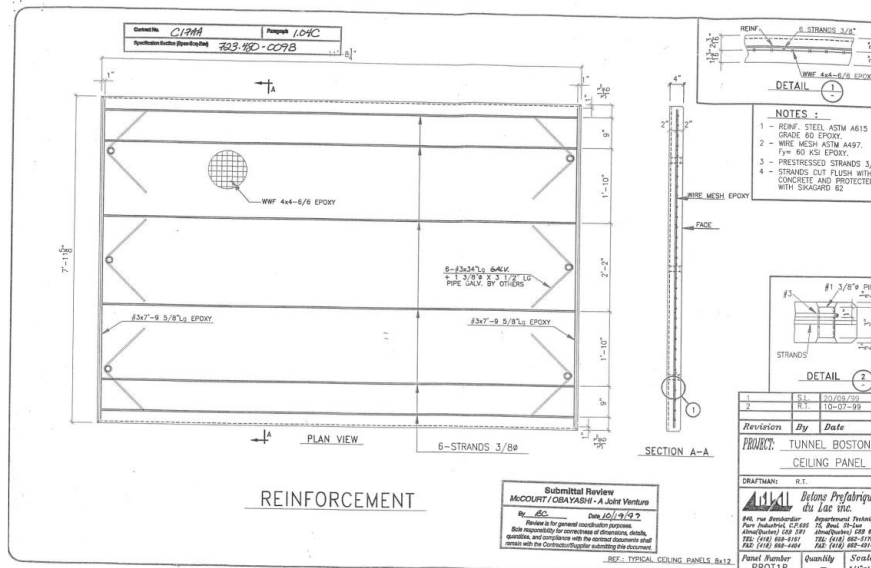
(b)

Figure 6.2: Original shop drawings of MassDOT-owned concrete ceiling panels (a) plan view and elevation view (b) reinforcement view

Shop drawings of the structural concrete slab specimens show the specified design of the specimens (Figures 6.3, 6.4, and 6.5)
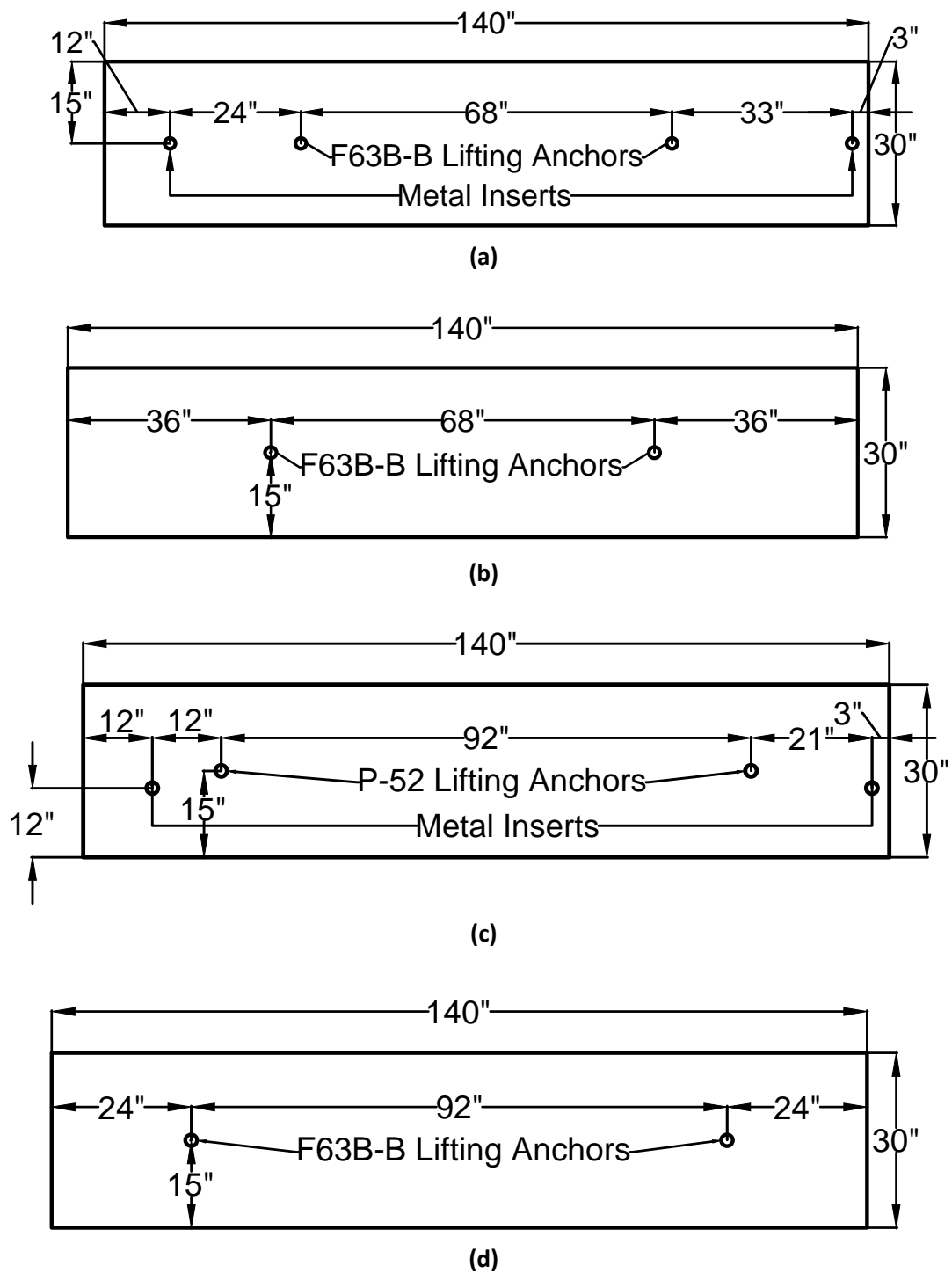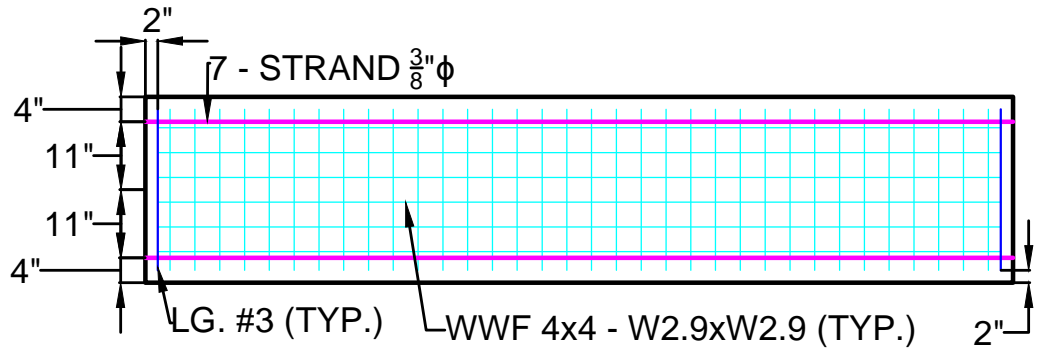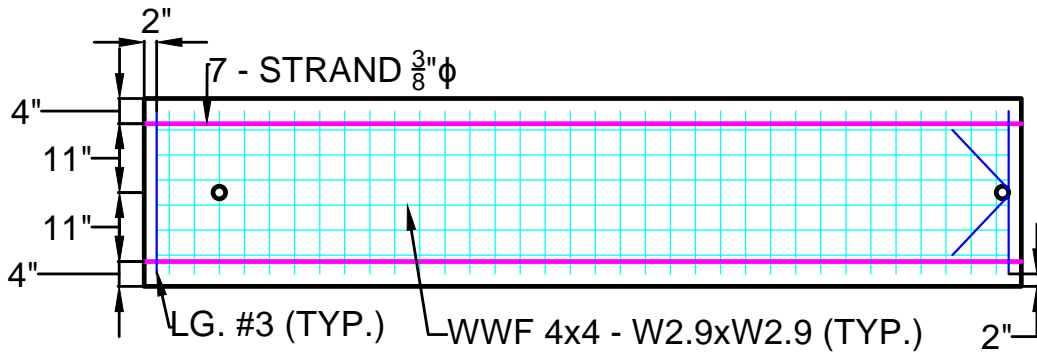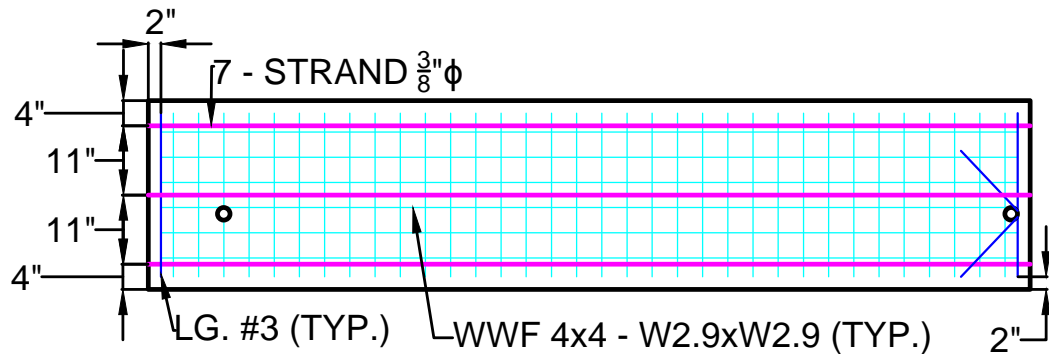

Figure 6.3: Concrete slab specimen design—plan view (a) batch 1 specimens without inserts (b) batch 1 specimens with inserts (c) batch 2 specimens (d) batch 3 specimens
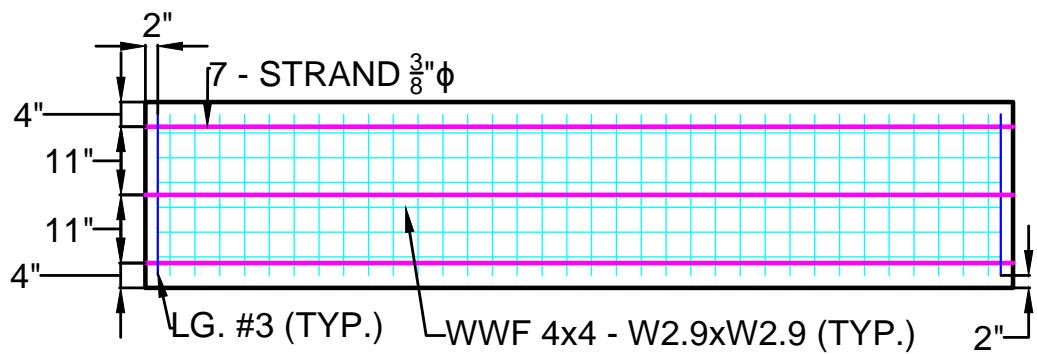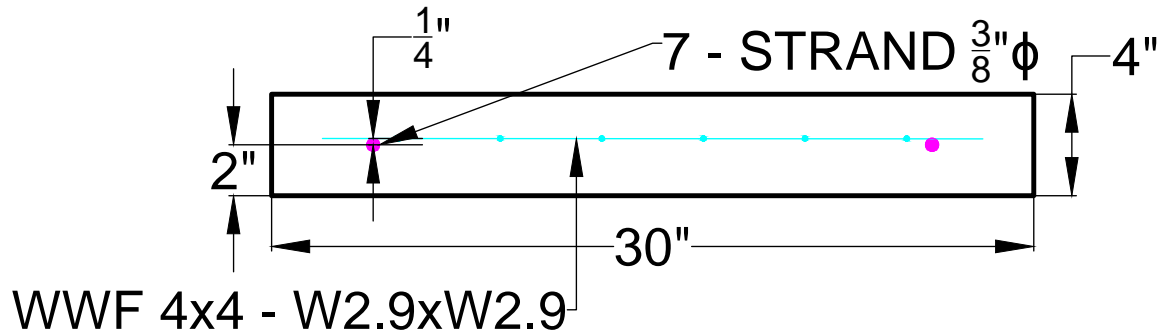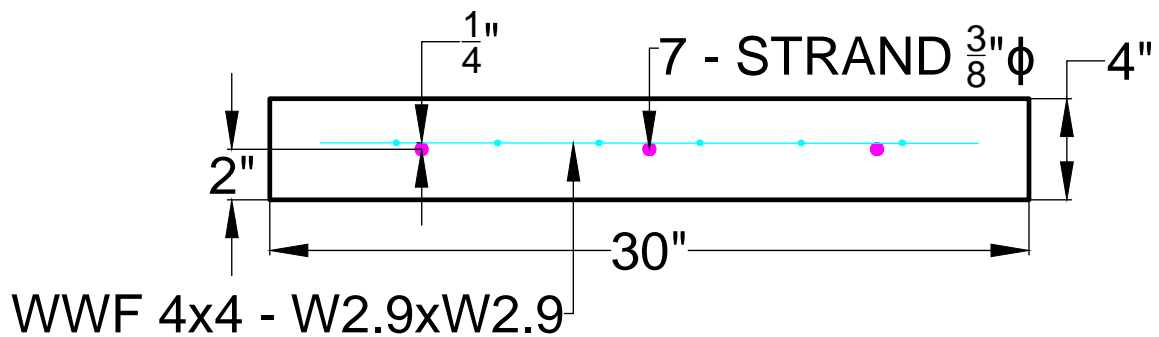
Figure 6.4: Concrete slab specimen reinforcement—plan view(a) batch 1 specimens without inserts (b) batch 1 specimens with inserts (c) batch 2 specimens (d) batch 3 specimens

(a)

(b)

Figure 6.5: Concrete slab specimen reinforcement—elevation view (a) batch 1 two strand members (b) batch 2 and 3 three strand members

6.2 Heat Testing

Concrete slab specimens from all three batches were heat tested. The purpose of heat testing was to investigate visual and physical responses of these specimens with heat exposure. Heat testing of concrete slab specimens utilized the equipment used for nonstructural components detailed in Section 3.0 of this report. All temperatures represent the temperature at the surface of concrete, as thermocouples were positioned to be touching the heated surface of the specimens.

The specimens used to investigate visual responses of concrete with heat exposure were heated as shown in Figure 6.6. Up to four potential heating zones were available on each slab given their geometry. Heated regions were considered to be continuously supported.
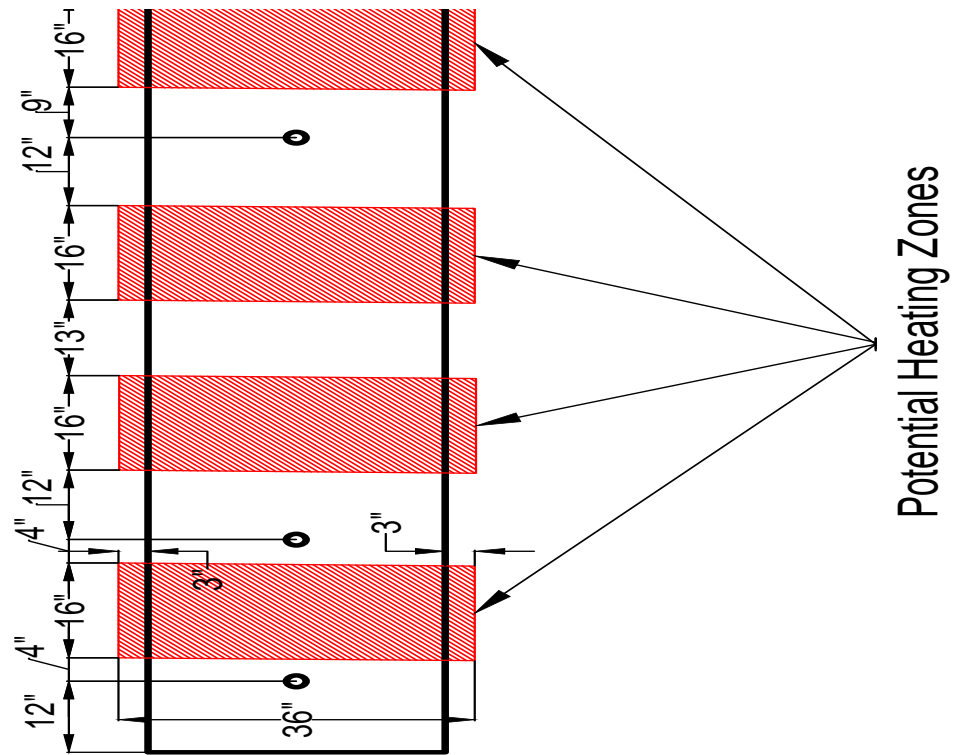
Figure 6.6: Potential heating zones for visual slabs—plan view

Specimens heated for mechanical testing purposes were heated in the center of their span as shown in Figure 6.7. Actual ceilings panels found in MassDOT-owned tunnels are simply supported by steel angles on their ends. The tension face resulting from the self-weight of a slab is exposed to the roadway and, in the case of most tunnel fires, would be directly heated (as opposed to the compression face). All concrete slab specimens that were used for mechanical testing and subject to heating were heated so that the directly heated face of the specimen was in equivalent tension from simply supported self-weight conditions.

Figure 6.7: Example heating setup for mechanical concrete slab specimens—plan view

6.2.1. Visual Characteristics of Concrete Slabs Resulting from Heat Exposure

The visual characteristics of concrete slabs with heat exposure was of interest. Two slabs from batch 1 and two slabs from batch 2 were used for this purpose. T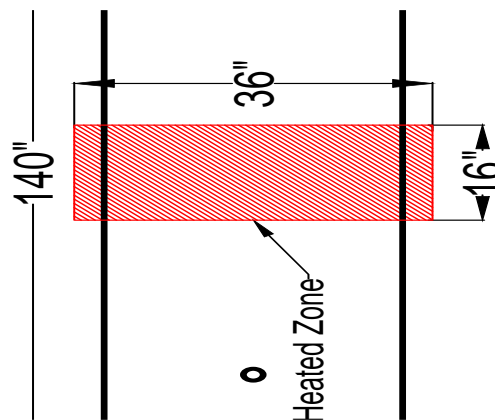he slabs were heated to target temperatures of 300°C (572°F), 400°C (752°F), and 500°C (932°F) in different potential heating zone locations. These target temperatures were held for one hour and three hours to investigate the influence of the duration of heat exposure on the visual characteristics of the concrete slabs.

Figure 6.8a represents different areas of a batch 1 concrete slab specimen held at the defined target temperatures for three hours, and Figure 6.8b represents areas of a batch 1 concrete slab specimen held at the defined target temperatures for one hour. One visual characteristic of interest is the change in color of concrete associated with heat exposure. Different target temperatures did have an influence on the color of the concrete. Notably, 300°C (572°F) did not have a major influence on concrete color, but a slight red tint began to be present at this temperature. At 400°C (752°F), the slight red tint became more significant, and at 500°C (932°F), the red tint was strongly apparent and the contrast in color when compared to the control ambient condition is easily observable. No significant differences in visual appearance relating to color is observed between the two durations of time of one hour and three hours that target temperatures were sustained. Figure 6.8c and Figure 6.8d represent batch 2 concrete slab specimens held at defined target temperatures for three hours and one hour, respectively. Visual color results for batch 1 and batch 2 specimens appear to be the same.
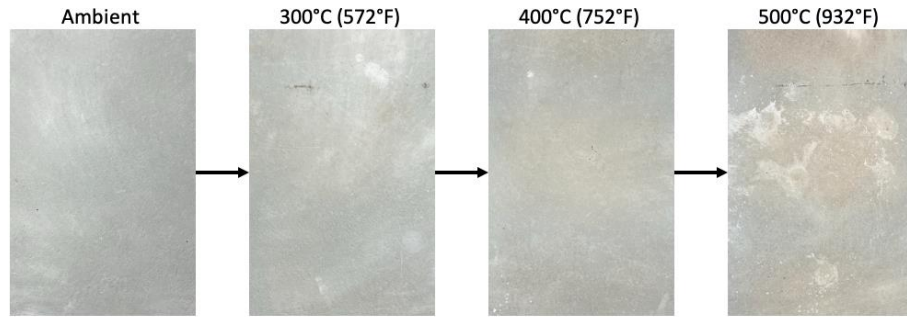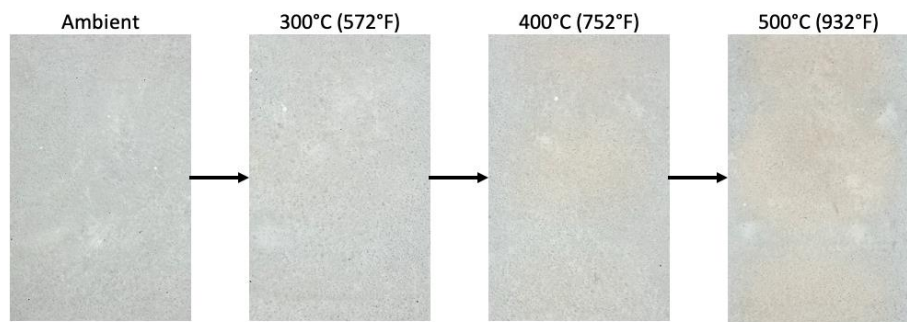
(a) CS-1E
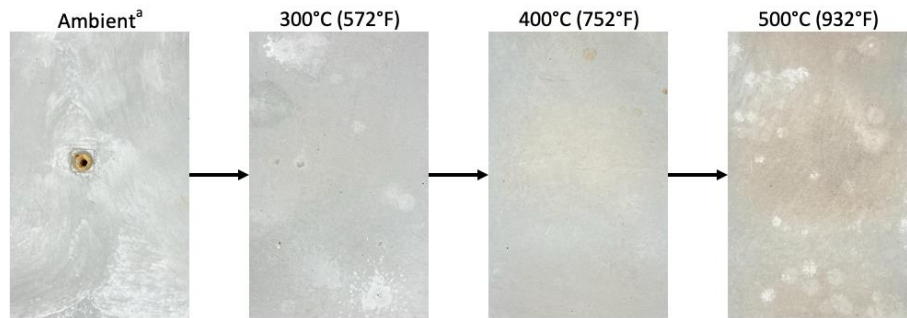
(b) CS-1F
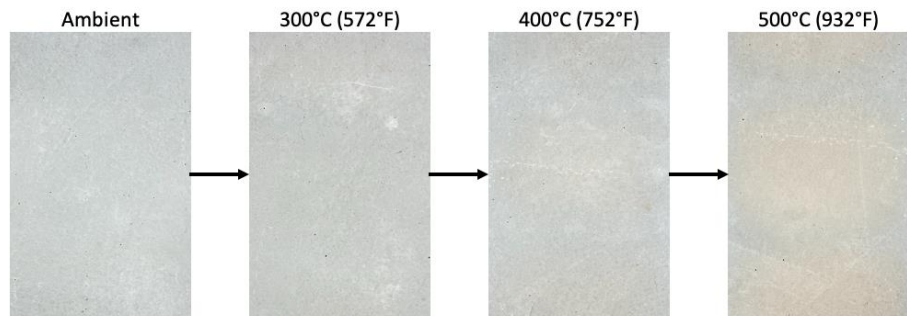
(c) CS-2E

(d) CS-2F

[a] Picture of specimen includes metal insert (seen at mid height)

Figure 6.8: Visual results of (a) batch 1, temperatures held for 3 hours, (b) batch 1, temperatures held for 1 hour, (c) batch 2, temperatures held for 3 hours, (d) batch 2, temperatures held for 1 hour

Another visual characteristic that was observed was the cracking of the concrete resulting from heat exposure. All slabs that were heated for visual investigation were observed to have surface cracking after heat exposure (with the exception of slab CS-1E heated to 300°C (572°F) for three hours). In general, all surface cracking was hairline and ranged from less than 0.1 mm to 0.3 mm in width. In general, cracking frequency increased with higher temperatures. Figure 6.9 illustrates variations in cracking with different target temperatures for slab CS-1F, batch 1 heated to target temperatures for three hours, and slab CS-2E, batch 2 heated to target temperatures for one hour. Differences in cracking relating to the duration of exposure to the target temperature and mixture design appear to be negligible.
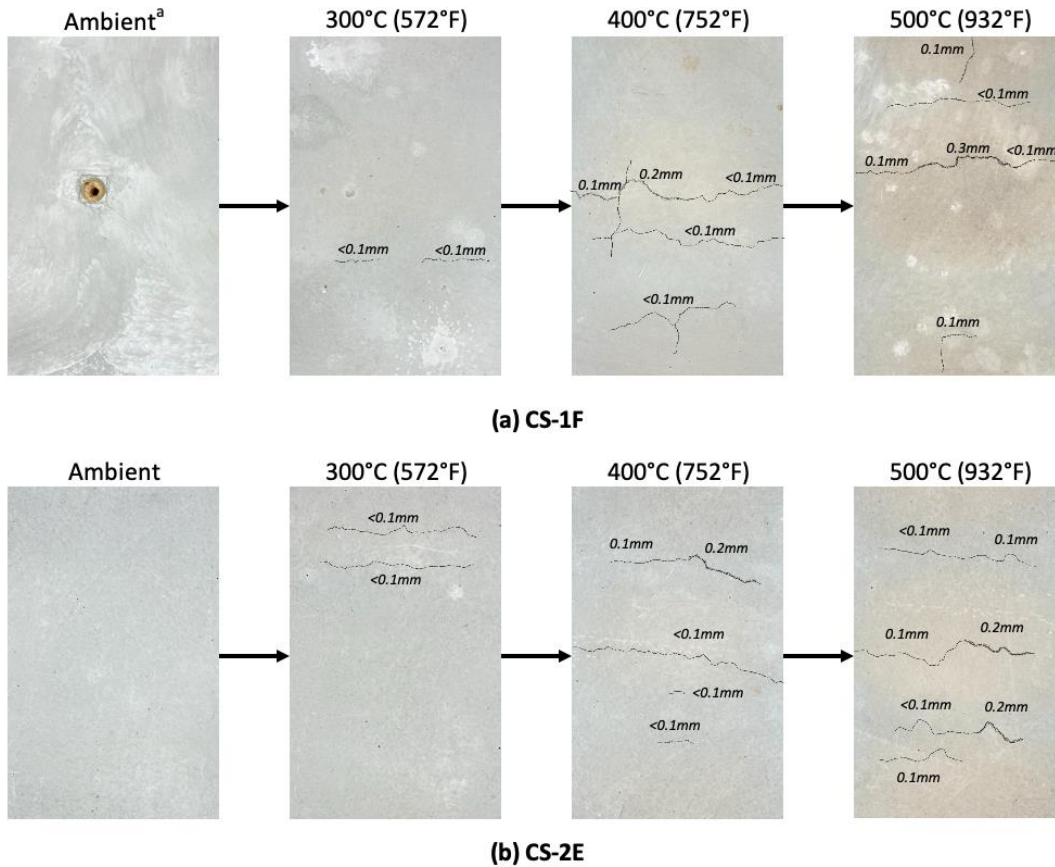
^a Picture of specimen includes metal insert (seen at mid height)

Figure 6.9: Surface cracking of concrete slab specimen CS-1F, batch 1 heated to target temperatures for 3 hours, and concrete specimen CS-2E, batch 2 heated to target temperatures for 1 hour, with cracks enhanced/highlighted

In addition to heating slabs to 300°C (572°F), 400°C (752°F), and 500°C (932°F), the investigators attempted to heat one slab, CS-1F from batch 1, to 700°C (1292°F) to see the concrete slab response at higher temperatures. When this specimen reached 670°C (1238°F), it spalled explosively (Figure 6.10), and the test was stopped.

64
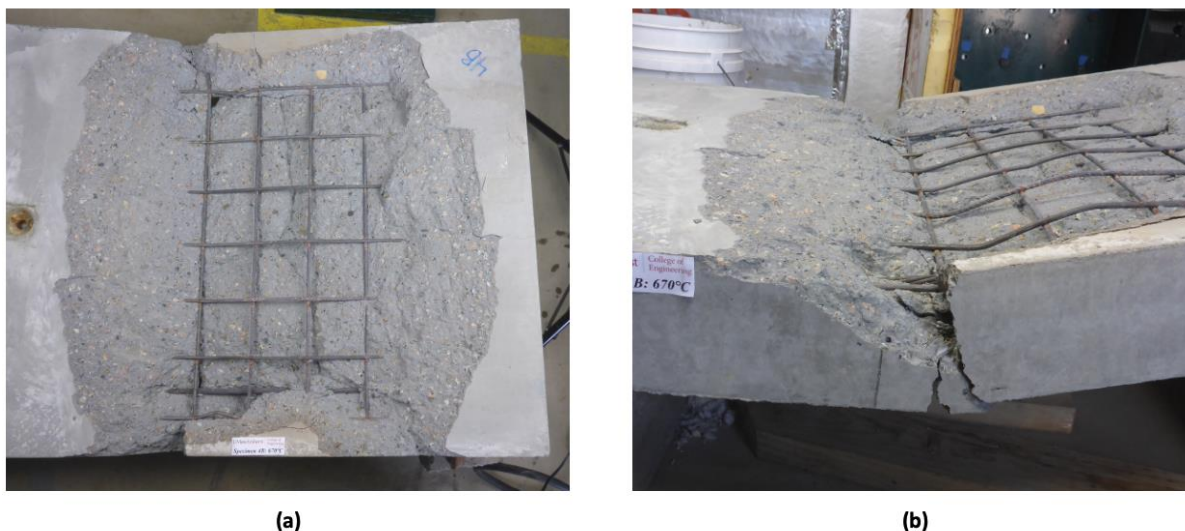
Figure 6.10: Concrete slab specimen CS-1F explosive spalling at 670°C (1238°F) (a) top view (b) side view)

6.2.2. Visual and Physical Responses of Metal Inserts and Lifting Anchors in Concrete Slabs

Metal inserts and metal lifting anchors cast in slabs from batches 1 and 2 were exposed to elevated temperatures to understand their visual and physical responses to heat. Metal inserts serve as a pipe for supporting angles to physically attach to the ceiling slabs (Figure 6.11). The ceiling slabs are further connected to hanger rods which are embedded into tunnel roofing using post-installed adhesive anchors. Lifting anchors are used to move the precast ceiling panels.
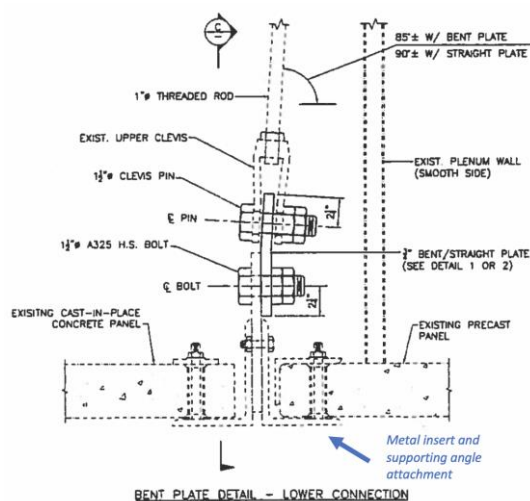
Figure 6.11: Metal insert and supporting angle attachment

It was of interest if the variability in material properties (e.g., coefficients of thermal expansion and thermal conductivity) of metal inserts and anchors and surrounding concrete would elicit visual or physical responses at elevated temperatures. Some inserts had mild reinforcement surrounding them (as shown in Figure 6.4) while others did not. Inserts without mild reinforcement surrounding them were meant to introduce a worst-case scenario (when compared with inserts with mild reinforcement).

6.2.2.1. Visual and Physical Responses of Metal Inserts

Concrete surrounding the metal inserts was heated to 500°C (932°F) for three hours to investigate the visual and physical responses to heat exposure. The heating chamber was opened at temperatures of 300°C (572°F) and 400°C (752°F) to observe any visual or physical changes while ramping up to 500°C (932°F). Metal inserts penetrate the entire depth of the concrete slab specimens and are hollow, introducing a hole through the depth of the specimen. In all testing of inserts, unless otherwise stated, ambient air was not restricted from flowing around and through the insert from the bottom of the slab surface. Thermocouples were placed touching specimens' top surfaces, bottom surfaces, and the interior of the metal inserts to record associated temperatures. It was of interest to see if differences in the temperature of the concrete slab and metal inserts would influence the slab's behavior with heat exposure.

General observations showed that the inclusion of metal inserts in slab specimens did not significantly influence surface cracking patterns during heat testing when compared with heat testing of slab specimens with no inclusion of metal inserts. In most insert heating tests, some cracking did stem from the inserts, and can be referenced in detail for each test in this section. The distance of an insert from its edge boundary of the slab did influence the inserts' responses to heating and may have influenced cracking patterns slightly. Notably, spalling was observed in one insert test and is detailed further in this section.

When heating around an insert located 12 in. from the left edge of a specimen from batch 1, it was observed that after the concrete was heated at 500°C (932°F) for three hours, there was some cracking around the metal insert (Figure 6.12). No cracking was observed prior to this. General surface cracking trends were comparable to those in concrete without a metal insert, with exception of the enhanced/highlighted cracks surrounding the insert. Temperature trends of the top surface, bottom surface, and metal insert can be found in Figure 6.13. The sharp drops and spikes in the temperature-time curves (Figures 6.13 and 6.15) after the top of the slab reached approximately 300°C (572°F), 400°C (752°F), and 500°C (932°F) can be explained by the opening of the heat chamber to visually investigate the specimen at these temperatures. When the heat chamber was opened, the heat chamber would be exposed to ambient laboratory conditions briefly, influencing the temperature-time curves. There was no mild reinforcement around this insert.

Figure 6.12: Cracking around metal insert, batch 1, 12in from left edge, after 500°C (932°F) for 3 hours with cracks enhanced (picture taken once cooled to ambient conditions)

Figure 6.13: Temperature-time curve for metal insert test, batch 1, 12in from left edge

An insert 2 in. from the right edge of a slab from batch 1 was also investigated to understand how boundary conditions influence test results. This test had results identical to the previous test except that a crack formed that ran from the insert to the edge boundary beginning at 300°C (572°F) (Figure 6.14). As seen in Figure 6.15, the temperature-time data show that the metal insert maintained a cooler temperature when it was 2 in. from the edge than when it was 12 in. due to the change in proximity of the insert to the boundary edge. Notably, the bottom surface temperature of the concrete surpassed the insert temperature toward the end of the testing period. There was mild reinforcement around this insert.
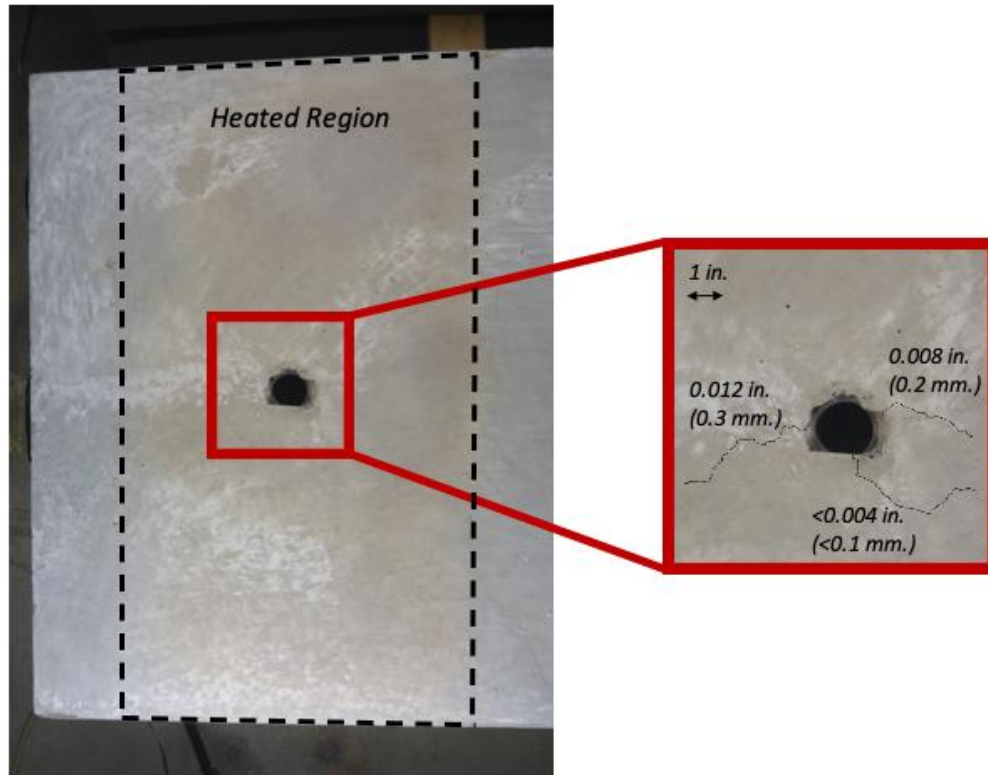

Figure 6.14: Cracking around metal insert, batch 1, 2in from left edge, after 500°C (932°F) for 3 hours with cracks enhanced (picture taken once cooled to ambient conditions)
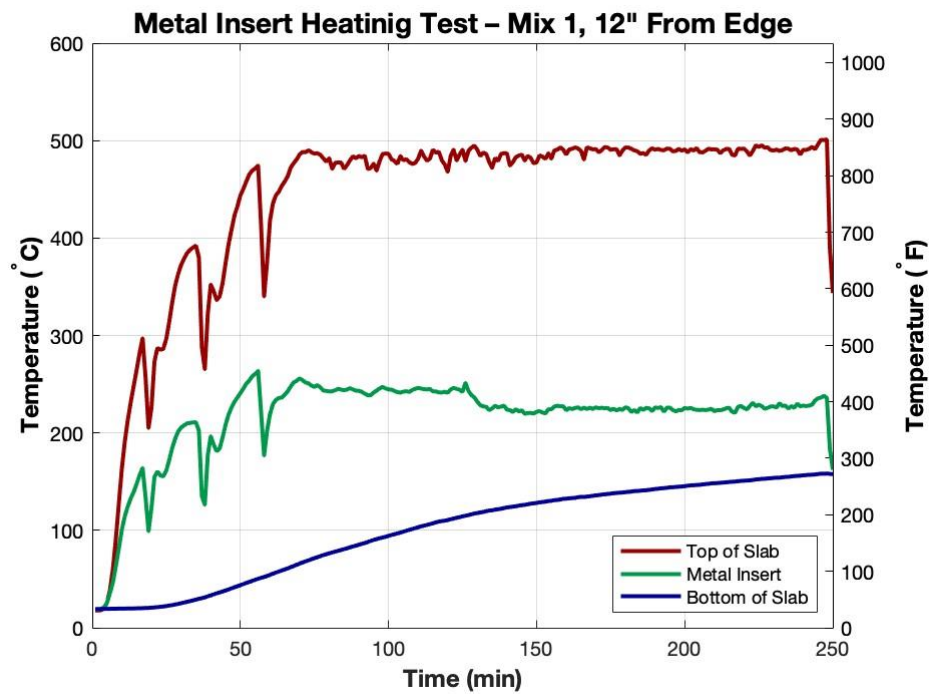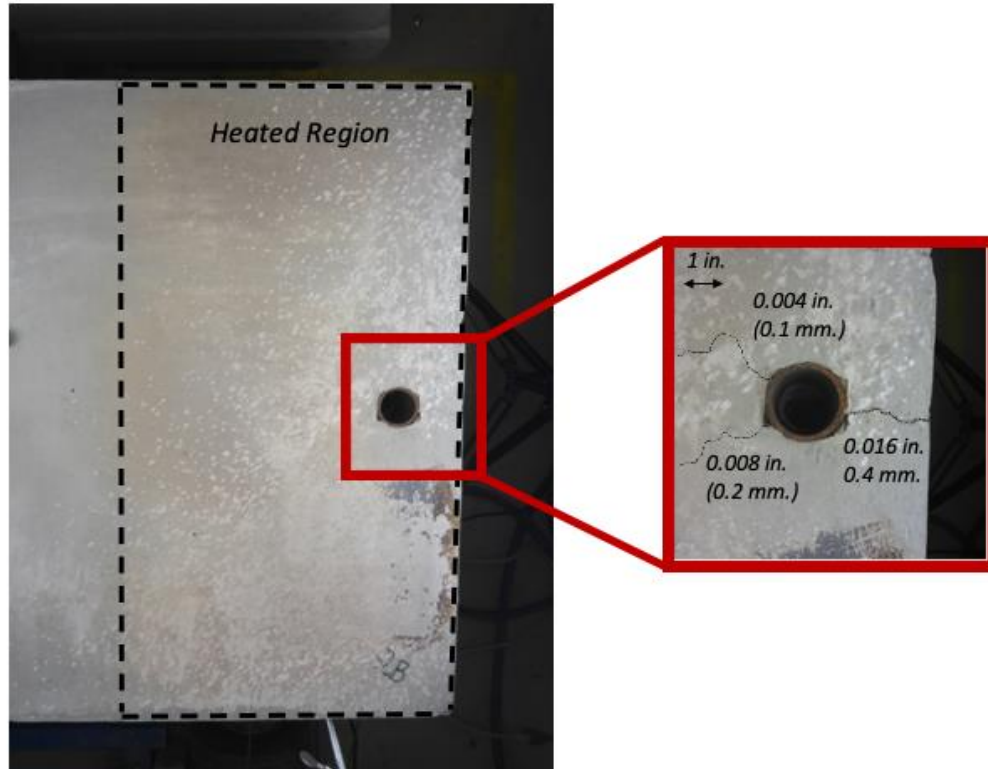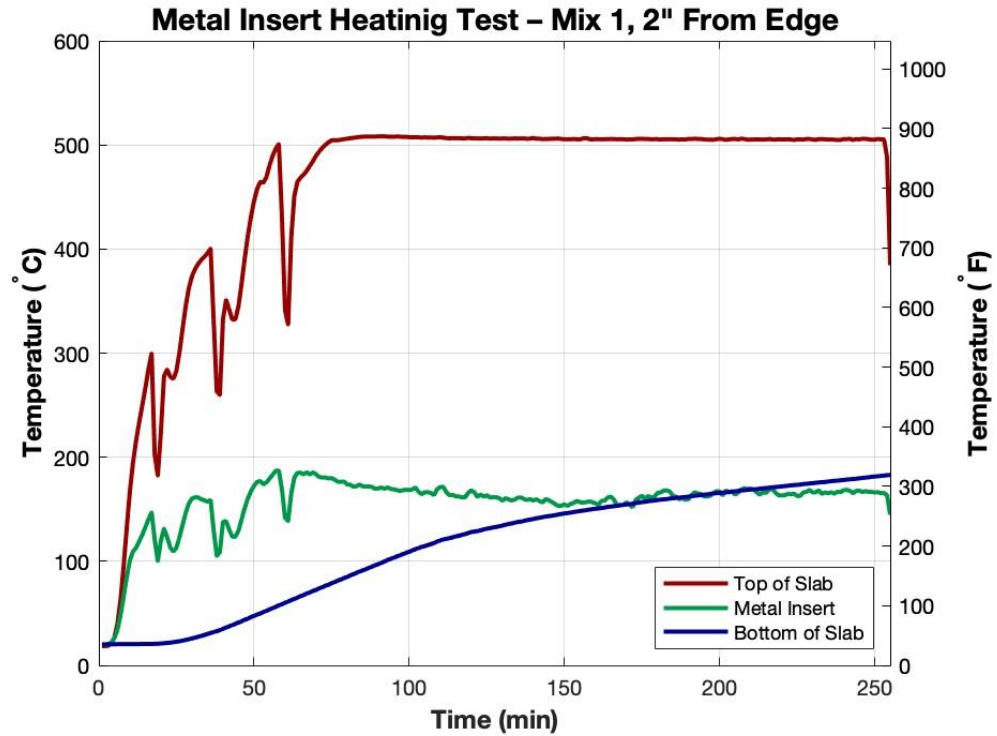
Figure 6.15: Temperature-time curve for metal insert test, batch 1, 2in from left edge

An insert 12 in. from the left edge of a slab from batch 2 was tested. This specimen explosively spalled after the top surface concrete temperatures were held at 500°C (932°F) for four minutes (Figure 6.16). The spalled concrete surrounded the metal insert. No cracking was observed on the piece of spalled concrete that was touching the metal insert. All spalled concrete did not extend to edge boundaries of the slab. The spall was approximately 1.75 in. in depth and did not exceed the depth of the reinforcing wire mesh. The test was concluded after spalling occurred. A replica of this test was conducted to further investigate the spalling phenomenon. It was found that the replica test did not induce spalling and showed normal surface cracking trends. Notably, there was no cracking around the insert during the replica test. There was no mild reinforcement around the insert in either test.

(a)   (b)
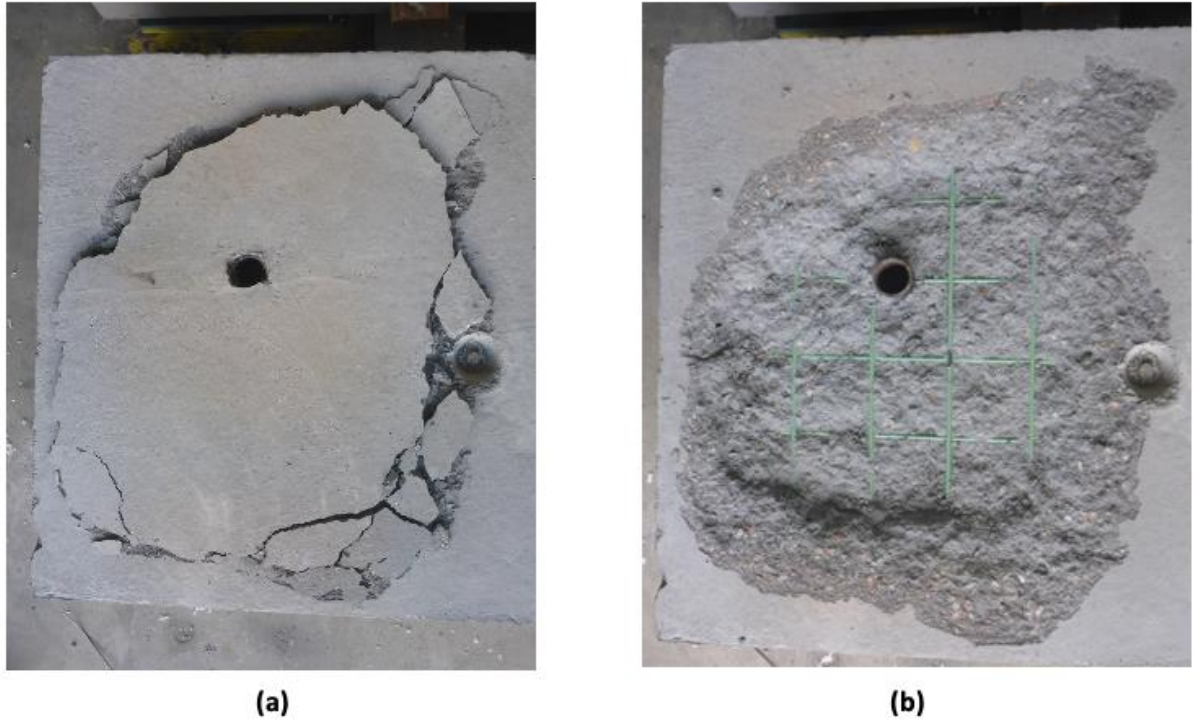
Figure 6.16: Spalling around metal insert, batch 2, 12in from left edge, 4 minutes after being at 500°C (932°F) (a) spalled concrete in place on specimen (b) after removal of spalled concrete

An insert 2 in. from the right edge of a batch 2 specimen was tested and found to show general surface cracking trends that were comparable to concrete without a metal insert with the exception of the enhanced/highlighted cracks surrounding the insert, which formed at 400°C (752°F) and ran from the insert to the edge boundary (Figure 6.17). There was mild reinforcement around this insert.

Figure 6.17: Cracking around metal insert, batch 2, 2in from left edge, after 500°C (932°F) for 3 hours with cracks enhanced (picture taken once cooled to ambient conditions)

Metal inserts are used so that supporting metal angles can be physically attached to the slab by fitting a metal cylinder into the insert. This causes restricted airflow through the insert, so to imitate this, an insert was filled with insulation. This test showed general surface cracking trends that were comparable to concrete without a metal insert with exception of the enhanced/highlighted cracks surrounding the insert, which formed at 400°C (752°F) and ran from the insert to the edge boundary (Figure 6.18). There was mild reinforcement around this insert.
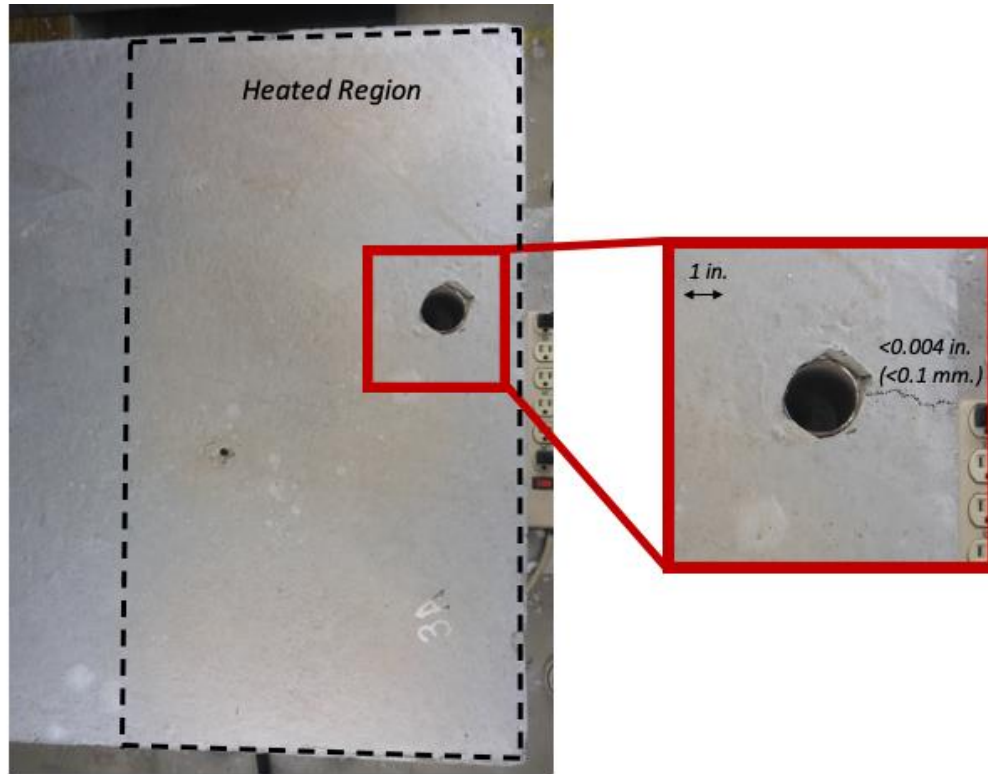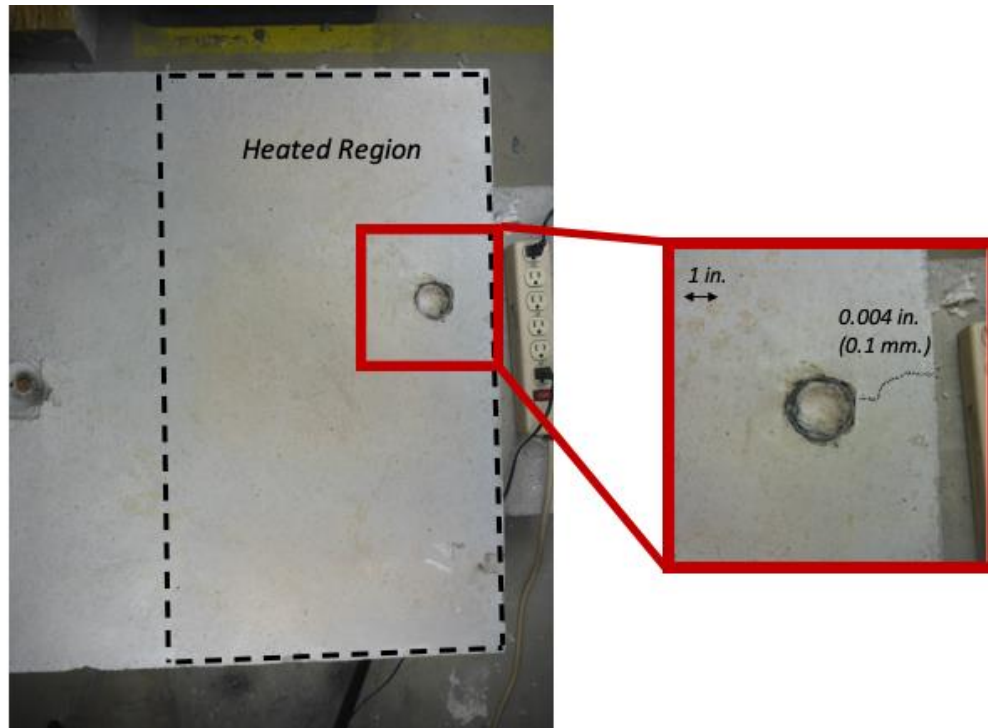
Figure 6.18: Cracking around metal insert, batch 2, 2in from right edge, after 500°C (932°F) for 3 hours with cracks enhanced (picture taken once cooled to ambient conditions)

6.2.2.1 Visual and Physical Responses of Lifting Anchors

Concrete surrounding the metal lifting anchors was heated to 500°C (932°F) for three hours to investigate their visual and physical response to heat exposure. The heating chamber was opened at temperatures of 300°C (572°F) and 400°C (752°F) to observe any visual or physical changes while ramping up to 500°C (932°F). Notably, different lifting anchors were used in batches 1 and 2, with batch 1 utilizing F63B-B lifting anchors and batch 2 using P-52 lifting anchors, extending approximately 2 in. and 3 in. into the depth of the slab, respectively.

General observations showed that the inclusion of metal lifting anchors during heat testing on slab specimens did not significantly influence surface cracking patterns when compared with heat testing of slab specimens with no inclusion of metal lifting anchors. In the lifting anchor heating tests, some cracking did stem from the lifting anchors and can be referenced in detail for each test in this section. The type of lifting anchor did not have a significant effect on the specimens' response to heat.

An anchor 36 in. from the edge of a batch 1 specimen was tested and found to show general surface cracking trends that were comparable to concrete without lifting anchors with the exception of the enhanced/highlighted cracks surrounding the anchor, which were observed after the slab top surface was maintained at 500°C (932°F) for three hours (Figure 6.19). A replica test was conducted and found identical results.

Figure 6.19: Cracking around F63B-B lifting anchor, batch 1, 36in from edge, after 500°C (932°F) for 3 hours with cracks enhanced (picture taken once cooled to ambient conditions)

An anchor 24 in. from the edge of a batch 2 specimen was tested and found to show general surface cracking trends that were comparable to concrete without a lifting anchor with the exception of the enhanced/highlighted cracks surrounding the anchor, which were observed after the slab surface was at 500°C (932°F) for three hours. (Figure 6.20).
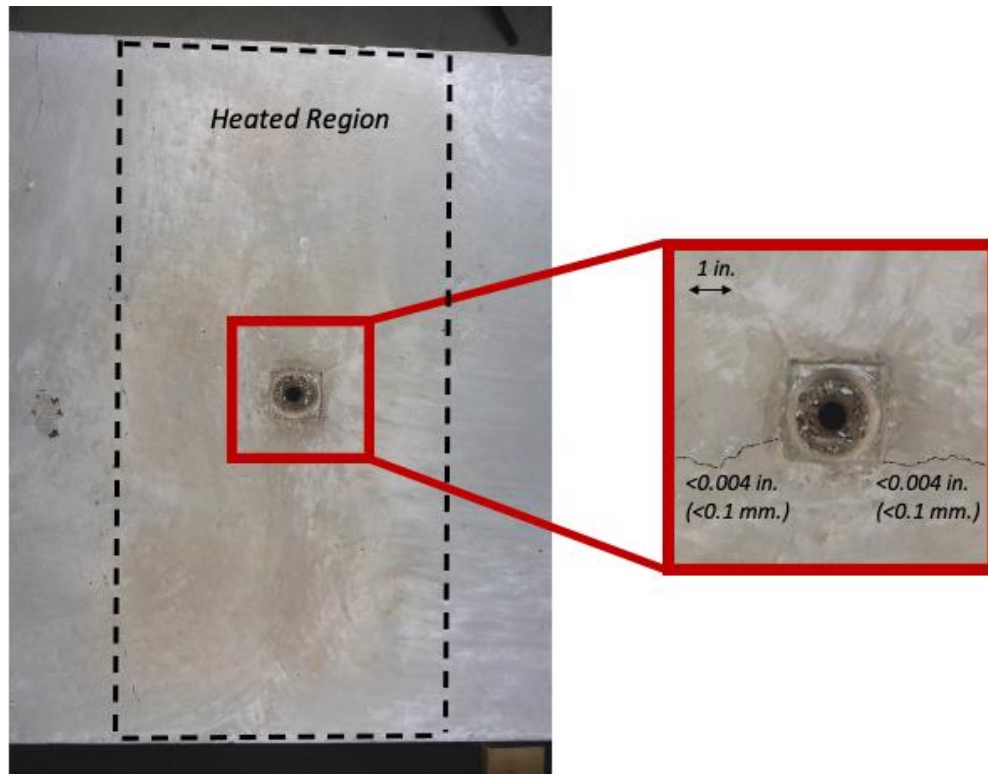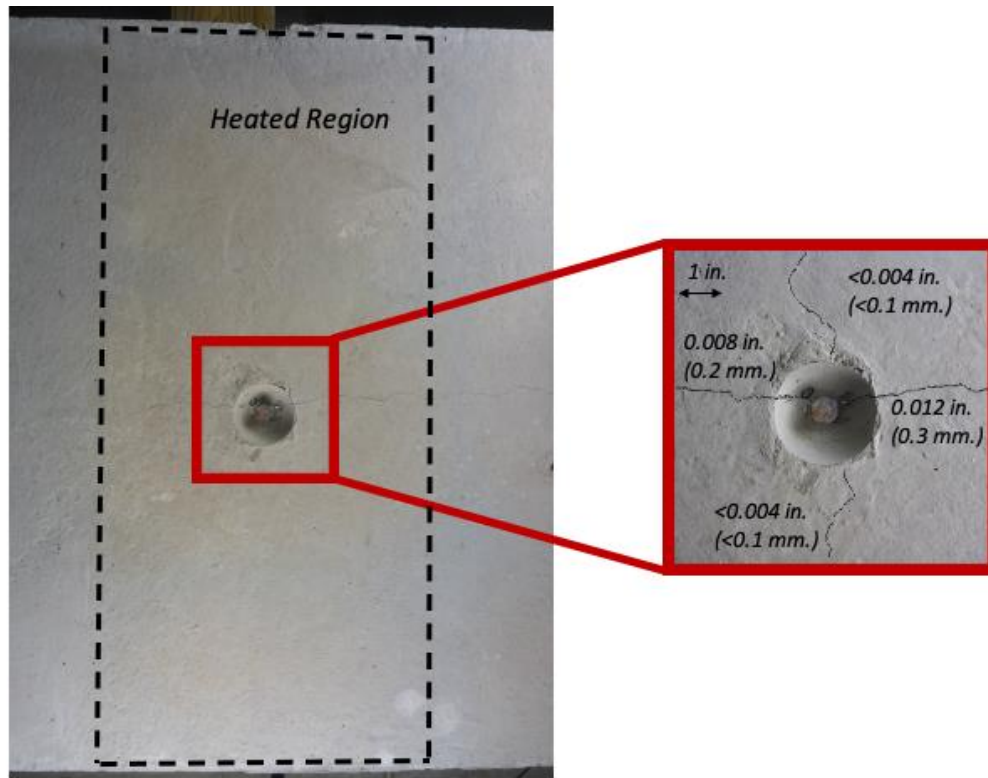
Figure 6.20: Cracking around P-52 lifting anchor, batch 2, 24in from edge, after 500°C (932°F) for 3 hours with cracks enhanced (picture taken once cooled to ambient conditions)

6.2.3. Structural Concrete Wall Panel

Two structural concrete wall panel specimens were heat tested in Phase II of this project. These were pieces of concrete wall panels that were in service in tunnel structures, provided by MassDOT. Other structural concrete wall panel specimens were tested during Phase I of this project. The specimens tested in Phase I were tested both with heat and mechanically to investigate the residual capacities and associated deflections. Detailed results may be referenced in the Phase I report. Figure 6.21 demonstrates the original wall panel provided to the research group and the process of saw cutting it into smaller specimens for research purposes. Figure 6.22 shows the wall panel dimensions and reinforcement layout.

Wall panel before saw cutting   *Saw cutting of panel*   *Example of some wall panel sections after being saw cut*

Figure 6.21: Original wall panel before and after being sawcut
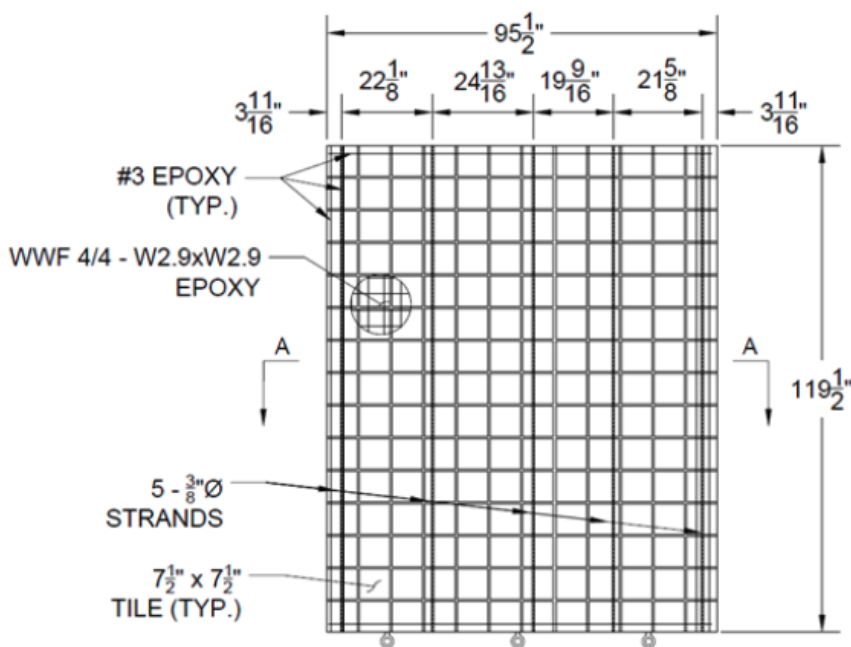
Figure 6.22: Wall panel dimensions and reinforcement *(1)*

Figure 6.23 shows a wall panel specimen from Phase I of this research project. This specimen suddenly spalled (explosive spalling) after being heated to 600°C (1112°F) for twenty-three minutes. Another wall panel specimen from Phase I, also heated to 600°C (1112°F), explosively spalled after twenty-seven minutes (Figure 6.24). These specimens are detailed in this report to show what spalling may look like on a wall panel in a tunnel structure. Notably, these specimens were heated on their untiled side.

75

Figure 6.23: First spalled wall panel specimen from Phase I experimental testing *(1)*

Figure 6.24: Second spalled wall panel specimen from Phase I experimental testing *(1)*

The specimens tested for Phase II had metal inserts as well as ceramic tiling. The first specimen (wall panel specimen #1) was first tested with a stepped heat loading regimen applied directly to its tiled face (Figure 6.25). After, the specimen was reheated, exposed to a direct heat loading regimen on its untiled side (Figure 6.26). The second specimen (wall panel specimen #2) was heated on its tiled face to higher temperatures than the previous specimen (Figure 6.27). Visual observations can be noted in the figures.

Figure 6.25 shows that discoloration of tiles and grout begins at 300°C (572°F). The tiles began to brown in color, and the grout began to darken in color. At 500°C (932°F), the grout began to change color to a reddish brown. At 600°C (1112°F), after 120 minutes, cracking in the tiles was noticed and charring was observed around the metal inserts and exposed epoxy coated rebar. Also, minor corner spalling (sloughing off) occurred where concrete was in contact with the metal insert. The grout was red and powder-like after the test and easy to remove (once returned to ambient temperature conditions). Figure 6.26 shows the same specimen reheated on its non-tiled side, directly to 600°C (1112°F) for 120 minutes. Slight discoloration of the specimen is observable as a result of heat exposure.

Figure 6.27 shows a second concrete wall panel specimen step heated to 800°C (1472°F) and 900°C (1652°F). Brown discoloration of both the tiles and grout was observed at 800°C

76

(1472°F). At 900°C (1652°F), significant cracking of the tiles was seen and charring of the epoxy from the exposed coated rebar. The grout and tiles both have red tints at 900°C (1652°F), which is also noticeable on some of the concrete. Once the specimen returned to ambient temperature conditions, the grout was red and powder-like, and easily removable from the specimen.

Temperature (time @ temp.)	Visual Condition			Observations
Ambient Before				*Lifting anchor and metal insert (imbedded in panels)*
300°C (572°F) *(30 minutes)*				*-Initial discoloration of tiles* *-Initial discoloration of grout (darkens in color)*
400°C (752°F) *(30 minutes)*				*-Discoloration of tiles and grout continues*
500°C (932°F) *(30 minutes)*		*Minor cracking (enhanced to show more detail*		*-Grout discoloration changes (turns red)*
600°C (1112°F) *(120 minutes)*				*-Minor cracking observed in tiles (picture on right side to show cracking in more detail, enhanced)*
Ambient After				*-Metal inserts charred* *-Exposed epoxy coated rebar melting and charring* *-Corner spalling*

Figure 6.25: Wall panel specimen #1 tiled face visual response to stepped heat loading

Temperature (time @ temp.)	Visual Condition	Observations
Ambient Before		
600°C (1112°F) *(120 minutes)*		*-Slight discoloration of specimen*
Ambient After		

Figure 6.26: Wall panel specimen #1 untiled face visual response to direct heat loading
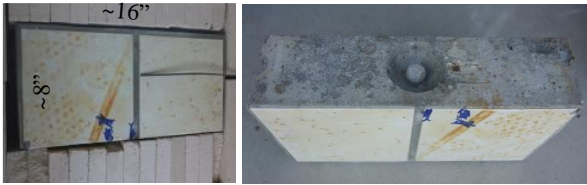
Temperature (time @ temp.)	Visual Condition	Observations
Ambient Before	~16" ~8"	*Lifting anchor (imbedded in panels)*
800°C (1472°F) (0 minutes)		*-Discoloration of tiles -Discoloration of grout (red in color)*
900°C (1652°F) (120 minutes)		*-Significant cracking in tiles (picture on right side to show cracking in more detail)*
Ambient After		*-Brown colors changed to red colors -Epoxy coated rebar melting and charring*

Figure 6.27: Wall panel specimen #2 tiled face visual response to direct heat loading

6.3 Mechanical Testing

Concrete slab specimens from all three batches were mechanically tested. The purpose of mechanical testing was to demonstrate the residual capacity and deflection behavior of specimens after being exposed to elevated temperatures in comparison with control specimens. Specifically, specimens were tested in flexure. By investigating flexural capacity of specimens exposed to elevated temperatures, post-fire tunnel inspection risk analysis of structural members can be enhanced.

All specimens were simply supported during mechanical testing. All specimens were loaded at their third points to induce a constant moment region in the center third of the specimens' span. All specimens were brought to failure, which can be defined as the instance in which a specimen's flexural capacity becomes reduced due to loading. Table 6.3 shows the calculated

flexural capacity and the contribution of mild reinforcement to flexural capacity for each batch of slabs in the control conditions.

Table 6.3: Calculated flexural capacity of concrete slab specimens

Batch	Number of Prestressed Strands	Approximate Concrete Compressive Strength[a] (psi)	Calculated Design Flexural Capacity (lbs.)	Percent Contribution of Mild Reinforcement to Flexural Capacity
1	2	10,883	4,107	30.62%
2	3	7,758	5,425	20.62%
3	3	9,645	5,628	20.79%

[a] Approximate concrete compressive strength at time of testing

A control specimen and a specimen heated to 500°C (932°F) for three hours were tested from each batch to compare the baseline capacity with the residual capacity after being exposed to elevated temperatures. 500°C (932°F) was chosen as an upper bound temperature as this was determined to be an appropriate temperature for an intermediate tunnel fire. Additional mechanical testing of concrete slab specimens with other heating regimens and physical characteristics was conducted and is detailed in the respective sections.

Due to concrete's minimal strength in tension, the influence of heat on the tension face of concrete was not expected to alter strength significantly, unless heat were to propagate through the entire depth of the slab into the compression zone. It was of interest, however, to see if the stiffness would be significantly influenced by heat exposure on the tension face of slab specimens.

Mechanical testing utilized four five-ton hydraulic cylinders to apply force to the specimens to test specimens in flexure. A pressure transducer was used to record the pressure being applied in the hydraulic cylinders. Load cells were used to record the reaction forces of the specimens when tested in flexure. String potentiometers were used to record deflections of the specimens during mechanical testing. A data acquisition system was used to record data from the pressure transducer, load cells, and string potentiometers.

Figure 6.28: (a) Hydraulic cylinder [63], (b) load cell [64], (c) pressure transducer
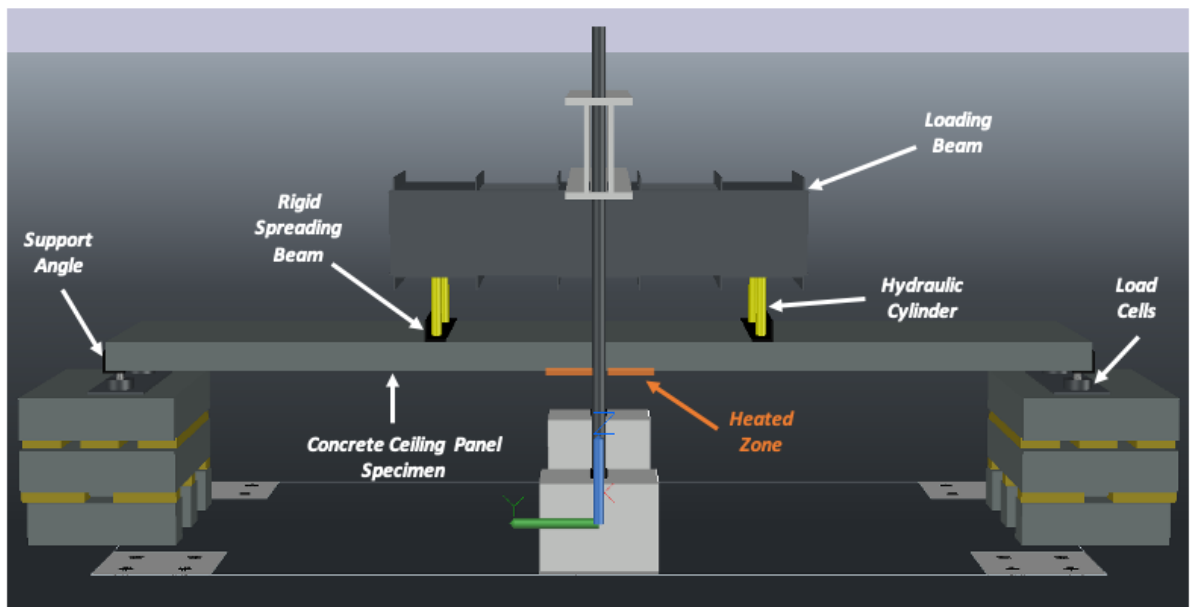

Figure 6.29: Schematic of mechanical loading rig

Figure 6.30: Actual mechanical loading rig

6.3.1. Batch 1

Four specimens (CS-1A, CS-1B, CS-1C, and CS-1D) were mechanically tested from batch 1. These included two control specimens, one specimen heated to 300°C (572°F), and one specimen heated to 500°C (932°F). While 500°C (932°F) was chosen as an upper bound temperature for intermediate fire testing, 300°C (572°F) was chosen to allow for an investigation of a heating regimen considered to be applicable to a moderate fire and its influence on the structural behavior of concrete slab specimens. Load-deflection plots for each test can be found in Figure 6.31. The peak capacity of each specimen is highlighted and presented in Table 6.4.
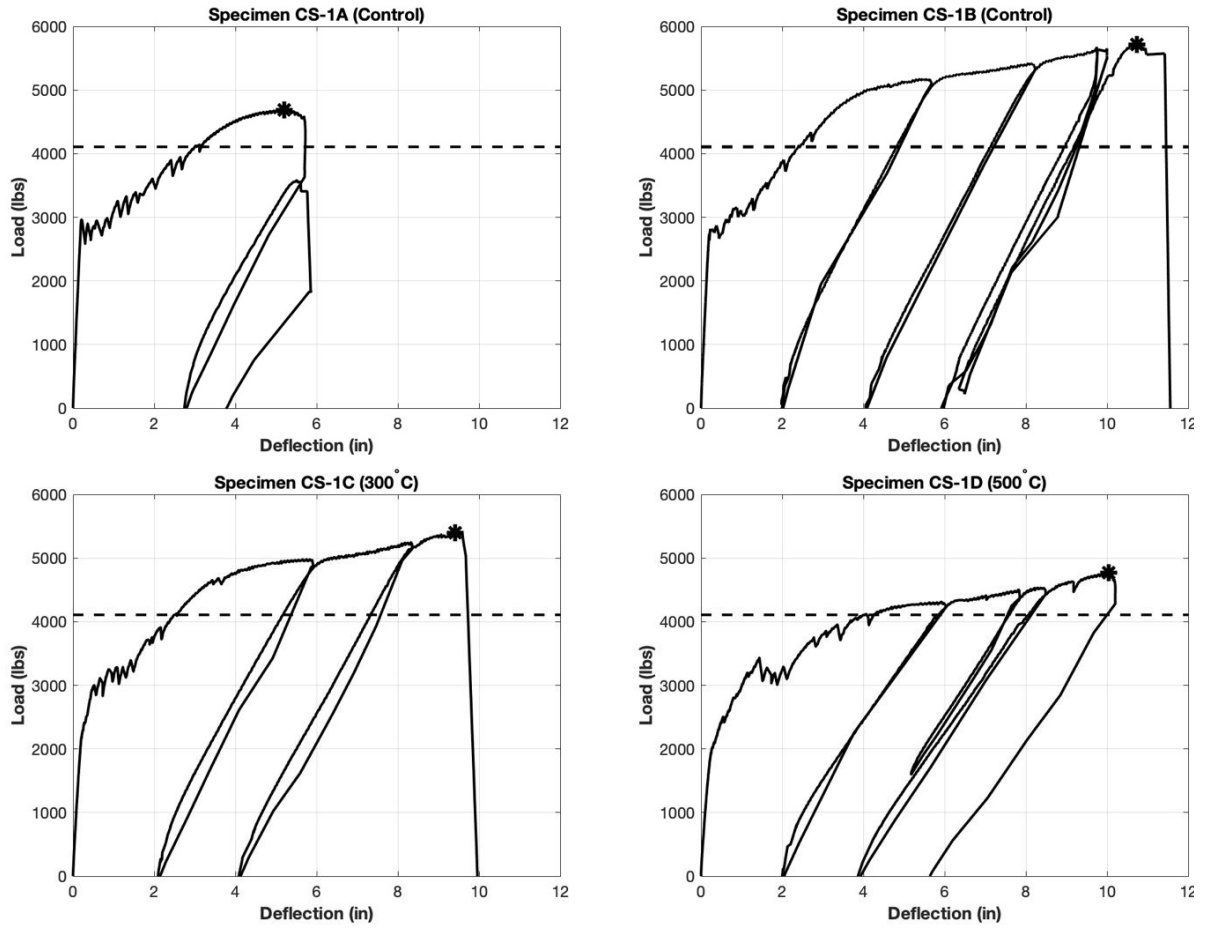
Figure 6.31: Mechanical testing results of batch 1 specimens CS-1A (Control), CS-1B (Control), CS-1C (300°C), and CS-1D (500°C), *dashed lines represent calculated design flexural capacity of unheated batch 1 concrete slab specimens (4,107lbs) and stars represent respective peak capacities during each test*
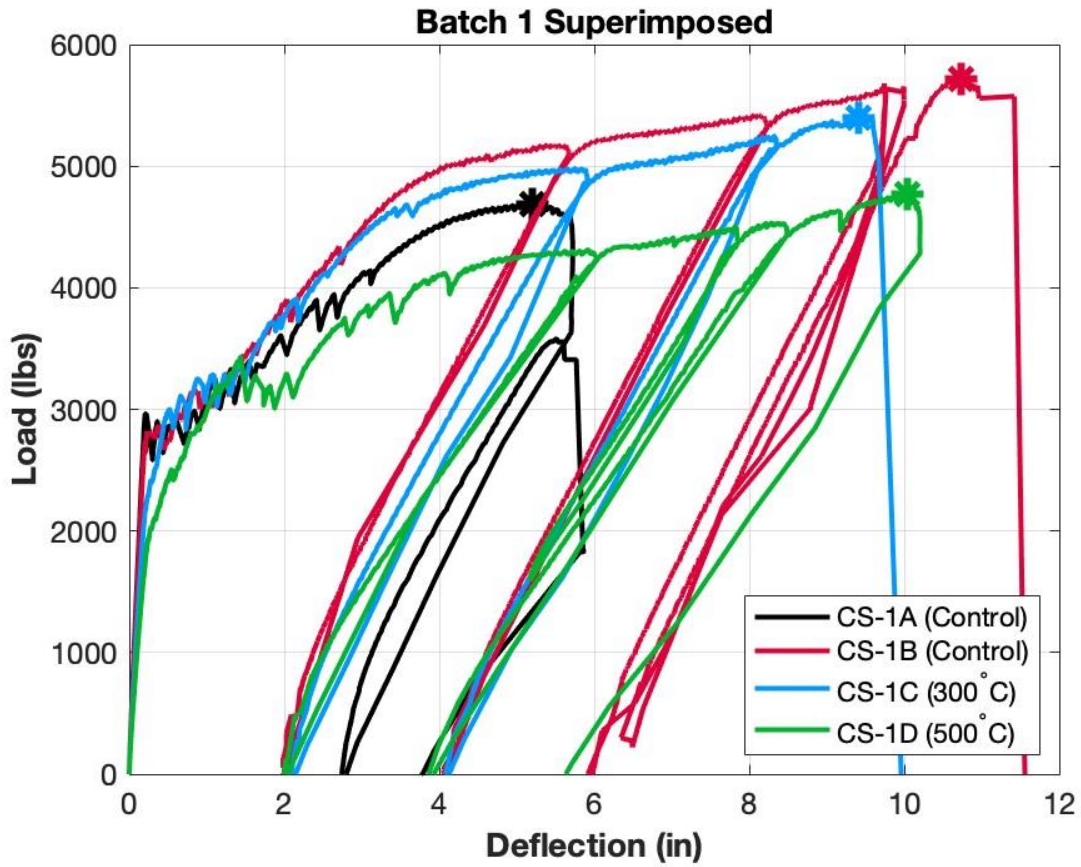
Figure 6.32: Batch 1 mechanical testing results superimposed, *stars represent respective peak capacities during each test*

Table 6.4: Summary of results from mechanical testing—batch 1

Slab	Heating Regimen	Maximum Capacity (lbs.)	Deflection at Maximum Capacity (in)	Failure Mode[a]	Failure Inside Heated Region?
CS-1A	None (Control)	4,685	5.20	1	N/A
CS-1B	None (Control)	5,721	10.73	2	N/A
CS-1C	300°C – 3 hours	5,400	9.41	2	Yes
CS-1D	500°C – 3 hours	4,770	10.04	1	No

[a] Failure mode "1" is yielding of steel followed by crushing of concrete and failure mode "2" is rupture of steel

(a) CS-1A

(b) CS-1B

(c) CS-1C

(d) CS-1D

Figure 6.33: Batch 1 mechanical testing failure locations (indicated by red lines)

When conducting tests on concrete slab specimens from batch 1, it was found that the different heating regimens may have had a negligible influence on the specimens' maximum capacities. All specimens' deflections at maximum capacity were within 14 percent of each other, when excluding specimen CS-1A. CS-1A reached its maximum capacity with significantly different behavior with regard to ductility than the rest of the batch 1 specimens, and the cause is unknown. The CS-1A and CS-1D maximum capacities were approximately 1000 lb. lower than those of CS-1B and CS-1C, and this can be explained by the failure modes of the specimens. All specimens were loaded until a decrease in carrying capacity was observed. CS-1A and CS-1D failed due to yielding of steel followed by crushing of concrete (Figure 6.34). CS-1B and CS-1C failed due to the rupture of reinforcing steel (Figure 6.35). CS-1A and CS-1D had maximum capacities within 2 percent of each other, and CS-1B and CS-1C had maximum capacities within 6 percent of each other. The data do not support that heat exposure caused a decrease in maximum capacity of the member or significantly influenced associated deflections at maximum capacity when excluding the deflection results of specimen CS-1A. All specimens from batch 1 failed inside the constant moment region. Specimen CS-1C failed inside the heated region, and specimen CS-1D failed outside the heated region (Figure 6.33).

**Figure 6.34: Yielding of steel followed by crushing of concrete failure (a) top view (b) side view**

Figure 6.35: Rupture of steel failure (a) top view (b) side view

6.3.2. Batch 2

Four specimens (CS-2A, CS-2B, CS-2C, and CS-2D) were mechanically tested from batch 2. These included two control specimens (one with epoxy coated wire mesh and one with wire mesh that was not epoxy coated), and two specimens heated to 500°C (932°F) (one with epoxy coated wire mesh and one with wire mesh that was not epoxy coaated). Specimens

with epoxy coated wire mesh were tested to understand if the epoxy coated wire mesh would cause different behavior than that of slabs with uncoated wire mesh. The primary interest was to observe if epoxy coated mesh would experience melting of the epoxy with heat exposure, and if that could lead to changes in the mechanical behavior of the specimens (e.g., spalling, variations in bond strength). Load-deflection plots for each test can be found in Figure 6.36. The peak capacity of each specimen is highlighted and presented in Table 6.5.
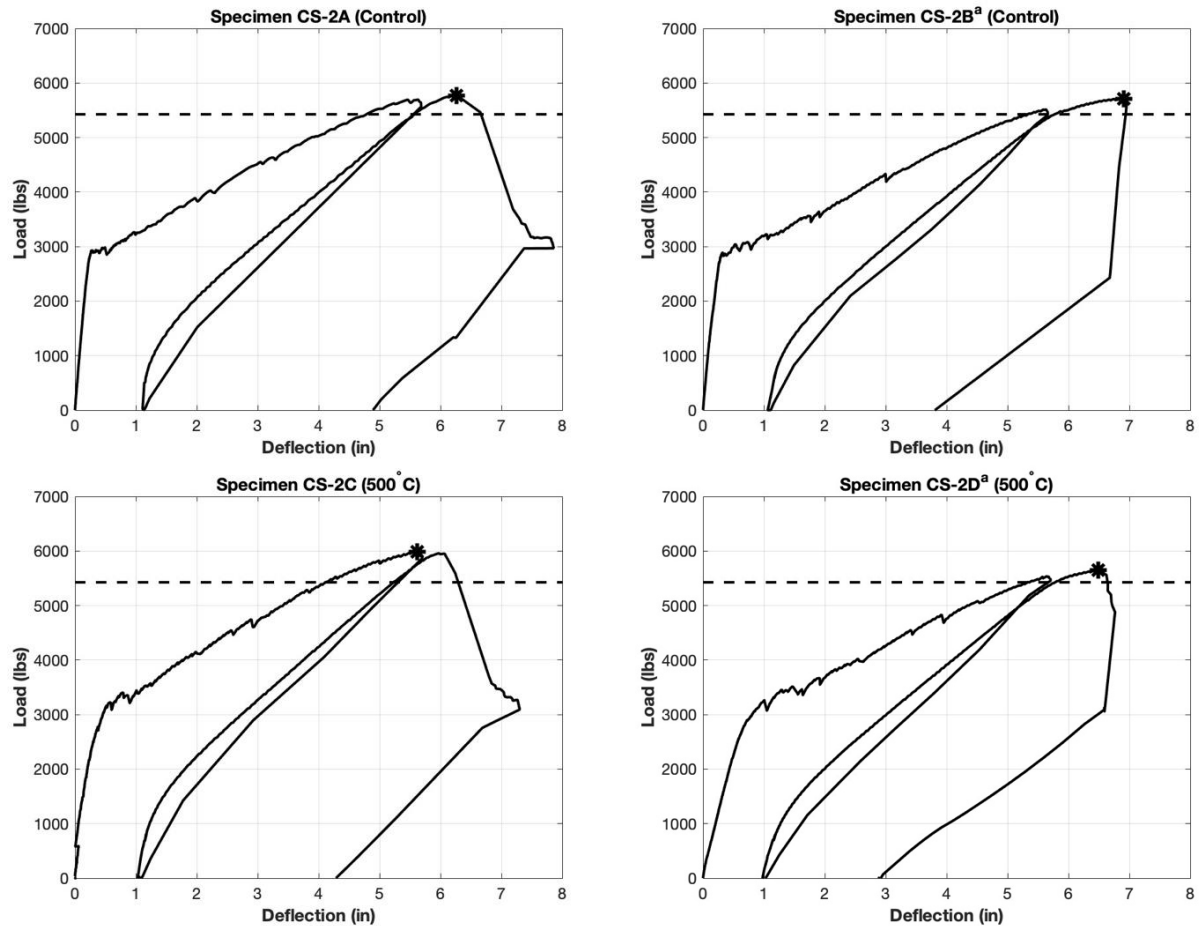
[a] Specimen has epoxy coated wire mesh.

Figure 6.36: Mechanical testing results of batch 2 specimens CS-2A (Control), CS-2B[a] (Control), CS-2C (500°C), and CS-2D[a] (500°C), *dashed lines represent calculated design flexural capacity of unheated batch 2 concrete slab specimens (5,425lbs) and stars represent respective peak capacities during each test*

Batch 2 Superimposed
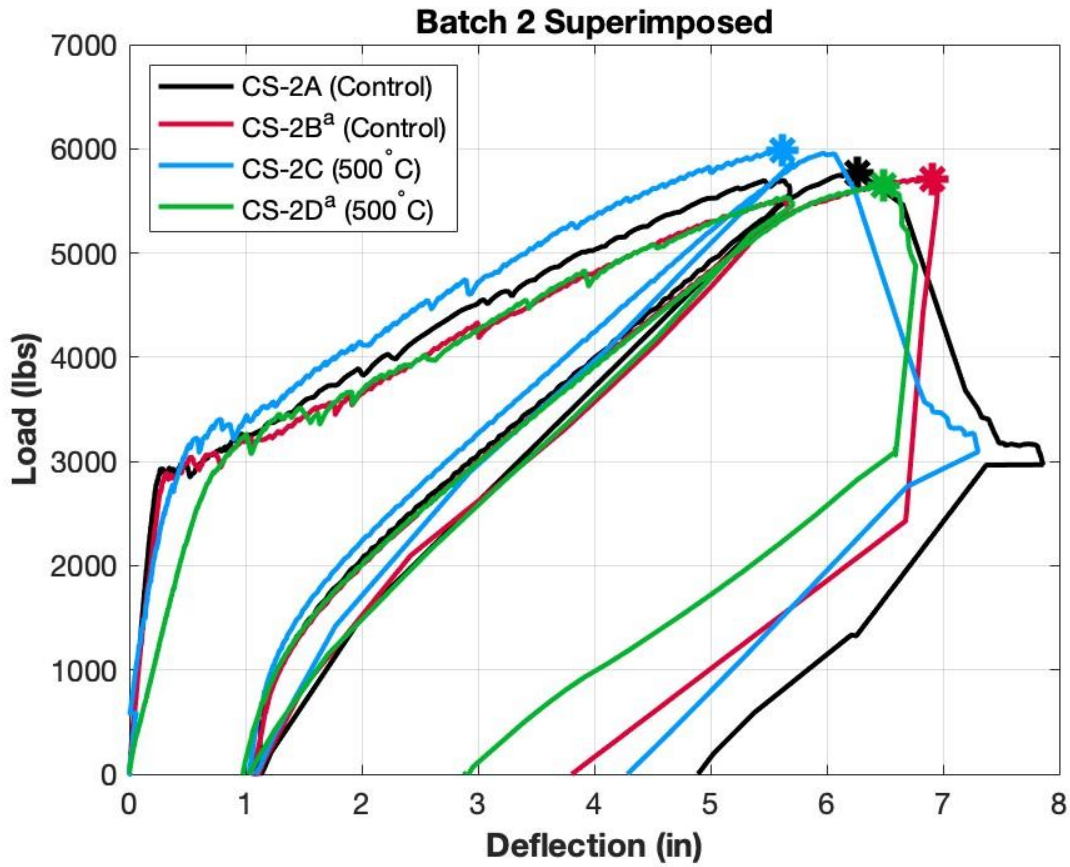
ᵃ Specimen has epoxy coated wire mesh.

Figure 6.37: Batch 2 mechanical testing results superimposed, *stars represent respective peak capacities during each test*

Table 6.5: Summary of results from mechanical testing—batch 2

Slab	Heating Regimen	Maximum Capacity (lbs.)	Deflection at Maximum Capacity (in)	Failure Modeᵃ	Failure Inside Heated Region?
CS-2A	None (Control)	5,770	6.26	1	N/A
CS-2Bᵇ	None (Control)	5,715	6.91	1	N/A
CS-2C	500°C – 3 hours	5,983	5.62	1	Yes
CS-2Dᵇ	500°C – 3 hours	5,647	6.49	1	No

ᵃ Failure mode "1" is yielding of steel followed by crushing of concrete
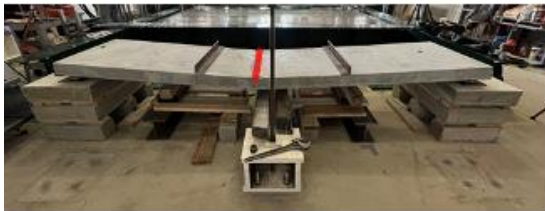ᵇ Specimens with epoxy coated wire mesh
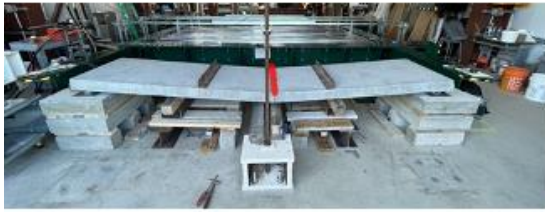
(a) CS-2A

(b) CS-2B

(c) CS-2C

(d) CS-2D

Figure 6.38: Batch 2 mechanical testing failure locations (indicated by red lines)

When conducting tests on concrete slab specimens from batch 2, it was found that the different heating regimens may have had a negligible influence on the specimens' maximum capacities and associated deflections. All batch 2 specimens' maximum capacities were within 6 percent of each other, and all deflections at maximum capacity were within 23 percent of each other. Notably, Slab CS-2D, heated to 500°C (932°F), experienced spalling while at elevated temperatures purely from heat loading, as shown in Figure 6.39. Despite losing a significant area of its cross section, the specimen still maintained a maximum capacity comparable to that of the other specimens from batch 2. This can be explained by the fact that the spalled concrete was located in the tension zone of the specimen, thus having a negligible influence on flexural capacity (as concrete has minimal strength in tension and is a material primarily used for its compressive strength). Also of interest is the influence of epoxy coated wire mesh on the structural behavior of concrete slab specimens. Test data suggest that there were no significant differences between the structural behavior of specimens with epoxy coated wire mesh and those with uncoated wire mesh in control conditions and after being exposed to elevated temperatures. All specimens from batch 2 failed inside the constant moment region. Specimen CS-2C failed inside the heated region and specimen CS-2D failed outside the heated region (Figure 6.38).

Figure 6.39: Specimen CS-2D spalled tensile face

6.3.3. Batch 3

Three specimens from batch 3(CS-3A, CS-3B, and CS-3C) were mechanically tested. These included one control specimen and two specimens heated to 500°C (932°F). Notably, specimen CS-3C heated to 500°C (932°F) was mechanically tested such that the heated region was on the compressive face of the specimen as opposed to all of the other specimens in mechanical testing that were heated on the tension face. The purpose of mechanically testing the heated region in compression was to investigate differences in structural behavior of the concrete slab specimens based on a fire occurring above or below the ceiling panel. In a tunnel structure, a ceiling panel may be exposed to elevated temperatures on its compressive face in the case of an electrical fire, where wireways are present above the ceiling panels. The peak capacity of each specimen is highlighted and presented in Table 6.6.
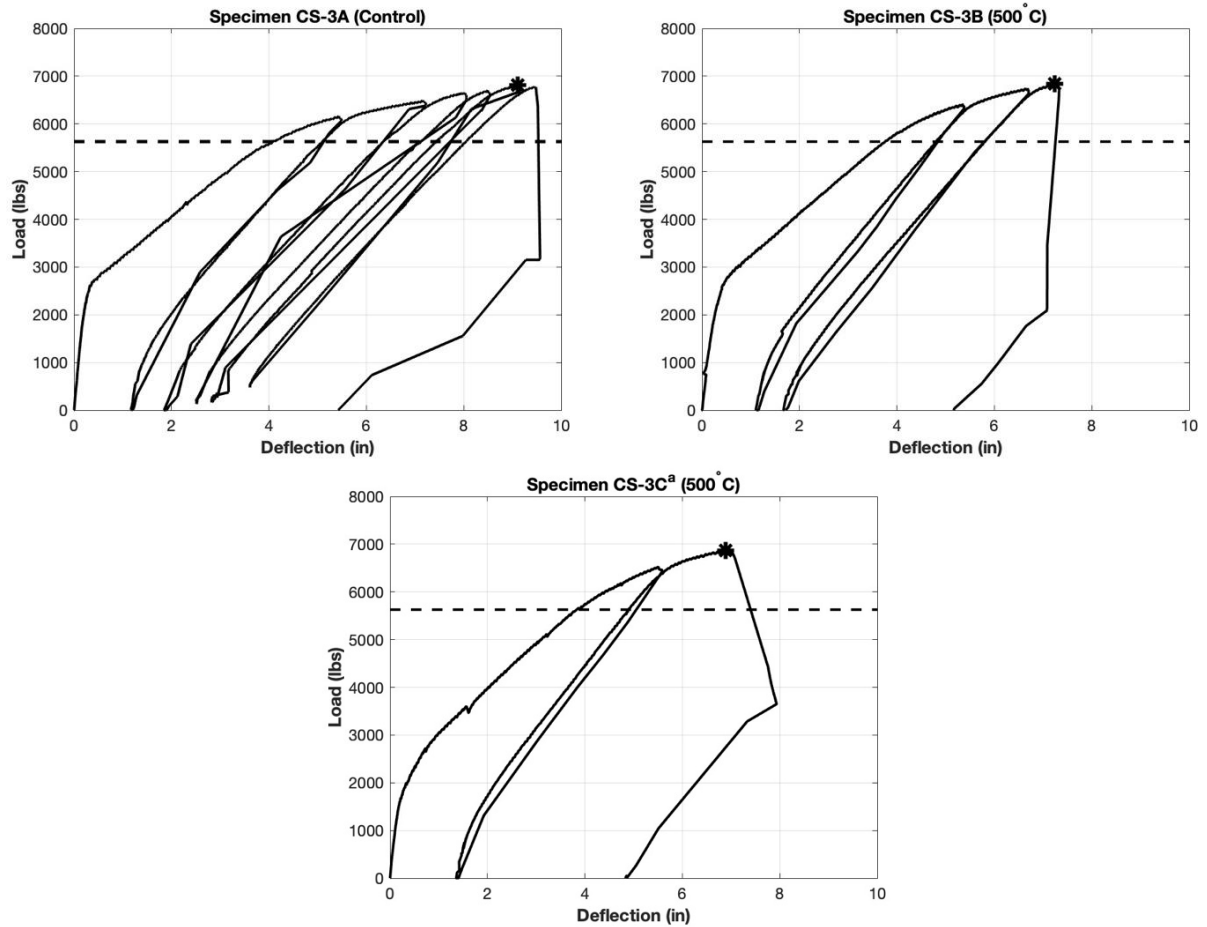
Figure 6.40

[a] Specimen was mechanically tested with its heated face in compression.

Figure 6.40: Mechanical testing results of batch 3 specimens CS-3A (Control), CS-3B (500°C), and CS-3Cª (500°C), *dashed lines represent calculated design flexural capacity of unheated batch 3 concrete slab specimens (5,628lbs) and stars represent respective peak capacities during each test*

Batch 3 Superimposed
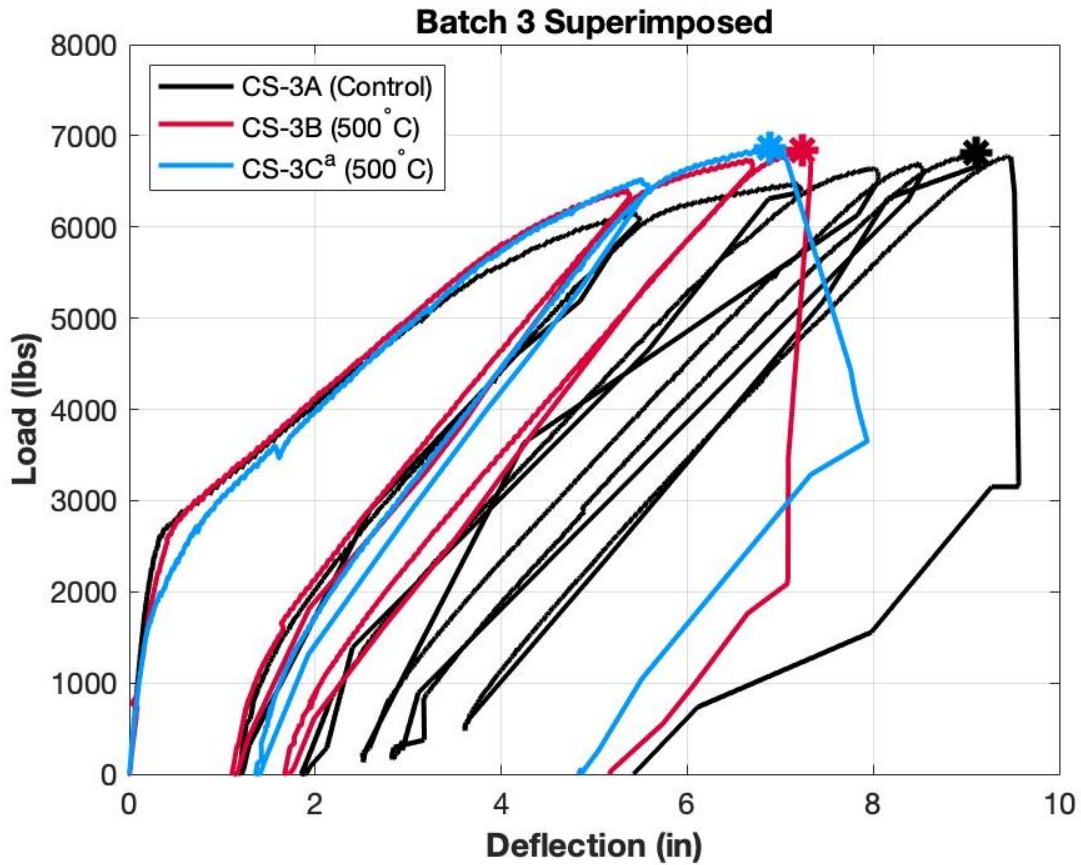
[a] Specimen was mechanically tested with its heated face in compression

Figure 6.41: Batch 3 mechanical testing results superimposed, *stars represent respective peak capacities during each test*

Table 6.6: Summary of results from mechanical testing—batch 3

Slab	Heating Regimen	Maximum Capacity (lbs.)	Deflection at Maximum Capacity (in)	Failure Mode[a]	Failure Inside Heated Region?
CS-3A	None (Control)	6,808	9.10	1	N/A
CS-3B	500°C – 3 hours	6,840	7.24	1	No
CS-3C[b]	500°C – 3 hours	6,869	6.89	1	Yes

[a] Failure mode "1" is yielding of steel followed by crushing of concrete
[b] Specimen was tested with its heated face in compression, opposed to tension

(a) CS-3A

(b) CS-3B

(c) CS-3C

Figure 6.42: Batch 3 mechanical testing failure locations (indicated by red lines)

When conducting tests on the concrete slab specimens from batch 3, it was found that heating regimens may have had a negligible influence on their capacities and deflections at maximum capacity. All specimens in batch 3 that were mechanically tested had capacities within 1percent of each other. Deflections at maximum capacity were similar between specimens CS-3B, heated to 500°C (932°F), and CS-3C, heated to 500°C (932°F), measuring within 5 percent of each other. Specimen CS-3A (control) appeared to be more ductile than the two heated specimens, but this behavior is not necessarily attributed to lack of heat exposure. Deflections of all three specimens at maximum capacity were within 32 percent of each other. Specimen CS-3C, mechanically tested with its heated face in compression, did not show any significant differences when compared with specimens mechanically tested with their heated face in tension. All specimens from batch 3 failed inside the constant moment region. Specimen CS-3C failed inside the heated region and CS-3B failed outside the heated region (Figure 6.42).

6.4 Structural Hanger Rod

Hanger rods are used to support ceiling panels in MassDOT-owned tunnels. These rods are made with galvanized steel and connect to metal angles which hold slabs on their ends. The other end is embedded in the tunnel roof using post-installed adhesive anchors (Figure 6.43). These anchors can be compromised when exposed to even moderately elevated temperatures *(65)*. An investigation of heat propagation through the rod was of interest to understand what parts of the rod may be at risk of heat damage or if heat can propagate through its length, potentially causing anchor failures. For testing purposes, a steel plate was attached to the hanger rod to mimic the steel angle ceiling panel support, and the plate was brought to

94

elevated temperatures. As described in Figure 6.43, the steel angle supports would be directly exposed to a tunnel fire, and the hanger rod itself would be exposed to conditions above the steel angle supports and ceiling panels. As the hanger rod would not be directly exposed to a fire due to the cover by the ceiling panels, during testing, the rod was put in ambient laboratory conditions. All fasteners of the rod were tightened to ensure maximum surface area connection between parts of the hanger rod to provide a worst-case scenario for heat propagation. The detailed test setup can be viewed in Figures 6.44 and 6.45. This testing utilized a Fluke TI400 thermal camera to capture the approximate temperatures of the rod at different locations.
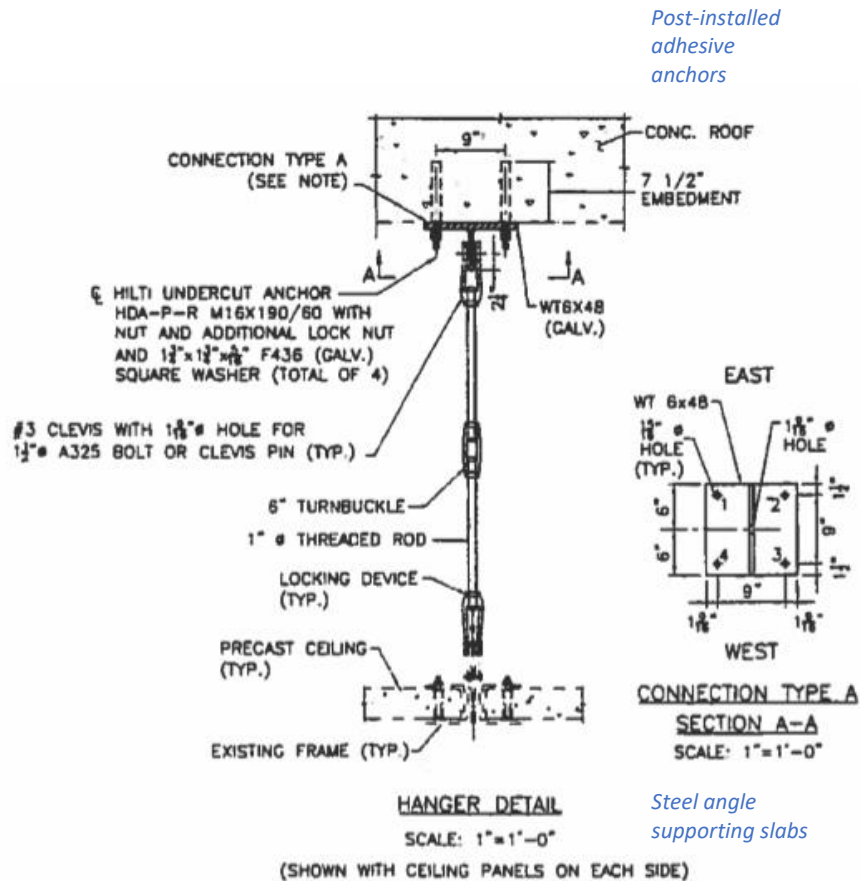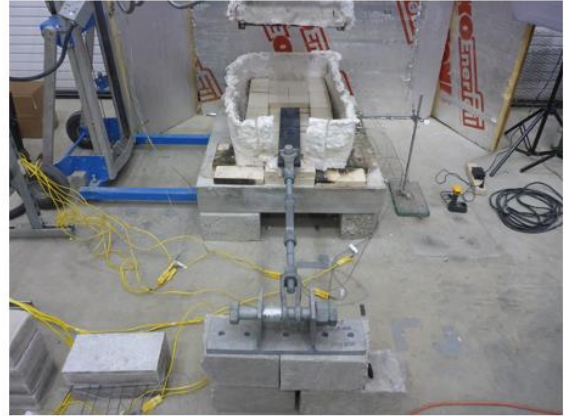

Figure 6.43: Hanger rod tunnel schematic detail

Figure 6.44: (a) Hanger rod (b) hanger rod and attached steel plate in heating chamber (c) close up of steel plate in heating chamber (d) closed heating chamber
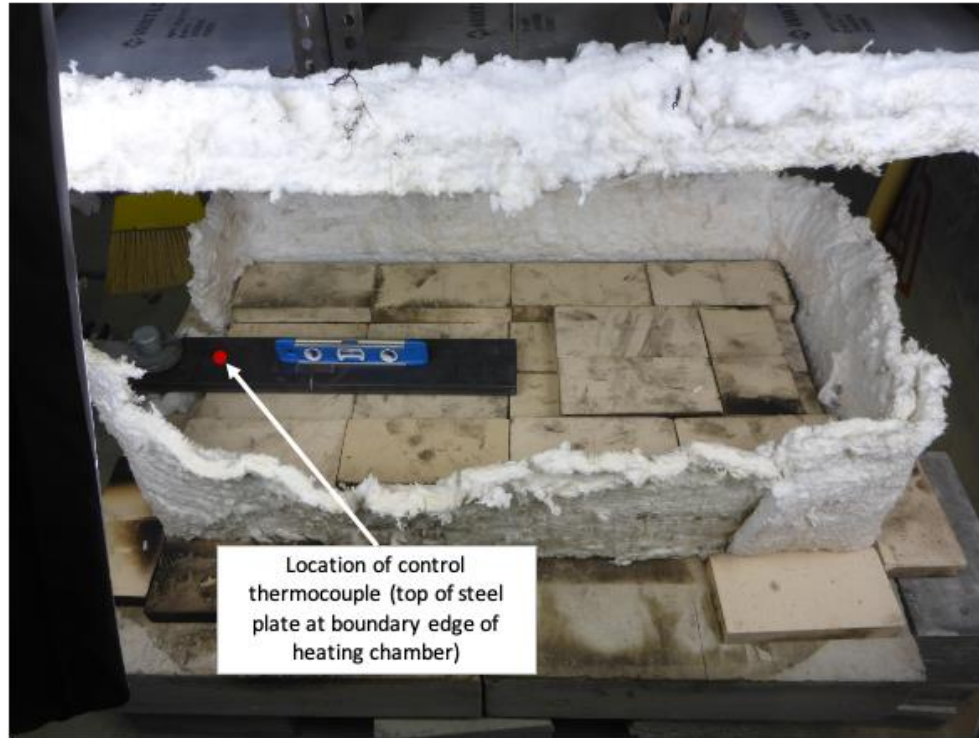
Figure 6.45: Location of control thermocouple for hanger rod heating test

A stepped loading procedure was applied to the specimen in which the attached steel plate was brought to temperatures of 300°C (572°F) and 500°C (932°F) for thirty minutes each, and 570°C (1058°F) for two hours. 570°C (1058°F) was the maximum plate temperature that could be achieved at the location of the control thermocouple (Figure 6.45) with the given test setup and equipment. Temperature data were taken at three different locations: *plate location*, *mid length*, and *anchor location* (Figure 6.46). The temperature data of the entire assembly were recorded and reported at the described three points using a Fluke TI400 thermal camera. *Plate location* references the point closest to the heat source of the rod, *mid length* refers to the middle connection of the rod, and *anchor location* is the end plate of the rod. Temperature data (Figures 6.47 and 6.48) show that the anchor location and mid length temperature data points are constant throughout testing, never experiencing a significant increase in temperature. The plate location temperature point, during the 300°C (572°F) step, increased by approximately 20°C (36°F) over the thirty-minute time period. The plate location temperature point at the 500°C (932°F) and 570°C (1058°F) maintained temperatures fluctuated between 75°C (167°F) and 85°C (185°F), reaching steady state conditions with an average slope of approximately 0°C/min (0°F/min) over the course of thirty minutes (Figure 6.47). The 570°C (1048°F) step was maintained for two hours during which there was no significant fluctuations in temperature at any of the defined points (Figure 6.48). This proved that heat propagation through the length of the rod was minimal given the described heating regimen and test setup. Therefore, a fire in a tunnel should theoretically not have any effect on post-installed adhesive anchor temperatures.
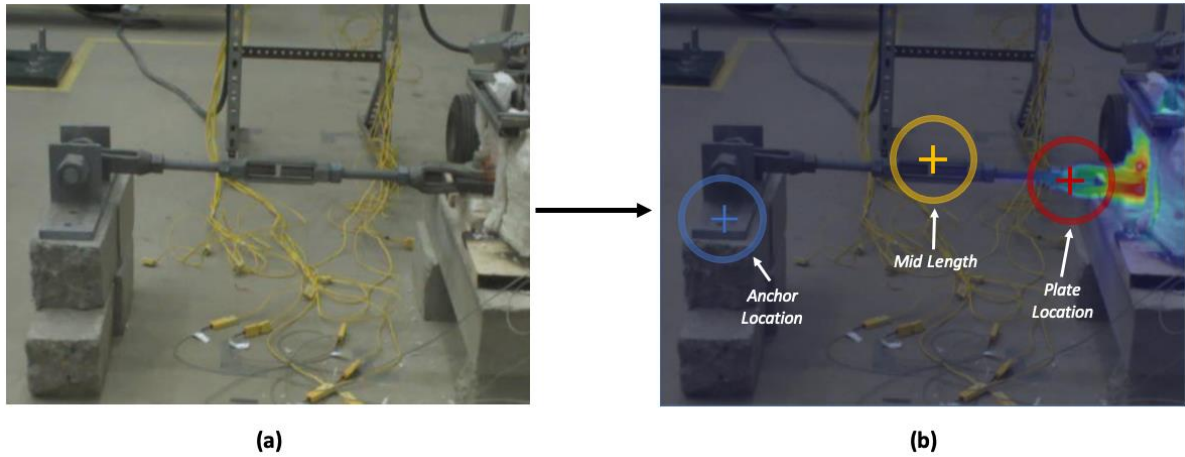
Figure 6.46: Example of thermal imaging using Fluke TI400 Thermal Camera to measure temperature data at plate location, mid length, and anchor location of hanger rod (a) normal (b) infrared
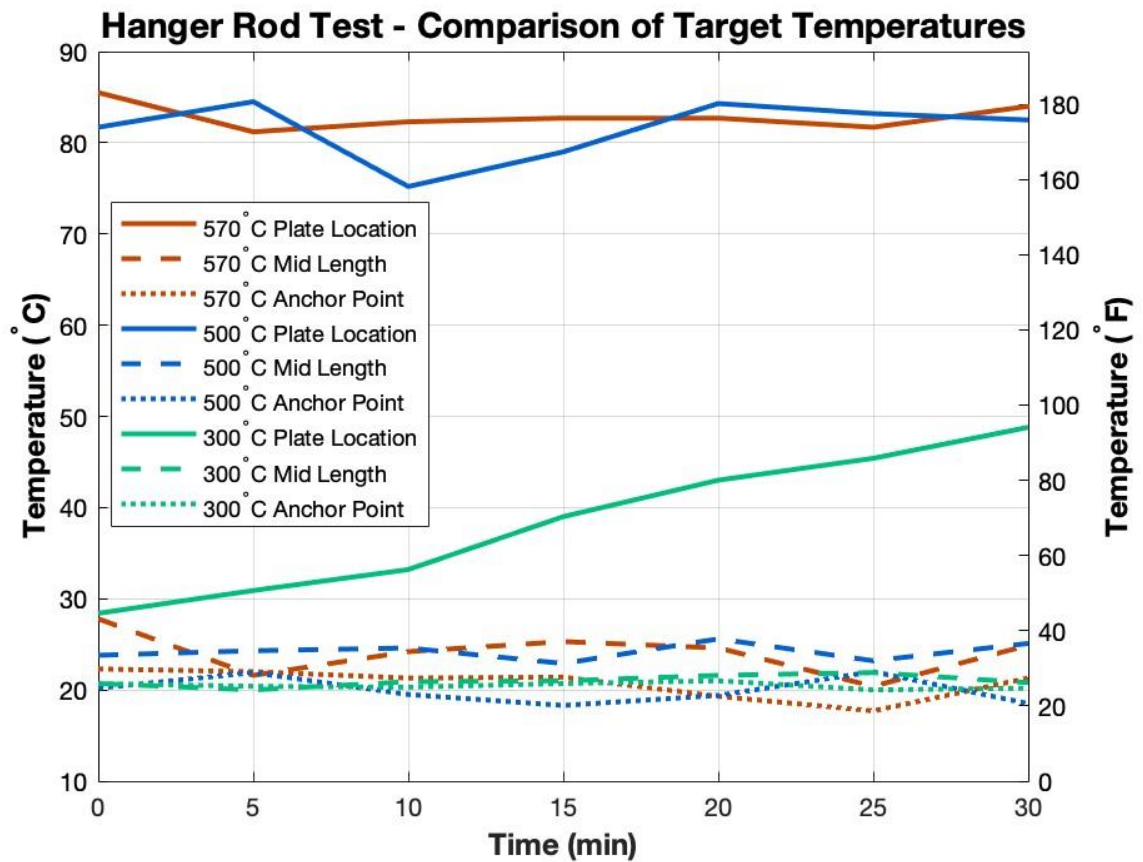

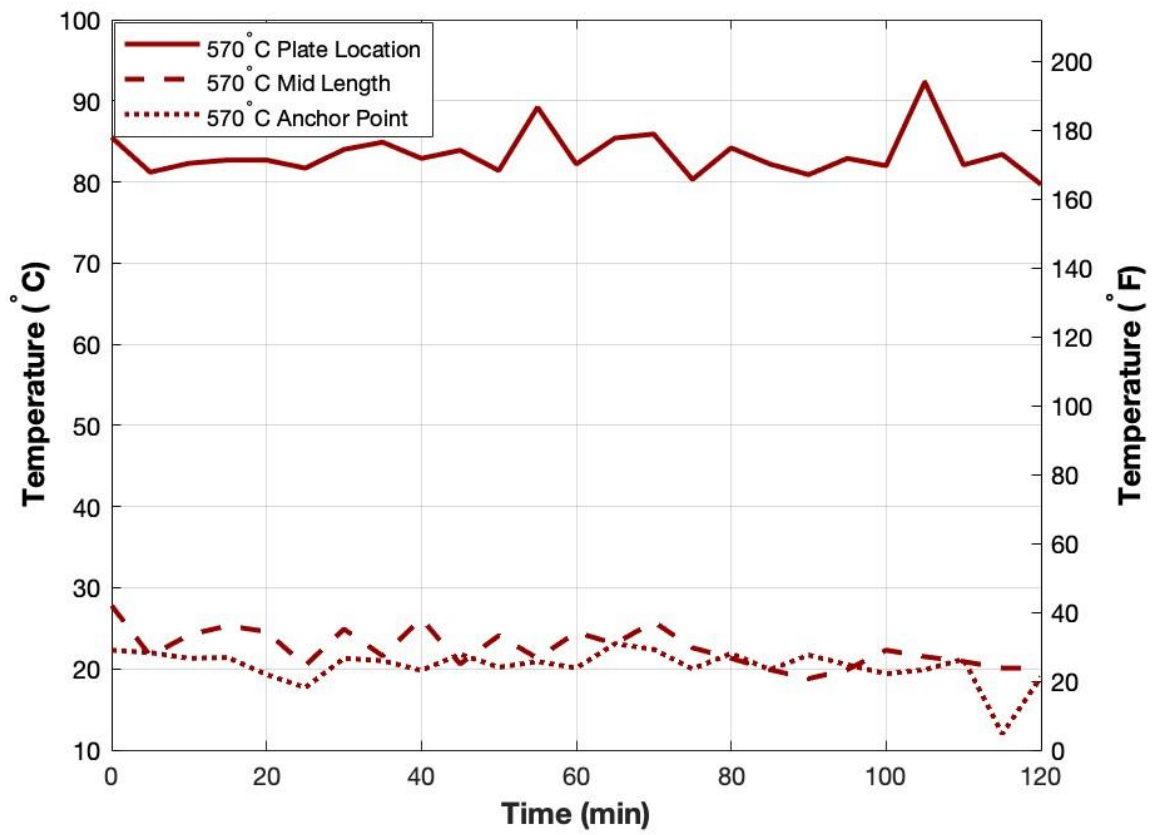**Figure 6.47: Hanger rod heat propagation comparison of target temperatures**

Figure 6.48: Hanger rod heat propagation maximum target temperature

This page left blank intentionally.

7.0 Conclusions

The experimental results from Phase II of this project provide important conclusions for post-fire investigation in tunnel structures. The goal of this project was to establish methods of evaluating the structural condition of a tunnel after an intermediate fire event.

Proper assessment of post-fire conditions is essential to reduce safety risks, interruption of commerce, negative economic impacts, and social ramifications. This project has aimed to create a collection of visual data that could help identify the condition of a wide range of materials and tunnel components exposed to various temperatures for different amounts of time (variable fire scenarios). Mechanical testing of structural tunnel components (ceiling panels) has given insight into the influence of heat exposure on structural members as well. This information has been compiled into a checklist presented in Appendix A so that it may be used to enhance post-fire inspection protocols.

Tunnel structures vary in design, making post-fire inspection unique to each tunnel. The use of a post-fire inspection protocol is therefore not straightforward and requires extensive engineering judgement. This project also aimed to study materials and components that may be common in tunnels in general, but with a specific focus on MassDOT-owned tunnels. It must be noted that the response of material and structural elements to heat can be variable depending on a number of factors, emphasizing the importance of engineering judgement in a case-by-case basis.

With a primary goal of this research being the evaluation of structural members exposed to heat, it is important to consider that a wide range of members exist in tunnels and may respond variably depending on factors such as material properties, geometry, and also exposure to specific fire conditions. This work is limited to mechanical testing of ceiling panel members specifically. Also, visual investigation is limited to specific materials and tunnel components and can be expanded in future work.

7.1 Nonstructural Components/Materials

Phenolic Conduit
- A phenolic conduit specimen showed visual responses that varied depending on the different levels of temperature exposure.
- A phenolic conduit specimen reached internal steady state conditions of approximately 100°C when the top surface was directly heat loaded to 600°C for 120 minutes.

Aluminum/Aluminum Wireway
- Aluminum wireway specimens showed visual responses, including color change and deformation, that varied with different levels of temperature exposure.
- Aluminum deformation appears to be a function of time once exceeding its melting point of 660°C (1220°F).

Light Fixture
- A light fixture specimen showed variable visual responses, including discoloration of its glass lens and aluminum casing, and deformation of its aluminum casing, dependent on different levels of temperature exposure.

Steel
- Galvanized steel and miscellaneous steel specimens showed visual responses that varied dependent on different levels of temperature exposure and on factors such as geometry and exterior coating.

Concrete
- There did not appear to be a difference in visual response of concrete sidewalk block specimens exposed to heat that was related to their mixture design or curing method.

7.2 Structural Components

Concrete Slab Specimens (Ceiling Panels)
- Concrete slab specimens showed pink/red discoloration and cracking with heat exposure which became more apparent as temperature increased from 300°C (572°F) to 400°C (752°F) to 500°C (932°F) (results are consistent with corresponding cylinders).
- Concrete slab specimens did not show significant differences in discoloration or cracking between batches or duration of heat exposure (one hour vs. three hours).
- Concrete slab specimens heated around metal inserts and lifting anchors showed general surface cracking trends comparable to concrete without inserts/anchors, with exception of some cracking stemming from the locations of inserts/anchors.
- No significant change in slab capacity was observed in slabs heated up to 500°C (932°F) for three hours.
- All slab specimens deflected significantly before failing (> 5in.).
- All specimens did fail inside the applied constant moment region; however, not all specimens failed in their heated zones.
- Two failure modes were observed: yielding of steel followed by crushing of concrete, and rupture of steel, with the latter only being observed in specimens with two prestressed strands.
- Higher temperatures may cause spalling which would be apparent in an inspection; the remaining cross section should be evaluated due to effects this might have on strength.

Wall Panel

- Wall panel specimens show visual responses in their grout color, discoloration of surrounding inserts, and burning/discoloration of exposed epoxy coated rebar that varied dependent on the different levels of temperature exposure.
- Wall panel specimens showed cracking of ceramic tiling at elevated temperatures.

Hanger Rod

- A hanger rod specimen did not show signs of significant heat propagation when an attached steel plate was heated to 570°C (1058°F) for 120 minutes.

This page left blank intentionally.

8.0 Recommendations for Future Testing

Phase II of this project has provided a collection of visual and mechanical data that can be used to enhance post-fire protocols in tunnel structures. Phase III of this project aims to continue the study of fire and tunnel structures through an investigation of patching materials with heat exposure as well as through on-site testing of tunnel members/components.

8.1 Patching Materials

A primary goal of Phase III of this project is to investigate patching materials and their behavior in response to heat exposure. Patching materials are used to fill in missing/removed sections of concrete members. Two main types of patching materials are of interest: polymer modified and cementitious. An investigation of the different types of patching materials under a range of heating regimens is recommended. This can not only enhance post-fire protocols, as patches are common in tunnel structures and can serve as a visual aid for estimating fire intensity and duration, but also enable a better understanding of how an applied patch may respond in the event of a fire.

8.2 On-Site Testing

Thus far, Phase I and Phase II testing has been conducted in a laboratory setting. In Phase III, it is recommended to test actual structural members/components on-site at a decommissioned location (so as not to influence the functionality of an in-use structure). This can further enhance the understanding of tunnel structures in a fire event through direct observation. It is recommended to expand the heating units from three units to six units. Testing on-site will also require a mobile generator to supply power to the heating units and data acquisition system(s).

This page left blank intentionally.

9.0 References

1. Menz, N., S. Gerasimidis, S. Civjan, J. Czach, and J. Rigney. Review of Post-Fire Inspection Procedures for Concrete Tunnels. In *Transportation Research Record:Journal of the Transportaion Research Board,* No. 2675(9), Transportation Research Board of the National Academies, Washington, D.C., 2021, pp.1304–1315.
2. Gerasimidis, S., and B. Ellingwood. Twenty Years of Advances in Disproportionate Collapse Research and Best Practices since 9/11/2001. *Journal of Structural Engineering*, Vol.149, No. 2, 2021, p. 02022002.
3. Gerasimidis, S., and M. Ettouney. On the Definition of Resilience, *Objective resilience: Policies and strategies*, 2022, pp. 1-24.
4. Pantidis, P., and S. Gerasimidis. Progressive collapse of 3D steel composite buildings under interior gravity column loss. *Journal of Constructional Steel Research*, Vol. 150, 2018, pp. 60-75.
5. Gerasimidis, S., N. E. Khorasani, M. Garlock, P. Pantidis, and J. Glassman. Resilience of Tall Steel Moment Resisting Frame Buildings with Multi-Hazard Post-Event Fire. *Journal of Constructional Steel Research,* Vol.139, 2017, pp. 202-219.
6. Sideri, J., C. L. Mullen, S. Gerasimidis, and G. Deodatis. Distributed Column Damage Effect on Progressive Collapse Vulnerability in Steel Buildings Exposed to an External Blast Event. *Journal of Performance of constructed Facilities,* Vol.31, 2015, No. 5, p. 04017077
7. Gerasimidis S., and J. Sideri. A New Partial-Distributed Damage Method for Progressive Collapse Analysis of Steel Frames. *Journal of Constructional Steel Research,* Vol. 119, 2016, pp. 233-245.
8. Gerasimidis, S. Analytical Assessment of Steel Frames Progressive Collapse Vulnerability to Corner Column Loss. *Journal of Constructional Steel Research,* Vol. 95, pp.1-9.
9. Khoury, G. A. Effect of Fire on Concrete and Concrete Structures. *Progress in Structural Engineering and Materials,* Vol. 2, No. 4, 2000, pp. 429-447.
10. Naus, D. J. *The Effect of Elevated Temperature on Concrete Materials and Structures*. U.S. Nuclear Regulatory Commission, Washington, D.C., 2006.
11. Shao, Z., X. Zha, and C. Wan. Load Capacity of Concrete-Filled Steel Tubular Members with Multilayer Confinement Subjected to Coupled Axial Compression-Bending and Fire. *Fire Safety Journal*, Vol. 135, 2023, p. 103711., https://doi.org/10.1016/j.firesaf.2022.103711. Accessed 5 Feb. 2023.
12. Promat. International Fire Curves and Fire Safety Design. https://www.promat.com/en/construction/your-project/expert-area/33637/international-fire-curves-fire-safety/. Accessed 15 Dec. 2022.
13. Maraveas, C. and A. A. Vrakas. Design of Concrete Tunnel Linings for Fire Safety. *Structural Engineering International,* 2014, pp. 1-11.
14. Priorit. Fire Protection in Tunnelling - Test Method Rabt. https://www.priorit.de/en/fire-protection-tunnels-test-method-rabt/. Accessed Oct. 4, 2022.
15. Fletcher, I. A., S. Welch, J. L. Torero, R. O. Carvel, and A. Usmani. The Behavior of Concrete Structures in Fire. *Thermal Science,* Vol. 11, No. 2, 2007, pp. 37-52.

16. Lie, T. T. Structural Fire Protection. *American Society of Civil Engineers*, 1992, https://doi.org/10.1061/9780872628885. Accessed 5 Feb. 2023.
17. European Committee for Standardization. *Eurocode 2: Design of Concrete Structures - Part 1- 2: General rules - Structural fire design*, EN 1992-1-2:2004: E, 2004.
18. European Committee for Standardization. *Eurocode 3: Design of Steel Structures – Part 1-2: General Rules – Structural Fire Design*, EN 1993-1-2:2005: E, 2004
19. European Committee for Standardization. *Eurocode 4: Design of Composite Steel and Concrete Structures – Part 1-2: General rules - Structural fire design,* EN 1994-1-2:2005: E, 2005.
20. Concrete Society. *Assessment, Design, and Depair of Fire-Damaged Concrete Structures*, Camberley : Concrete Society, No. 68, 2008.
21. International Federation for Structural Concrete (fib). Fire Design of Concrete Structures - Structural Behavior and Assessment. Bulletin 46, Lausanne, 2008.
22. The Institution of Structural Engineers. *Appraisal of existing structures.* London, 2010.
23. American Concrete Institute. *Code Requirements for Determining Fire Resistance of Concrete and Masonry Construction Assemblies*. American Concrete Institute, Farmington Hills, 2014.
24. Knaack, A. M., Y. C. Kurama, and D. J. Kirkner. Compressive Strength Relationships for Concrete under Elevated Temperatures. *ACI Materials Journal,* Vol. 107, No. 2, 2010, pp. 164-175.
25. Tao, Z., X.-Q. Wang, and B. Uy. Stress-Strain Curves of Structural and Reinforcing Steels after Exposure to Elevated Temperatures. *Journal of Materials in Civil Engineering,* Vol. 25, No. 9, 2013, pp. 1306-1316.
26. Ingham, J. Forensic Engineering of Fire-Damaged Structures. In *Proceedings of The Institution of Civil Engineers-Civil Engineering*, Vol. 162, 2009, pp. 12-17.
27. Phan, L. T. *Fire Performance of High-Strength Concrete: A Report of the State-of-the-Art. National Institute of Standards and Technology*, Gaithersburg, 1996.
28. Shahraki, M., N. Hua, N. Elhami-Khorasani, A. Tessari, and M. Garlock. Residual Compressive Strength of Concrete after Exposure to High Temperatures: A Review and Probabilistic Models. *Fire Safety Journal*, Vol. 135, 2023, p. 103698., https://doi.org/10.1016/j.firesaf.2022.103698.
29. Hertz, K. D. Limits of Spalling of Fire-Exposed Concrete. *Fire Safety Journal,* Vol. 38, No. 2, 2003, pp. 103-116.
30. Bostrom L., and C. Larsen. Concrete Tunnel Linings Exposed to Severe Fire Exposure. *Fire Technology,* Vol. 42, 2006, pp. 351-362.
31. Msaad, Y., and G. Bonnet. Analyses of Heated Concrete Spalling Due to Restrained Thermal Dilation: Application to the "Chunnel" Fire. *Journal of Engineering Mechanics,* Vol. 132, No. 10, 2006, pp. 1124-1132.
32. Zeiml, M., R. Lackner, and H. A. Mang.Experimental Insight into Spalling Behavior of Concrete Tunnel Linings under Fire Loading. *Acta Geotechnica,* Vol. 3, 2008, pp. 295-308.
33. Jansson, R. Fire Spalling of Concrete: Theoretical and Experimental Studies. KTH Royal Institute of Technology, Stockholm. *Doctoral Thesis* 2013.
34. Klingsch, E. W. Explosive Spalling of Concrete in Fire. Institut für Baustatik und Konstruktion, 2014.

35. Hedayati, M., M Sofi, P. A. Mendis, and T. Ngo. A Comprehensive Review of Spalling and Fire Performance of Concrete Members. *Electronic Journal of Structural Engineering,* Vol. 15, No. 1, 2015.
36. Liu, J. C., K. H. Tan, and Y. Yao. A New Perspective on Nature of Fire-Induced Spalling in Concrete. *Construction and Building Materials,* Vol. 184, 2018, pp. 581-590.
37. Khoury G. A, and Y. Anderberg. Concrete Spalling Review. *Fire Safety Design*, 2000, pp. 1-60.
38. American Concrete Institute. *Code Requirements for Determining Fire Resistance of Concrete and Masonry Construction Assemblies.* American Concrete Institute, Farmington Hills, 2014.
39. Tao, Z. Mechanical Properties of Prestressing Steel after Fire Exposure. *Materials and Structures,* Vol. 48, 2015, pp. 3037-3047.
40. Outinen J., and P. Makelainen. Mechanical Properties of Structural Steel at Elevated Temperatures and after Cooling Down. *Fire and Materials,* Vol. 28, 2004, pp. 237-251.
41. Jinwoo, L., M. D. Engelhardt, and E. M. Taleff. Mechanical Properties of ASTM A992 Steel After Fire. *Engineering Journal,* Vol. 49, 2012, pp. 33-44.
42. Crook,R. N., The Elevated Temperature Properties of Reinforced Concrete. University of Aston in Birmingham, Birmingham, 1980.
43. Neves, I. C., J. P. C. Rodrigues, and A. D. P. Loureiro. Mechanical Properties of Reinforcing and Prestressing Steels After Heating. *Journal of Civil Engineering Materials,* Vol. 8, No. 4, 1996, pp. 189-194.
44. Felicetti, R., P. G. Gambarova, and A. Meda. Residual Behavior of Steel Rebars and R/C Sections after a Fire. *Construction and Building Materials,* Vol. 23, 2009, pp. 3546-3555.
45. Zhang, L., F. T. K. Au, Y. We,i and J. Li. Mechanical Properties of Prestressing Steel in and after Fire. *Magazine of Concrete Research,* Vol. 69, No. 8, 2017, pp. 379-388.
46. The Institution of Structural Engineers. *Appraisal of existing structures*. The Institution of Structural Engineers, London, 2010.
47. Bingol A. F., and R. Gul. Residual Bond Strength between Steel Bars and Concrete after Elevated Temperatures. *Fire Safety Journal,* Vol. 44, No. 6, 2009, pp. 854-859.
48. Schneider U., and D. Drysdale. Repairability of Fire-Damaged Structures. *Fire Safety Journal,* Vol. 16, 1990, pp. 251-336.
49. Khalaf, J., Z. Huang, and M. Fan. Analysis of Bond-Slip between Concrete and Steel Bar in Fire. *Computers and Structures,* Vol. 162, 2016, pp. 1-15.
50. Bosnjak, J., A. Sharma, and S. Bessert. Bond Performance of Reinforcement in Concrete after Exposure to Elevated Temperatures. In *3rd International Symposium on Connections between Steel and Concrete*, Stuttgart, 2017, pp. 850-861.
51. Bingol A. F., and R. Gul. Residual Bond Strength between Steel Bars and Concrete after Elevated Temperatures. *Fire Safety Journal,* Vol. 44, No. 6, 2009, pp. 854-859.
52. El-Hawary, M. M., A. M. Ragab, A. A. El-Azim, and S. Elibiari. Effect of Fire on Flexural Behaviour of RC Beams. *Construction and Building Materials,* Vol. 10, No. 2, 1996, pp. 147-150.
53. Graybeal, B. A. *Flexural Capacity of Fire-Damaged Prestressed Concrete Box Beams*. Federal Highway Administration (FHWA), Fairfax, 2007.

54. Kodur V., M. B. Dwaikat, and R. S. Fike. An Approach for Evaluating the Residual Strength of Fire-Exposed RC Beams. *Magazine of Concrete Research,* Vol. 62, No. 7, 2010, pp. 479–488.

55. Choi, E. G., Y.-S. Shin, and H. S. Kim. Structural Damage Evaluation of Reinforced Concrete Beams Exposed to High Temperatures. *Journal of Fire Protection Engineering,* Vol. 23, No. 2, 2013, pp. 135-151.

56. Kodur V., and A. Agrawal. Residual Response of Fire-Damaged High-Strength Concrete Beams. *Fire and Materials,* Vol. 43, 2019, pp. 310-322.

57. Hua, N., N. Elhami-Khorasani, A. Tessari, and R. Ranade. Experimental Study of Fire Damage to Reinforced Concrete Tunnel Slabs. *Fire Safety Journal*, Vol. 127, 2022, p. 103504.

58. Hager, I. Colour Change in Heated Concrete. *Fire Technology,* Vol. 50, 2014, pp. 945-958.

59. Short, N., J. Purkiss, and S. Guise. Assessment of Fire Damaged Concrete Using Colour Image Analysis. *Construction and Building Materials,* Vol. 15, No. 1, 2001, pp. 9-15.

60. The Institution of Structural Engineers. *Appraisal of existing structures.* The Institution of Structural Engineers, London, 2010.

61. Watlow. Thermocouples. Global Supplier of Industrial Electric Thermal Solutions, https://www.watlow.com/. Accessed 31 May 2022.

62. Brena, S., K. Peterman, and R. Sullivan. Construction and Materials Best Practice for Concrete Sidewalks. 2021.

63. RC55. Enerpac, https://www.enerpac.com/en-us/general-purpose-cylinders/general-purpose-cylinder/RC55. Accessed 15 Dec. 2022.

64. Rice Lake RL90000 Alloy Steel, Compression Disk Load *Cell*, https://www.ricelake.com/products/rice-lake-rl90000-alloy-steel-compression-disk-load-cell/. Accessed 15 Dec. 2022.

65. Mendoza, M., S. Civjan, and S. Brena. Performance of Adhesive and Cementitious Anchoring Systems. *Masters Thesis.* 2017.

66. Leitner, A. The Fire Catastrophe in the Tauern Tunnel: Experience and Conclusions for the Austrian Guidelines. *Tunnelling and Underground Space Technology*, Vol. 16, No. 3, 2001, pp. 217–223.

67. De Beer, J. A., A., J, Alascio, S. Stoliarov, and M. Gollner. Analysis of the Thermal Exposure and Ignition Propensity of a Lignocellulosic Building Material Subjected to a Controlled Deposition of Glowing Firebrands. *Fire Safety Journal*, Vol. 135, 2023, p. 103720. https://doi.org/10.1016/j.firesaf.2022.103720.

68. Voigt, S., F. Straubig, A. Kwade, J. Zehfub. An Empirical Model for Lithium-Ion Battery Fires for CFD Applications. *Fire Safety Journal*, Vol. 135, 2023, p. 103725. https://doi.org/10.1016/j.firesaf.2022.103725.

69. Dundar, U., and S. Serdar. Fire Load and Fire Growth Characteristics in Modern High-Rise Buildings. *Fire Safety Journal*, Vol. 135, 2023, p. 103710. https://doi.org/10.1016/j.firesaf.2022.103710.

70. Reismüller, R., M. Konigsberger, A. Jager, and J. Fussl. The Performance of Vertically Perforated Clay Block Masonry in Fire Tests Predicted by a Finite-Element Model Including an Energy-Based Criterion to Identify Spalling. *Fire Safety Journal*, Vol. 135, 2023, p. 103729. https://doi.org/10.1016/j.firesaf.2022.103729.

71. Law, A., G. Spinardi, and L. Bisby. The Rise of the Euroclass: Inside the Black Box of Fire Test Standardisation. *Fire Safety Journal*, Vol. 135, 2023, p. 103712. https://doi.org/10.1016/j.firesaf.2022.103712.

This page left blank intentionally.

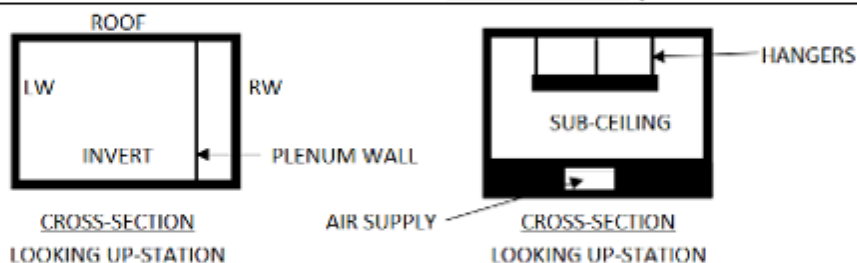# 10.0 Appendix

**10.1 Rapid Post-Fire tunnel Inspection
Checklist**

RAPID POST-FIRE TUNNEL INSPECTION CHECKLIST

GENERAL INFORMATION

INSPECTOR(S): _____   DATE/TIME: _____

TUNNEL NAME: _____   TUNNEL STATION: _____

AIR TEMPERATURE: _____   FIRE EXINGUISHING METHOD: _____

AIR FLOW: _____   _____

SURFACE TEMPERATURE MEASUREMENTS

LEFT WALL _____ (meas. or est. max.) (°C or °F)

RIGHT WALL _____ (meas. or est. max.) (°C or °F)

INVERT _____ (meas. or est. max.) (°C or °F)

ROOF _____ (meas. or est. max.) (°C or °F)

PLENUM WALL _____ (meas. or est. max.) (°C or °F)

SUB-CEILING _____ (meas. or est. max.) (°C or °F)

STEEL STRINGERS, HANGERS, OR BEAMS _____ (meas. or est. max.) (°C or °F)

ROOF

LW   RW

INVERT   PLENUM WALL

CROSS-SECTION
LOOKING UP-STATION

HANGERS

SUB-CEILING

AIR SUPPLY   CROSS-SECTION
LOOKING UP-STATION

SOUND & RECORD OBSERVED DAMAGE LIMITS

	TOTAL (ft x ft)		REMOVED CONCRETE (ft x ft)		C.S.	NOTES
LEFT WALL	_____ x	_____	_____ x	_____	_____	_____
RIGHT WALL	_____ x	_____	_____ x	_____	_____	_____
INVERT	_____ x	_____	_____ x	_____	_____	_____
ROOF	_____ x	_____	_____ x	_____	_____	_____
PLENUM WALL	_____ x	_____	_____ x	_____	_____	_____
SUB-CEILING	_____ x	_____	_____ x	_____	_____	_____

OTHER NOTES (DEFLECTIONS, SPALLING, ETC.)

_____

_____

_____

_____

_____

ITEMIZED CHECKLIST

CONCRETE CEILING PANEL

PINK/RED CONCRETE YES ☐ NO ☐
WHITENED CONCRETE YES ☐ NO ☐
NOTICEABLE CRACKING OF CONCRETE YES ☐ NO ☐
SPALLING OF CONCRETE YES ☐ NO ☐
NOTICEABLE DEFLECTION OF MEMBER YES ☐ NO ☐
REINFORCING STEEL DAMAGE YES ☐ NO ☐

STEEL HANGER RODS/SUPPORT ANGLES

GALVANIZING DISCOLORATION YES ☐ NO ☐
DISTORTION/DEFORMATION YES ☐ NO ☐

WALL PANEL

GROUT DISCOLORATION YES ☐ NO ☐
GROUT TURNS TO POWDER YES ☐ NO ☐
NOTICEABLE CRACKING OF TILES YES ☐ NO ☐
LOSS OF TILES YES ☐ NO ☐
REINFORCING STEEL DAMAGE YES ☐ NO ☐

LIGHT FIXTURE

DISCOLORATION OF ALUMINUM CASING YES ☐ NO ☐
DISCOLORATION OF GLASS LENS YES ☐ NO ☐
MELTING OF ALUMINUM CASING YES ☐ NO ☐
MELTING OF LENS YES ☒ NO ☐

ALUMINUM WIREWAY

DISCOLORATION OF ALUMINUM YES ☐ NO ☐
MELTING OF ALUMINUM YES ☐ NO ☐

PHENOLIC CONDUIT

DISCOLORATION OF CONDUIT YES ☐ NO ☐
DEFORMATION OF CONDUIT YES ☐ NO ☐

ROADWAY SURFACE

SLICK ROADWAY YES ☐ NO ☐
POTHOLES/SPALLING YES ☐ NO ☐

HOW TO USE ITEMIZED CHECKLIST

The itemized checklist should be further compared with the **REFERENCE GUIDE** of the **RAPID POST-FIRE TUNNEL INSPECTION CHECKLIST** to evaluate the maximum temperatures that components may have reached during a given fire.

REFERENCE GUIDE

Disclaimer: Many factors contribute to member strength reduction that should be considered as part of a post-fire inspection. Surface temperature may not always correlate with structural damage (such as explosive spalling resulting from rapid temperature rises). ***Tunnel closure recommendations are suggestions only, and engineering judgement must be used on a case-by-case basis.***

RECOMMENDED ACTION FLOW CHART

Start

Concrete surface temperature[a] $\geq$ 300 °C (532°F)
— yes → Nonstructural components damaged (tiles, lights, etc.) and/or conc. surface temp.[a] $\geq$ 500 °C (932°F)
— yes → Structural elements damaged (tunnel liners, etc.) and/or conc. surface temp.[a] $\geq$ 600 °C (1112°F)

no ↓   no ↓   no ↓   yes ↓

Minor spalling[b] and/or concrete surface crack widths $\geq$ 0.012in (0.3mm)
— yes → Spalling[c] exceeding reinforcement depth and/or conc. surface crack widths $\geq$ 0.025in (0.6mm) and/or any noticeable deflections[d]
— yes → Major spalling[c] exceeding reinforcement depth and/or conc. surface crack widths $\geq$ 0.025in (0.6mm) and/or any noticeable deflections[d]

no ↓   no ↓   no ↓   yes ↓

Tunnel section *most likely* safe to reopen after removal of loose components and clearing of debris
    Tunnel section *may* require closure and future repairs may be necessary
    Tunnel section is recommended for closure and *may not* be structurally sound (depending on thickness and loading)

Condition states[e] 1/2   Condition state[e] 3   Condition state[e] 4

[a] Concrete surface temperature may be determined using the aid of visuals provided in this guide in further sections
[b] Minor spalling refers to spalling greater than or equal to 1/8in in depth
[c] Specifically in reference to spalling on a tension face of a structural element, structural implications resulting from spalling in a compression zone of a structural element must be further assessed using engineering judgement
[d] If deflections are increasing, high risk for collapse
[e] Condition states can be further referenced on the following page

116

CONDITION STATES

Rating	Description	Recommended Actions
1	No damage	Likely safe to open; monitor condition
2	Slightly damaged surfaces / concrete cracking ≤ 0.012in (0.3mm)	Likely safe to open; minor repairs
3	Spalling not exceeding concrete reinforcement depth (tension face) / concrete cracking ≤ 0.025in (0.6mm)	Potential tunnel closure with future repairs
4	Major spalling exceeding concrete reinforcement depth (tension face) / concrete cracking ≥ 0.025in (0.6mm) / noticeable deflections	Recommended tunnel closure
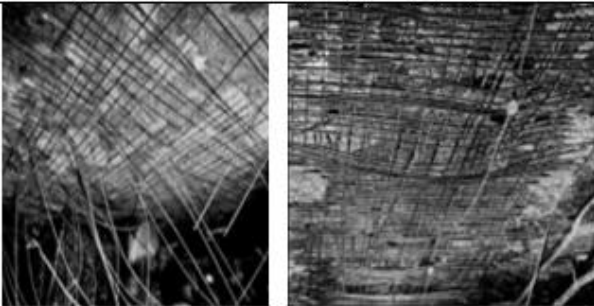
Example Condition State 1 Left: ceiling panels post-fire, bottom-up view; right: wall panel post-fire

Example Condition State 2 Wall panel post garbage truck fire

Example Condition State 3 Left: tunnel section with spalling post-fire, right: concrete spalling post-fire (67)

Example Condition State 4 Severe concrete spalling post-fire with damage reinforcement

CONCRETE CEILING PANELS[a]

Ambient	300°C (575°F)	400°C (750°F)	500°C (930°F)

~30"

~16"

Reddening discoloration →

Ambient	300°C (575°F)	400°C (750°F)	500°C (930°F)

~30"

~16"

Cracking frequency/width →

Concrete must be cleaned[b] of residue (e.g., soot build up from smoke) for evaluation, and comparison of a section not exposed to fire with a section exposed to fire should be used for reference in individual fire scenarios.

[a] Concrete ceiling panels were considered continuously supported during heat loading
[b] Cleaning of concrete surfaces should be done using a method that preserves important visual characteristics (e.g., color and crack widths) that may give insight into fire exposure levels of concrete and associated damage

118

WALL PANEL

Flipped over
(non-tiled
side)
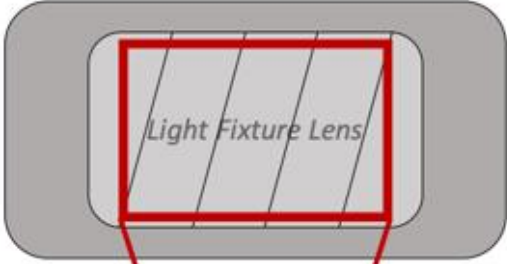
Use above picture in reference to other wall panel temperature-observation charts

WALL PANEL

Temperature (time @ temp.)	Visual Condition	Observations
Ambient Before		
300 ℃ (572 ℉) (30 minutes)		-Initial discoloration of tiles -Initial discoloration of grout (darkens in color)
400 ℃ (752 ℉) (30 minutes)		-Discoloration of tiles and grout continues
500 ℃ (932 ℉) (30 minutes)		-Grout discoloration changes (turns red)
600 ℃ (1112 ℉) (120 minutes)		-Minor cracking observed in tiles
Ambient After		-Metal inserts charred -Exposed epoxy coated rebar melting and charring -Corner spalling

WALL PANEL

Temperature (time @ temp.)	Visual Condition	Observations

Ambient Before

~16"

~8"

600 °C (1112 °F) (120 minutes)

-Slight discoloration of specimen

Ambient After

121

LIGHT FIXTURE

Temperature	Time at Elevated Temperature		Observations
	0 minutes	**30 minutes**	
Ambient Before			
300°C (572°F)			
400°C (752°F)			
500°C (932°F)			- Discoloration begins
600°C (1112°F) [a]			- Significant discoloration and smoke residue build up - First flames observed
700°C (1292°F) [a]			- Smoke residue build up continues - Flames continue (and influence lighting of picture)
Ambient After [a]			

[a] Diamond-like pattern on light fixture lens is a result of the heating system, not unique to the light fixture itself

LIGHT FIXTURE
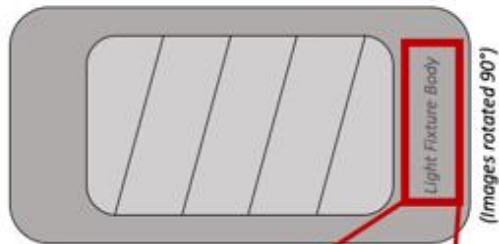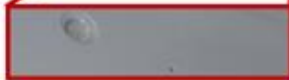
Temperature	Time at Elevated Temperature		Observations
	0 minutes	30 minutes	
Ambient			
300°C (572°F)			
400°C (752°F)			- Discoloration of paint begins
500°C (932°F)			- Discoloration continues - After 30min, flaking of paint
600°C (1112°F)			- Discoloration continues - First flames observed
700°C (1292°F)			- Discoloraation continues - Melting of aluminum begins - Flames continue (and influence lighting of picture
Cooled for 1 hour			- Discoloration of paint lightens in color
Cooled for 2 hours			
Cooled for 4 hours			
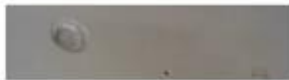
Light Fixture Body

(Images rotated 90°)

123

PHENOLIC CONDUIT

ALUMINUM WIREWAY

Temperature (time @ temp.)	Visual Condition	Observations
Ambient Before	~10"	
300 ℃ (572 ℉) (30 minutes)		-Initial color change
400 ℃ (752 ℉) (0 minutes)		-Color change continues
500 ℃ (932 ℉) (30 minutes)		-Color change continues
600 ℃ (1112 ℉) (0 minutes)		-Color change continues
700 ℃ (1292 ℉) (30 minutes)		-Color change continues -Melting of aluminum
800 ℃ (1472 ℉) (0 minutes)		-Melting of aluminum continues (red lighting due to heaters)
900 ℃ (1832 ℉) (0 minutes)		

MISCELLANEOUS METALS AND ASSOCIATED PROPERTIES

Metal	Temperature °C (°F)	Physical Change(s)
Galvanized Steel (33mil)	300 (572)	-Dulling of outer shine
	400 (752)	-Initial discoloration (yellow tint)
	600 (1112)	-Yellow discoloration continues
	700 (1292)	-Discoloration continues, charring begins
	1371 – 1540 (2500 – 2800)	-Melting point of steel
Galvanized Steel (54mil and 97mil)	500 (932)	-Dulling of outer shine
	700 (1292)	-Initial discoloration (yellow tint)
	800 (1472)	-Discoloration continues, charring begins
	900 (1832)	-Significant charring
	1371 – 1540 (2500 – 2800)	-Melting point of steel
Steel (general)	300 - 400 (572 – 752)	-Discoloration (browning/minor charring) begins
	600 – 700 (1112 – 1292)	-Charring becomes more significant
	1371 – 1540 (2500 – 2800)	-Melting point of steel
Steel (painted finish)	400 (752)	-Minor bubbling of paint
	500 (932)	-Significant flaking and discoloration of paint
	1371 – 1540 (2500 – 2800)	-Melting point of steel
Aluminum	660 (1221)	-Melting point of aluminum -Aluminum softens/deformations begin -Discoloration begins
	900 (1652)	-Significant charring
Brass	900 – 1050 (1652 – 1922)	-Melting point of brass
Bronze	900 – 1000 (1652 – 1832)	-Melting point of bronze
Copper	1000 – 1100 (1932 – 2012)	-Melting point of copper
Cast iron	1100 – 1250 (2012 – 2282)	-Melting point of cast iron
Lead	250 – 400 (482 – 752)	-Melting point of lead
Zinc	400 – 420 (752 – 788)	-Melting point of zinc

This information is general, and some metals may react differently to heat depending on their physical/chemical composition.